REQ. NO. 1-9093

SERVICE CONTRACT NO. 1495893

ROCK PERMEABILITY OF ROOF STRATA

Final Report

by

V. DE KOROMPAY

Work on this project was conducted under the auspices of
Canada Centre for Mineral and Energy Technology
Energy, Mines and Resources Canada

CANMET PROJECT NUMBER: 310007

CANMET SCIENTIFIC AUTHORITY: Dr. D.G.F. Hedley

Date: March 1983

Service Contract No: 1495893

111 pp

ABSTRACT

A novel method based on the ability of rocks to transmit liquid has been developed to detect fractures in rock and structures. The method establishes the location, width, dip, strike and areal extension of a fracture, consequently the stability and safety of an underground opening or of a structure can be evaluated. Vacuum is used for testing to prevent pressure build-up in the fracture, as would occur with a pressurized system.

Fractures of 0.5 to 1.0 mm width, located at 6 to 8 m deep in the rock mass,were detected with a high degree of accuracy. Successful correlation of fractures in holes 8 to 10 m apart was also proven. In situ permeability as low as 0.002 md was measured.

The method is sensitive because the flow rate through fractures is about 1000 to 2000 times higher than through solid rocks.

The method is suitable for establishing the physical condition of rock bolt holes and to monitor large underground openings. Effect of blasting on the rock mass can also be investigated by the vacuum method.

The measuring technique is simple, accurate, reliable and relatively inexpensive.

CONTENTS

	Page
ABSTRACT	i
INTRODUCTION	1
Review of the State-of-the-Art	2
Basic Concept of the Method	2
MATRIX PERMEABILITY	3
Permeability of Fractures	5
Permeability of Fractured Rock	6
FRACTURATION INDEX	8
Operating Principles	8
Sensitivity - Reliability	9
Safety Aspect of the System	12
Description of the System	12
MEASURING AND MONITORING PROCEDURE	18
Vacuum Test in CAN-MET Drift	21
Fracturation Profile Determination in the CAN-MET Drift	24
Permeability of Unfractured Rock	26
Response Test	27
Investigation of Blasting Effects	27
Leakage Test	28
Improvements and Modifications	28
VACUUM TEST IN THE SELECTED STOPE AT DENISON MINE	30
Fracturation Profile of the Test Stope	30
Correlation of the Fractures Between Holes	32
Roof Mapping by Vacuum Method	34
Roof Monitoring	39
Roof Stability	51
Development of Unstable Roofs	51
Immediate Roof Stability Evaluation	54
Main Roof Stability Evaluation	58
Stability of the Roof in the Test Stope	61
Formation Water Investigation	61
VACUUM TEST AT RIO ALGOM MINE	63
Description of the Test Stope	63
Fracturation Profile Logs	63

Correlation of Fractures 72
Interpretation of the Vacuum Test 72
ROOF STABILITY OF THE TIO ALGOM TEST STOPE 79
UTILIZATION OF CONVECTRON TYPE VACUUM GAUGES 81
CORRELATION OF LARGE FRACTURES BY USING CO_2 82
AIR PERMEABILITY - WATER PERMEABILITY 82
POSSIBLE FURTHER APPLICATION OF THE METHOD 84
CONCLUSIONS 86
ACKNOWLEDGEMENTS 87
REFERENCES 88
GLOSSARY OF TERMS USED IN CONNECTION WITH THE VACUUM METHOD 89
APPENDIX A - Fracturation Profile Log of Can-Met Drift A-91
APPENDIX B - Matrix Permeability Determination - Basic Information .. B-92
APPENDIX C - Matrix Permeability Determination - Calculation C-93
APPENDIX D - Fracturation Profile Log of Hole No. 231-74 ..... D-94
APPENDIX E - Fracturation Profile Log of Hole No. 231-76 ..... E-95
APPENDIX F - Observation Sheet of Hole No. 231-71 ..... F-96
APPENDIX G - Observation Sheet of Hole No. 231-73 ..... G-97
APPENDIX H - Observation Sheet of Hole No. 231-75 ..... H-98
APPENDIX I - Observation Sheet of Hole No. 231-77 ..... I-99
APPENDIX J - Observation Sheet of Hole No. 231-78 ..... J-100
APPENDIX K - Observation Sheet of Hole No. 231-80 ..... K-101
APPENDIX L - Fracturation Profile Log - Hole No. VH-1 ..... L-102
APPENDIX M - Fracturation Profile Log - Hole No. VH-3 ..... M-103
APPENDIX N - Fracturation Profile Log - Hole No. VH-4 ..... N-104
APPENDIX O - Fracturation Profile Log - Hole No. VH-9 ..... O-105
APPENDIX P - Fracturation Profile Log - Hole No. VH-11 ..... P-106

FIGURES

No.

1. Calculation of the permeability of fractured rock 7
2. Air flow through solid and fractured rock 10
3. Relationshik between the width and permeability of a fracture .. 11
4. Instrumentation - test stope 13
5. Instrumentation - measuring station 14
6. DEK-type straddle packer 16

7. DEK-type observation packer 17
8. Typical drilling pattern for roof monitoring holes 22
9. Location map of CAN-MET drift 23
10. Drilling pattern for vacuum test holes in CAN-MET drift 25
11. Location of fractures in the test stope's roof 31
12. Arrangement of the fracture correlation test 33
13. Areal extension of fracture B 36
14. Areal extension of fracture C 37
15. Areal extension of fracture D 38
16. Hole construction for roof monitoring 40
17. General arrangement of the roof monitoring 41
18. Effect of the first blasting 44
19. Effect of the first pneumatic fracturing 45
20. Effect of the second blasting 46
21. Effect of the third blasting 47
22. Effect of the second pneumatic fracturing 48
23. Typical mine roof 53
24. Development of coffin roof, parallel to the stope 55
25. Development of coffin roof, perpendicular to the stope 56
26. Sketch of the coffin type for stability calculation 59
27. A typical relative permeability - saturation relationship 62
28. Layout of the Rio Algom test stope 64
29. Vacuum hole transmissibility graph. Hole: VH-1 67
30. Vacuum hole transmissibility graph. Hole: VH-3 68
31. Vacuum hole transmissibility graph. Hole: VH-4 69
32. Vacuum hole transmissibility graph. Hole: VH-9 70
33. Vacuum hole transmissibility graph. Hole: VH-11 71
34. Cross-section A-A. R.A. 847 stope 73
35. Cross-section B-B. R.A. 847 stope 74
36. Cross-section C-C. R.A. 847 stope 75
37. Cross-section D-D. R.A. 847 stope 76
38. Cross-section of the 847 stope for roof stability calculation .. 80
39. Correlation of large fracture by using CO_2 83
40. Equivalent liquid permeability determination 85

INTRODUCTION

A comprehensive test program has been conducted with the vacuum method to establish the fracturation conditions of mine roofs in Denison Mine and Rio Algom Mines at Elliot Lake, Ontario.

The main objective of this report is to present a detailed account of the tests conducted at these mines.

The state-of-the-art for detecting fractures and unstable conditions in mine roofs is reviewed briefly. The vacuum method represents a novel approach to the problem of evaluating the stability of the mine roof.

The basic concept and the operating principles of the vacuum method are reviewed briefly.

It was realized that the determination of the permeability of hard rocks, especially in fractured conditions, is a fairly specialized field but it is the basis of the vacuum method.

For this reason the units and terms used in connection with the problem are presented in a glossary and discussed within the scope of the report.

The developed method being unique and unorthodox it is necessary to discuss in detail the instrumentation and measuring technique for detecting and monitoring fractures in mine roofs.

The sensitivity, reliability and safety aspect of the measuring technique are also discussed in the report. The theoretical aspects of the development of unstable roof conditions and the evaluation of roof stability are presented.

The economy and the further application of the vacuum method are discussed briefly.

REVIEW OF THE STATE-OF-THE-ART

Fractures present in the mine roof have a paramount effect on its stability. Accurate knowledge of the location, width, dip, strike and areal extension of the fracture is necessary to evaluate the stability and safety of the roof.

Predicting areas of imminent roof falls and determining the size and shape of the unstable area are the key factors of effective roof control because standard engineering methods could be used either to support the unstable area or blast it down.

In reality, fatal roof collapse may happen when all safety regulations as stipulated by mining law are meticulously and scrupulously observed by the workers and enforced by the mine operator.

It is not surprising, therefore, that visual inspection and the sounding of the rock with scaling bars, commonly used since the earliest days of mining, are the best methods available today to detect loose rocks (1).

The miner is the only industrial worker in our technologically advanced society who is working under a roof of completely unknown stability. The vacuum method applying so far unutilized rock properties can supply some information on roof stability and may advance the prediction of roof falls.

BASIC CONCEPT OF THE METHOD

The vacuum method uses the fluid transmitting property that is the permeability of the rock to establish the parameters of a fracture such as the location, width, dip, strike and the areal extension.

It is well known that the fluid transmitting capabilities of fractured rocks is about 1,000-2,000 times greater than that of massive rocks. Consequently, permeability can be used as a convenient parameter to establish the

fracture pattern.

The permeability of the rock as the best parameter for detecting fractures and correlating them between holes was not recognized before or used in connection with rock mechanics or ground control problems.

The novel feature of the method is to conduct the test with vacuum because it automatically prevents the dangerous pressure build-up in the fractured rock, which would occur with a pressure test.

A very simple air measuring system has been developed as the most practical method for detecting fractures in the roof and monitoring them during excavation.

Air was selected as a testing fluid because it can move more easily than water in very tight rocks due to its low viscosity. Viscosity of water = 1 cp, viscosity of air = 0.018 cp at room temperature.

For a better understanding of the operating principles of the system it is necessary to briefly review the theory of air movement in (1) porous media, (2) fractures, joints and separations, and (3) in fractured rocks themselves.

MATRIX PERMEABILITY

Media that allow the passage of fluid through them are said to be permeable. The commonly accepted units for permeability measurements are darcies and cm/sec. If pores and fractures are absent the fluid movement takes place through the solid rock and is called 'matrix permeability'. It is important to recognize that the matrix permeability represents the rock conditions before fracturation.

The absolute permeability (K) expresses the fluid transmitting capacity of the medium when the pore space is 100% saturated with the fluid

flowing in the medium.

The definition of the absolute permeability is given in the glossary.

Equations for calculating the absolute air permeability for linear and radial flow are as follows:

For linear air flow:

$$K = \frac{Q\ 2\mu\ L\ P}{A(P_1^2 - P_2^2)}$$

where: K = permeability - darcies

Q = flow rate cm^3/sec at 1 atm pressure and flowing temperature

μ = air viscosity cp

L = length of sample cm

A = cross section area cm^2

P_1 = upstream pressure, standard atm absolute

P_2 = downstream pressure, standard atm absolute

P = atmospheric pressure, standard atm.

For radial air flow:

$$K = \frac{0.3188\ Q\ \mu\ \ell n\ \frac{re}{rw}\ P}{h(P_e^2 - P_w^2)}$$

where, re = selected radius where the prevailing pressure is known, cm

rw = radius of hole, cm

h = thickness of the zone, cm

P_e = pressure at re, standard atm absolute

P_w = pressure at rw, standard atm absolute

ℓn = a logarithm to base e

The matrix permeability as mentioned previously is a very important physical parameter of the rock because it is used to establish the presence of fractures in the rock mass.

PERMEABILITY OF FRACTURES

It is well known that air moves more easily through fractures, joints, cracks and separation than through the matrix of the rock itself.

The permeability of such openings may be estimated roughly by using the formulae proposed by Buckingham (2). The formulae are:

For fractures:

$$K_F = 54 \times 10^6 \, W^2$$

For solution channels:

$$K_S = 20 \times 16^6 \, D^2$$

where: K_F = permeability of fracture in darcies

K_S = permeability of solution channel in darcies

W = width, in

D = diameter, in.

The short theoretical investigation has revealed the following significant facts in connection with fracture detection:

1. The permeability of a fracture is considerably higher than the matrix permeability of the rock generally encountered in underground mines.
2. The sharp contrast existing between the matrix and fracture permeability can be used to detect fractures in the roof and monitor them by simple air flow rate measurement.
3. The permeability of a fracture according to the equation increases with the second power of its width. Therefore, the enlargement of a fracture system, i.e., the deterioration of the stability of the roof is indicated by a rapid increment of its transmitting capacity.

PERMEABILITY OF FRACTURED ROCK

The characteristic feature of air flow through fractured rock is the simultaneous air migration through the matrix of the rock and the fractures present in the rock mass.

In order to calculate air flow through fractured rock, it is necessary to determine the average permeability of the fractured rock which expresses the combined transmitting capacity of the matrix and the fractures. The calculation formula is as follows:

$$K_{ER} = \frac{K_M A_M + K_F A_F}{A_M + A_F}$$

where: K_{ER} = permeability of fractured rock, md

K_M = matrix permeability, md

K_F = permeability of fracture, md

A_M = area of unfractured rock, cm^2

A_F = area of fracture, cm^2.

The calculation is illustrated with a numerical example on Fig. 1. The calculation has indicated that a 0.1 mm fracture in a 100 x 100 cm rock mass increases its original permeability of 0.1 md approximately 838 times. It is obvious that such a drastic increment can be easily detected with a simple and accurate flow rate measurement.

The main conclusion of the theoretical investigation is that fracturation drastically increases the fluid transmitting capability of otherwise very tight rocks, therefore, the permeability of the fractured rock directly expresses its fracturation condition.

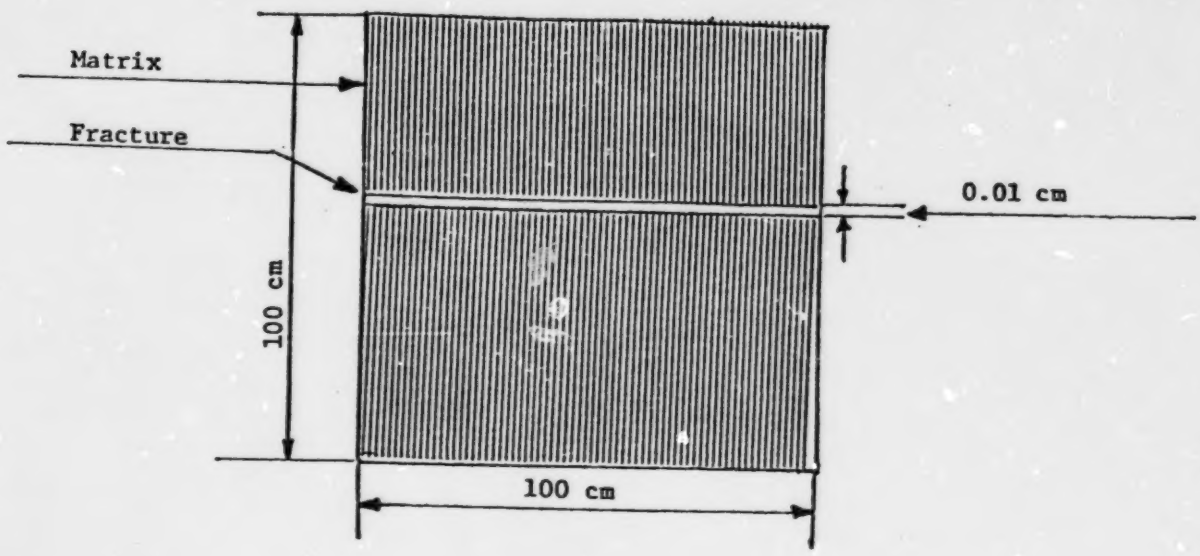

Basic information:

Matrix permeability: K_M = 0.1 md.
Permeability of fracture: K_F = 837,000 md.

Formula:

$$K_{FR} = \frac{K_M A_M + K_F A_F}{A_M + A_F}$$

where: K_{FR} = permeability of fractured rock, md
K_M = matrix permeability, md
K_F = fracture permeability, md
A_M = area of matrix, cm^2
A_F = area of fracture, cm^2

Therefore:

$$K_{FR} = \frac{0.1 \times 9{,}999 + 837{,}000 \times 1}{9{,}999 + 1} = 83.8 \text{ md}$$

and the fracturation index:

$$F = \frac{K_{FR}}{K_M} = \frac{83.8 \text{ md}}{0.1 \text{ md}} = 838$$

Fig. 1 - Calculation of the permeability of fractured rock.

FRACTURATION INDEX

In order to conveniently express the degree of the deterioration of the roof condition,the so called 'fracturation index' has been introduced.

The fracturation index is defined as the ratio between the permeability of a fractured rock and its matrix permeability. The formula expressing the relationship is:

$$F = \frac{K_{FR}}{K_M}$$

where: F = fracturation index, dimensionless

K_{FR} = permeability of fractured rock, md

K_M = matrix permeability of the same rock, md.

Therefore, the fracturation index can be conveniently used to express the roof condition and monitor its deterioration during excavation.

OPERATING PRINCIPLES

The vacuum method uses one hole as a vacuum hole and one or more holes for observation to establish the physical parameters of a fracture.

A straddle packer is installed at various depths in the vacuum hole then vacuum is created. In the case of a solid rock the vacuum in the hole will diminish very slowly. If a fracture is present, a definite flow rate can be measured. The continuity of the fracture between holes is established by observing the effect of the vacuum with a second straddle packer installed in the observation hole. By moving the packers in the holes and repeating the test, the exact location, dip, strike and areal extension of the fractures are established.

The equivalent fracture size is then calculated by the Darcy and Buckingham formulae using the measured flow rate and rock face pressure.

It is important to realize that if pneumatic or hydraulic pressure is

introduced to a parting or fracture present in the roof, the original load will be increased. It follows, that no method should be used for roof stability measurements which applies positive pressure. Even 1 atm pressure will create an extra load of 17 tons on a 4 ft x 4 ft roof area.

The vacuum method provides a profile of the fracture system in the rock mass under investigation, thus it is useful for the mapping of the roof.

SENSITIVITY - RELIABILITY

Sensitivity and reliability are the basic requirements for a detection system. The sensitivity is best illustrated by a simple example given in Fig. 2.

It is supposed that the fluid flowing through a solid rock block of 100 cm x 100 cm x 100 cm is 1 cm^3 per day.

If a fracture of 0.01 cm width develops in it, the fluid flow increases to 838 cm^3 per day.

Furthermore, if the 0.01 cm fracture widens to 0.02, the fluid flow through the rock will increase to 6704 cm^3 per day.

It is obvious that very simple instruments are able to detect such a drastic change in the flow rate.

The relationship between the width and the permeability of a fracture is presented in Fig. 3.

In situ underground tests have indicated that permeability as low as 0.003 md can be measured, and fractures of 0.5 to 1.0 mm width located at 6 to 8 m depth in the rock mass can be observed with a high degree of accuracy. The results obtained during testing are always reproducible.

The simplicity of the system is the guarantee for reliable and satisfactory service. The instruments have worked properly during the underground test at Denison and Rio Algom mines.

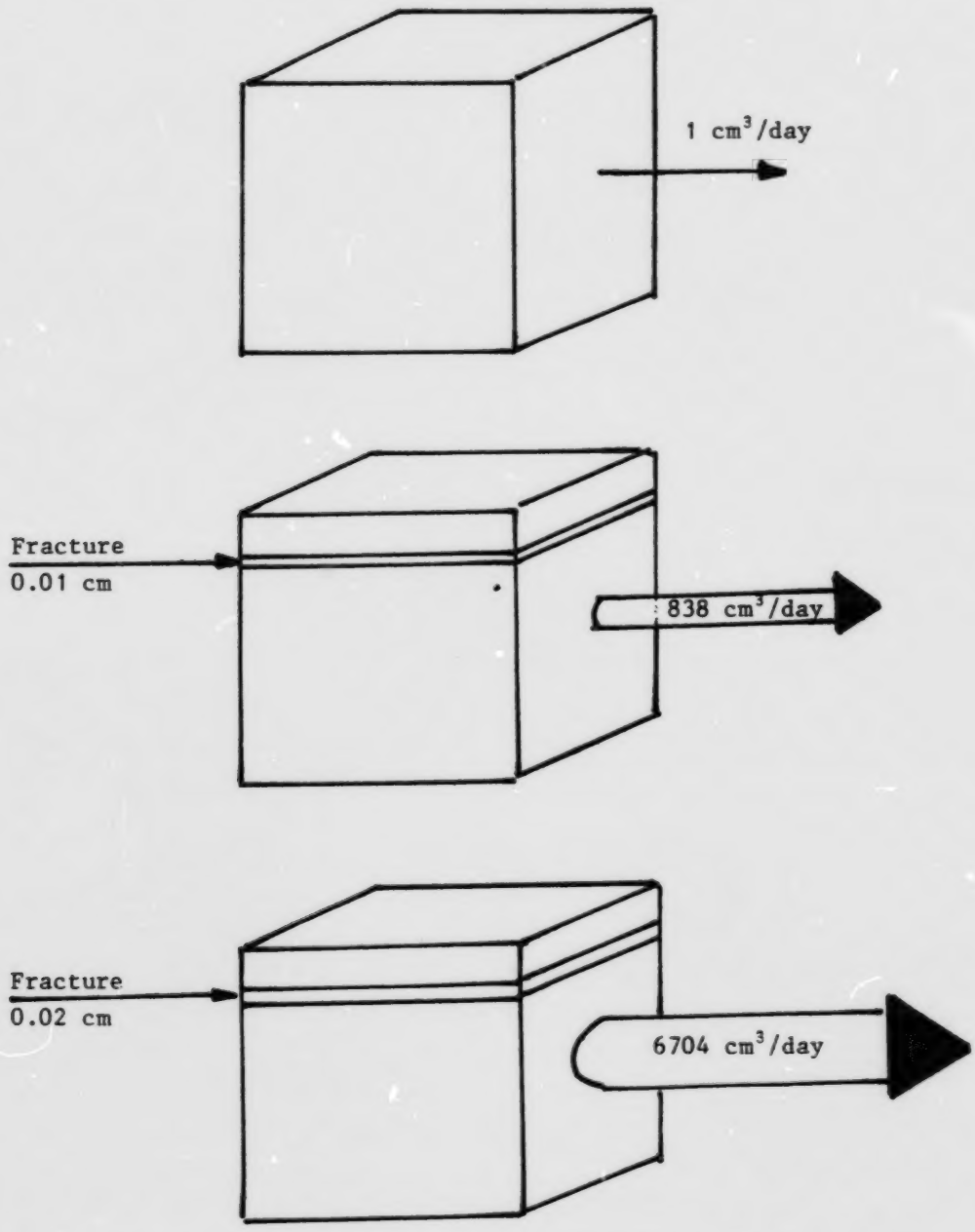

Dimension of the block 100 x 100 x 100 cm

Fig. 2 - Air flow through solid and fractured rock.

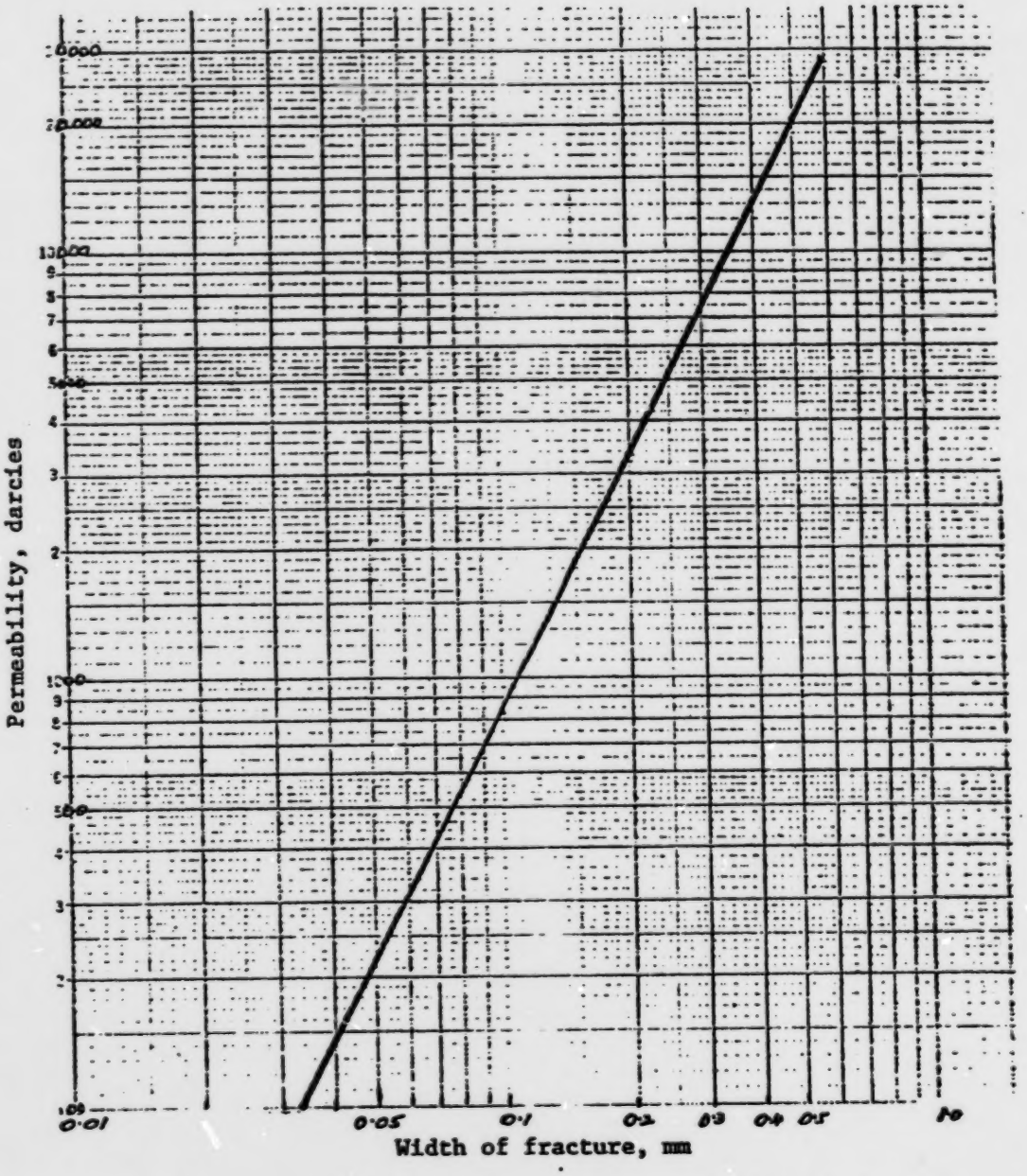

Matrix permeability of uranium ore = 0.0001 darcies

Fig. 3 - Relationship between the width and permeability of a fracture.

SAFETY ASPECT OF THE SYSTEM

Theoretically the developed system can utilize vacuum or compressed air for the investigation. However, it is important to realize that if a pneumatic or hydraulic pressure is introduced in the parting overlying a roof lamina an additional load will be imposed on the roof.

The formula to calculate the maximum tensile stress in this case, according to Obert and Duvall (3) is:

$$\sigma_{max} = \frac{\gamma S^2}{2t} + \frac{pS^2}{2t^2}$$

where: σ_{max} = maximum tensile stress

γ = unit weight of the rock

S = span of the stope

t = thickness of the immediate roof

p = pneumatic pressure.

DESCRIPTION OF THE SYSTEM

Schematic diagrams showing the general arrangement of the system in the stope and the measuring station are given in Fig. 4 and 5, respectively.

The vacuum system consists of:

A vacuum test hole

Observation holes

DEK-type mechanical straddle packers

DEK-type observation packers

Electrically operated vacuum pump and exhaust assembly

Flow meter assembly

Mercury and water manometers

Inclined manometer

Water traps

Stand and tubing spool

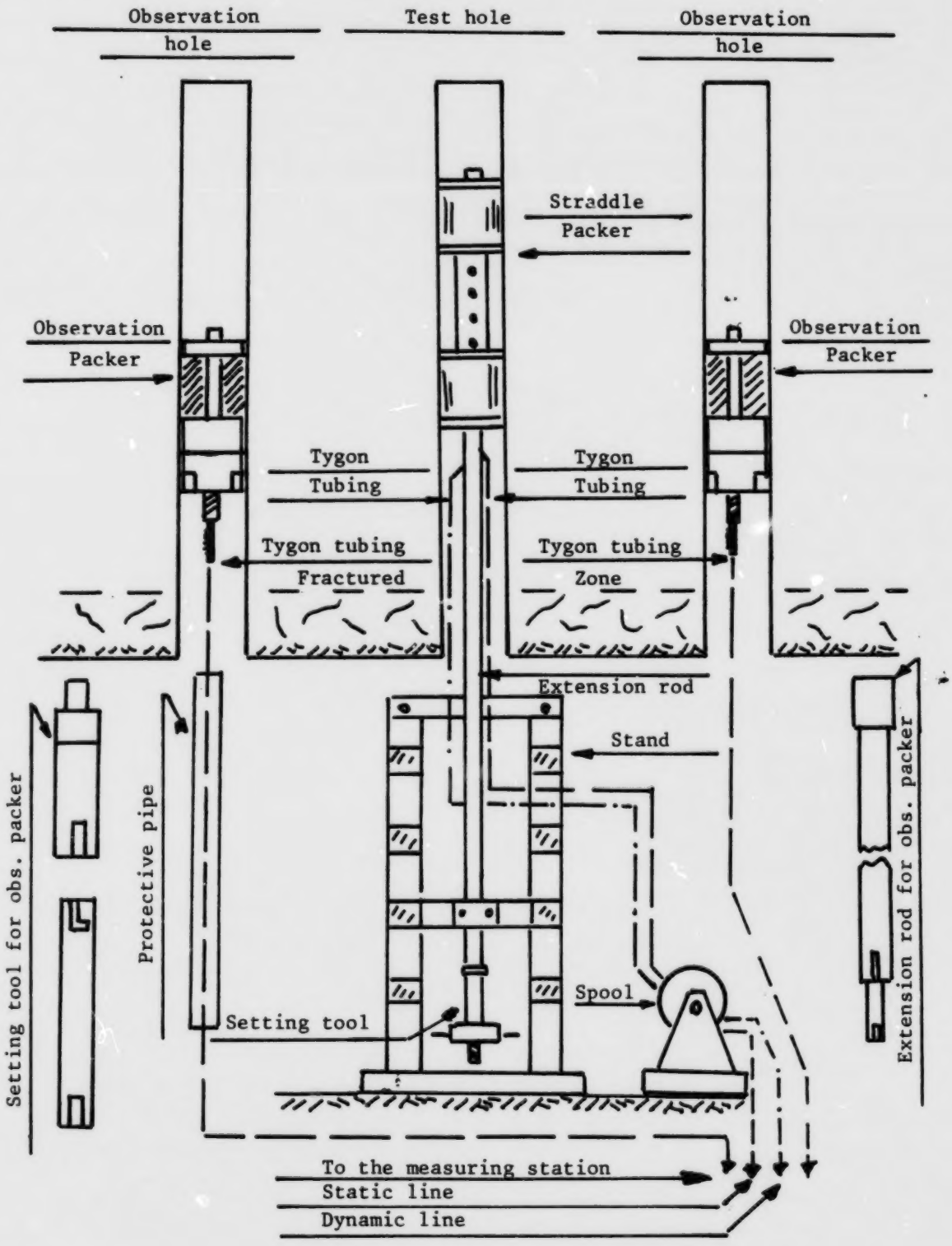

Fig. 4 - Instrumentation - test stope.

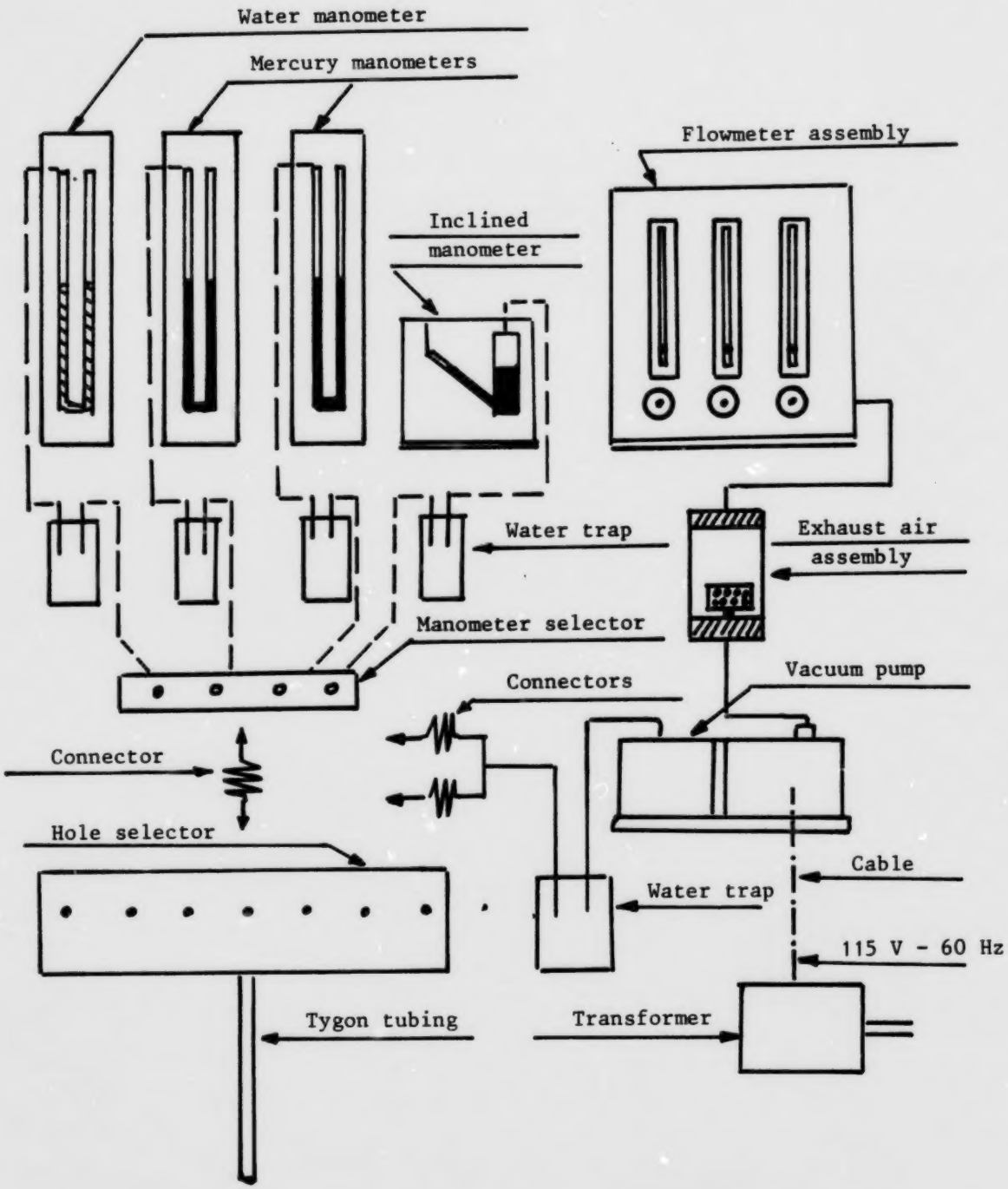

Fig. 5 - Instrumentation - measuring station.

Extension rods for straddle and observation packers.

Setting tool for observation packer.

Regular or longer rock bolt holes are used as vacuum test and observation holes.

A special effort was made to develop simple, but reliable packers, as the proper function of the packers is the key to the vacuum measurement. The main function of the straddle packer is to isolate the selected section in the hole during testing.

The packer, due to the special construction, measures the rock face pressure, i.e., the pressure between the sealing elements directly during testing, and the rock face pressure is used to calculate the permeability of the section.

The DEK-type straddle packer is the only vacuum packer capable of measuring the rock face pressure directly, see Fig. 6. The function of the observation packer is to close the hole in order to observe the effect of a vacuum created in the vacuum test hole, see Fig. 7. The observation packer can be installed at any depth in the hole by using the setting tool and extension rods. After the setting of the packer the setting tool and the extension rods are removed. It is obvious that blasting or other activities in the stope cannot damage the packer, because the only exposed part of the system is the tygon tubing which can be easily protected during blasting.

A very light, about 7.3 kg, SAR-VAC vacuum pump is used for the test.

The air flow rate, by utilizing the exhaust air assembly, is measured at atmospheric condition by Dwyer's variable area flow meter.

Mercury, water and inclined manometers were used to measure the vacuum during testing.

The introduction of Wallace and Tiernan dial vacuum gauges improves the mobility and utilization of high-vacuum thermistor gauge increases the accuracy and measuring range of the system considerably.

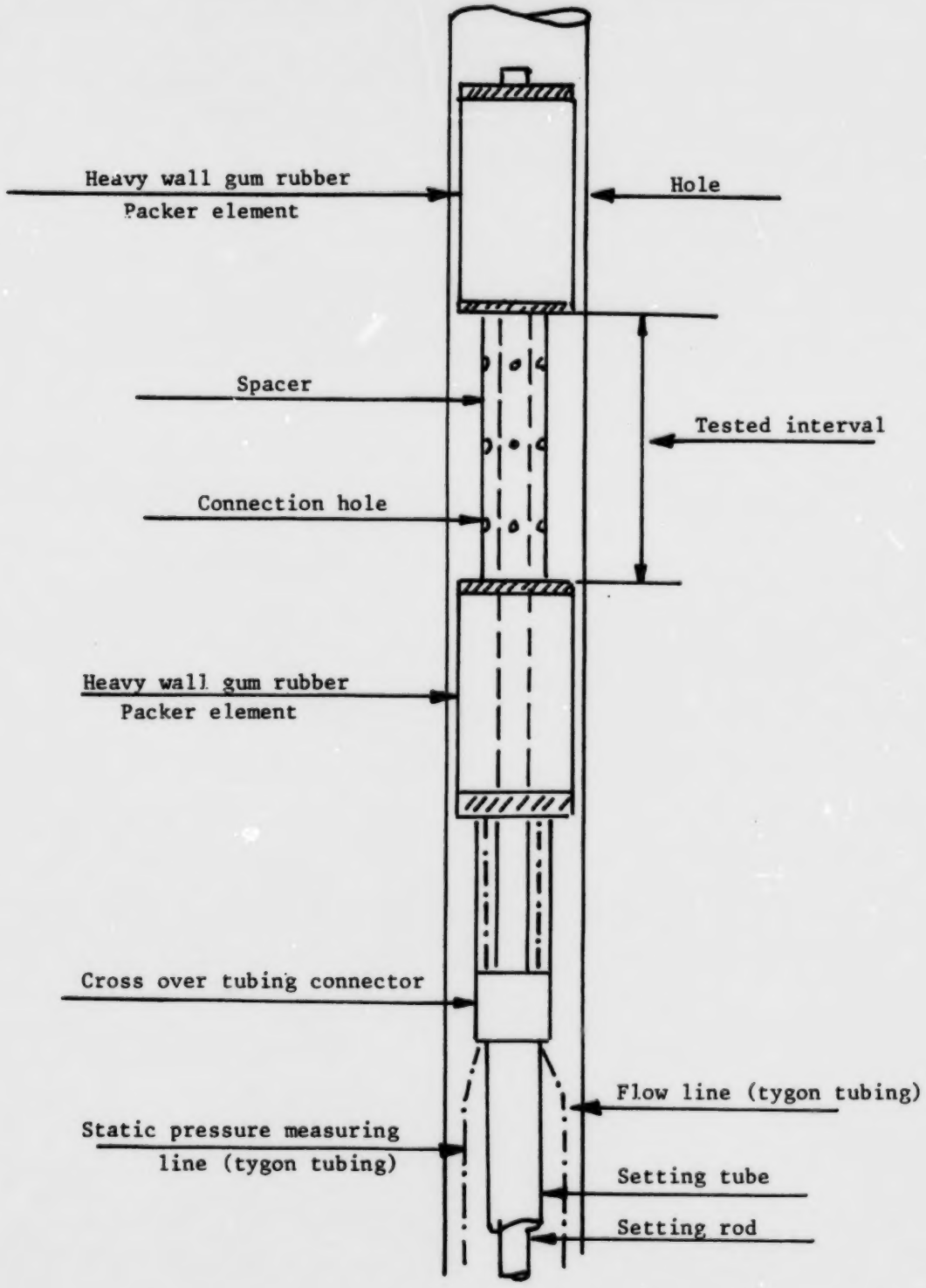

Fig. 6 - DEK-type straddle packer.

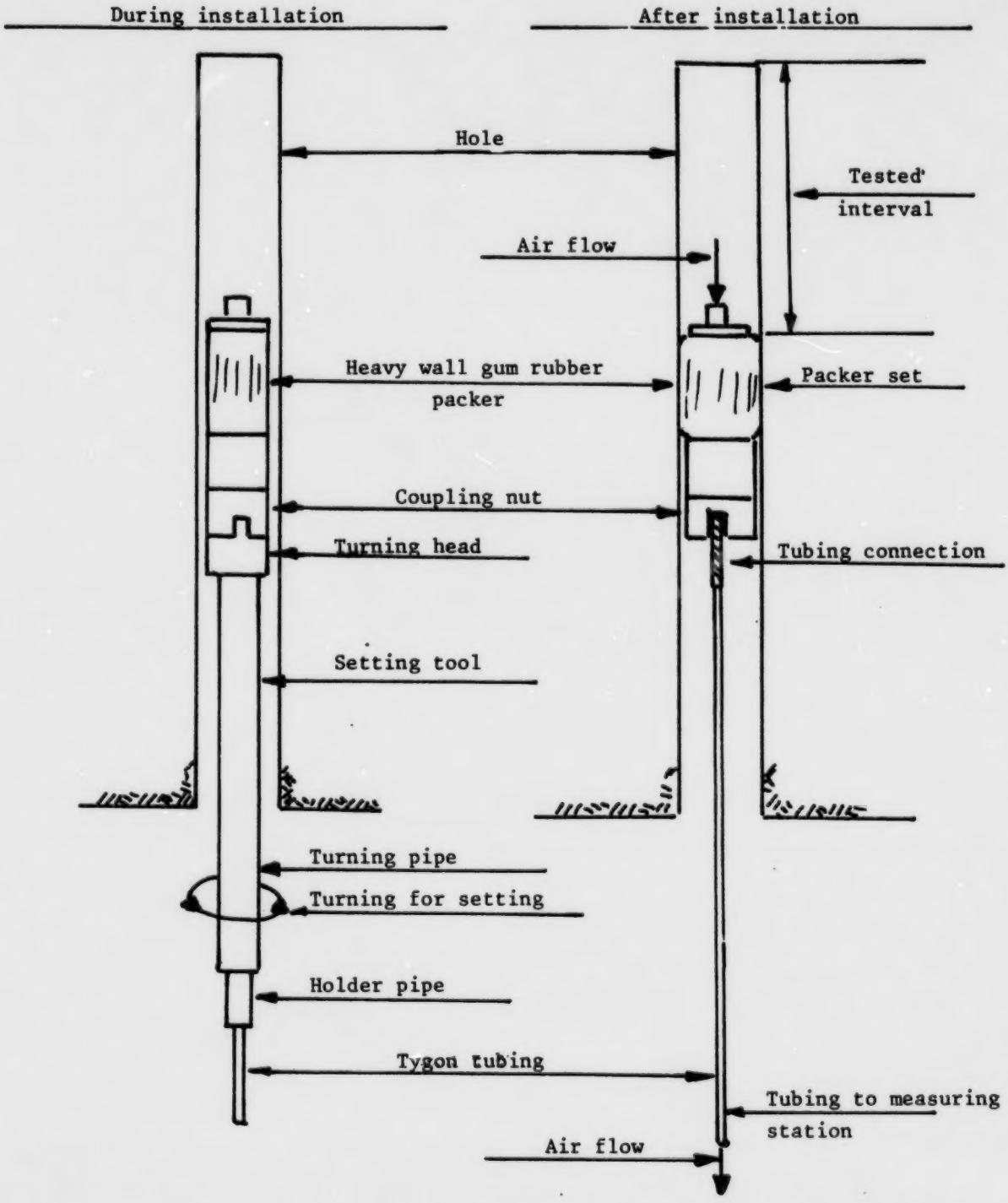

Fig. 7 - DEK-type observation packer

MEASURING AND MONITORING PROCEDURE

In order to establish the fracturation condition and the stability of the roof in the test stope, three measuring techniques were used, namely:

Fracture profile determination

Roof mapping

Monitoring the roof condition.

The main objective of the fracture profile determination is to provide information about the location and size of the fractures, if present, in the roof. A straddle packer with a 25 cm measuring distance is used for the test. By moving the packer in the hole and repeating the test, the location, permeability, size of fracture and the permeability of the unfractured rock are established.

The flow-rate and the pressure difference creating the flow are measured simultaneously during testing and the information obtained is used to calculate the permeability of the zone under investigation and estimate the size of the fracture, if present.

In the case of fracture the flow-rate can be directly measured by using a variable area type flowmeter. However, the flow through unfractured rock is very small and cannot be measured by any commercially available flowmeter.

In this case the flow-rate is indirectly measured by observing the absolute pressure change in a closed system and the volume of air entering is calculated by using Boyle's law.

The paramount advantage of the vacuum method is that the vacuum change of 1 millitorr (0.001 mm of Hg) in the closed system can be conveniently measured with a high-vacuum gauge. Therefore it is possible to measure air flow rates as low as 2×10^{-5} cm^3/min with the system.

The formula to calculate the flow-rate is:

$$Q = \frac{(H_1 - H_2)\ 520\ V}{760\ t(460 + T_f)}$$

where: Q = flow rate, cm^3/min

H_1-H_2 = vacuum, Torr, at the start and end of observation period

t = length of observation period, min

T_f = air temperature in the system, °F.

V = volume of the closed system, cm^3.

It is supposed that for a short period the barometric pressure and the air temperature in the closed system are constant.

After the determination of the flow rate the permeability of the rock is calculated by using Darcy's Equation for radial gas flow:

$$K = \frac{Q\ \mu\ \ln \frac{re}{rw}\ T_f\ 14.65}{10329\ h(P_e^2 - P_w^2)}$$

where: K = darcies

Q = cu ft/day at 60°F and 1 atm

h = ft

μ = cp at flowing temperature

P_e, P_w = psi a

r_e, r_w = ft

T_f = °R flowing temperature in the rock.

In the case of fractured rock the transmissibility of the test interval is calculated:

$$T = Kh\ \frac{Q\ \mu\ \ln \frac{re}{rw}\ Tf\ 14.65}{10320\ (P_e^2 - P_w^2)}$$

where: T = transmissibility, darcy/ft.

Neglecting the flow through the matrix the 'equivalent fracture size' can be estimated by using the following formula:

$$W = \sqrt[3]{\frac{12T}{54 \times 10^6}}$$

where: W = width of the fracture, in

T = transmissibility, darcy/ft.

The main objective of the roof mapping is to determine the basic parameters of the fracture, such as the dip, strike and areal extension.

The continuity of the fracture between holes is established by observing the effect of the vacuum with a second straddle packer installed in the adjacent observation hole.

Utilizing more observation holes drilled according to a proper pattern the areal extension of the fracture is established.

The roof monitoring has three basic functions, namely to:

a) detect the widening of the fractures already present in the roof

b) observe any change in the areal extension of the fracture

c) observe the development of any new fracture.

It is obvious that unchanged pneumatic parameters indicate unchanged physical roof condition and vice versa. Therefore, the roof monitoring in an active stope requires the drilling of the necessary observation holes to conduct the vacuum test and repeat the test at predetermined intervals.

The increased flow rate is used to establish the deterioration of the roof. The formula to estimate the relative widening of the fracture using the original fracture width as a unit is:

$$F = \frac{W_i}{W_o} = \sqrt[3]{\frac{Q_i}{Q_o}}$$

where: F = fracture size ratio

W_i = increased fracture size

W_o = original fracture size

Q_i = increased flow-rate

Q_o = original flow-rate.

Especially designed observation packers are used for monitoring which

cannot be damaged by blasting or by other activities at the working face, see Fig. 7. The packer can be removed after the completion of the work.

A typical drilling pattern for roof monitoring holes is presented in Fig. 8.

It is important to realize that according to Dr. D.G.F. Hedley's (4) previous investigation only 1-2% roof area represents unstable roof conditions in the Elliot Lake mining area. Consequently, it is very restrictive to conduct elaborate testing, but overlooking such an area can be fatal.

VACUUM TEST IN CAN-MET DRIFT

The vacuum method has been developed in connection with potash mining, where the physical condition of the salt roof differs considerably from the roof conditions encountered in hard rock mines.

Generally, the salt provides ideal mining conditions, but fractures, cracks, faults and other mechanical discontinuities can easily develop in the hard rock mass.

Cores obtained from diamond drilling in Denison Mine exhibit a very large number of fractures which could be interpreted as an indication of a very fractured roof.

It was realized that in a fractured roof, as is indicated by the cores, the vacuum method cannot be used. For this reason it was decided to conduct a short test in a drift in order to:

1) check the actual rock condition in Denison Mine,
2) establish the applicability of the vacuum method under such rock conditions before the commencement of the actual test program in the selected stope.

The so-called 'CAN-MET Drift' was selected to conduct the first test with the vacuum method. The location map showing the test site is attached, see Fig. 9.

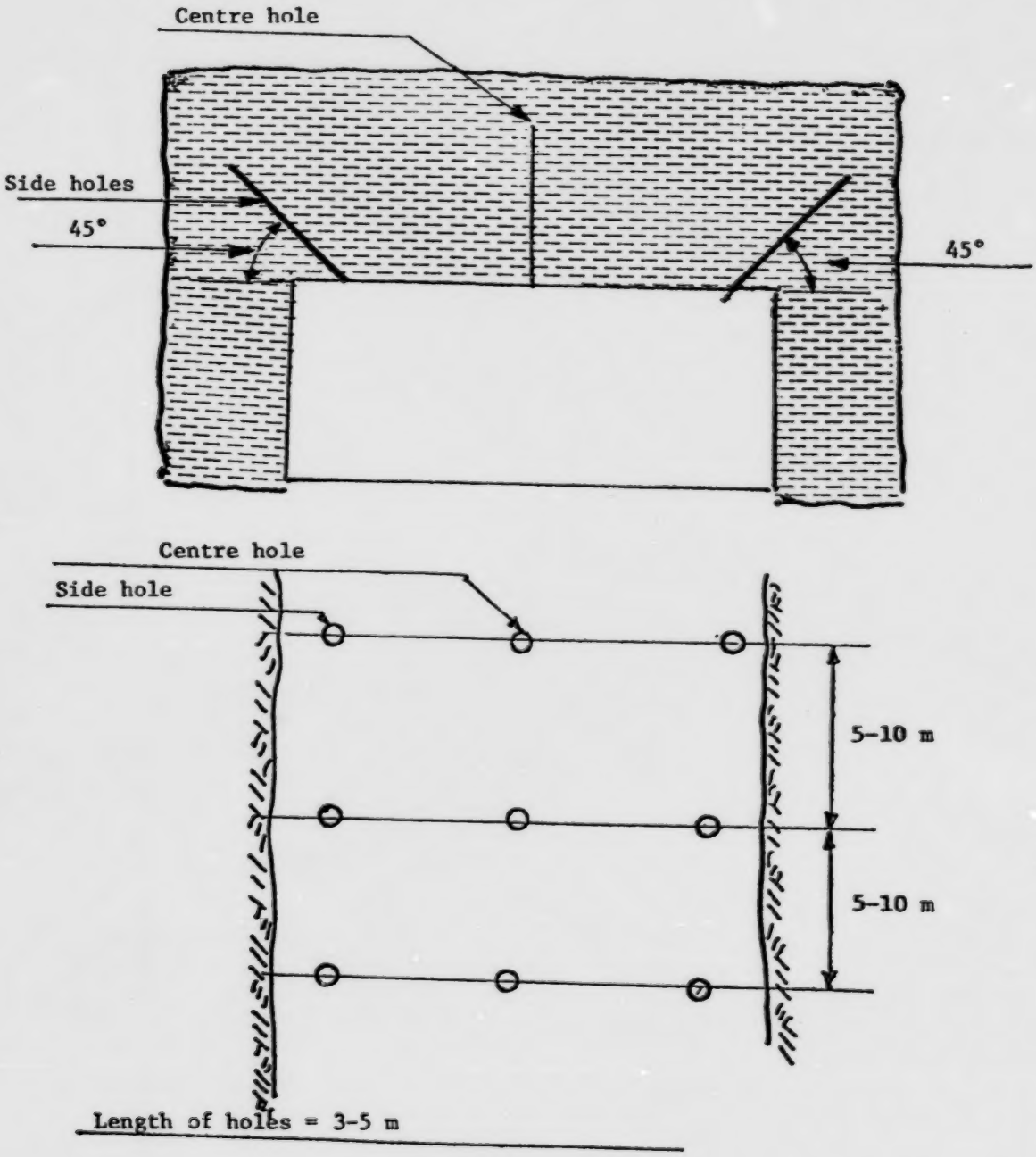

Fig. 8 - Typical drilling pattern for roof monitoring holes.

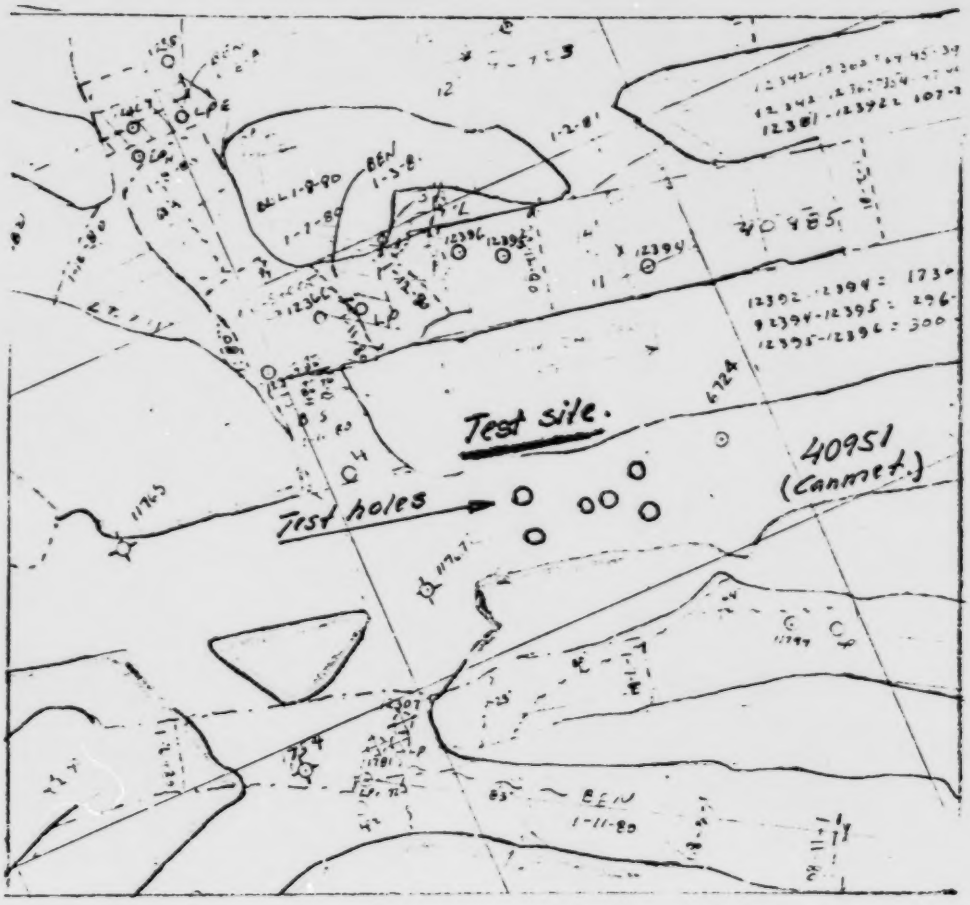

Scale 1" = 40 ft.

Fig. 9 - Location map of CAN-MET drift.

Six EX-holes drilled and cored in the roof were used for the test to establish the pneumatic characteristics of the rock in Denison Mine, see Fig. 10.

Furthermore, the tests conducted between March 18-31, 1981 provided an excellent opportunity to check the developed packers, instruments and vacuum pump arrangement under actual mining conditions.

As a result of the preliminary test some of the equipment was modified and the measuring technique improved. The results of the vacuum tests conducted in the CAN-MET Drift are briefly discussed in the following chapters.

FRACTURATION PROFILE DETERMINATION IN THE CAN-MET DRIFT

No. 6 test hole in the CAN-MET drift has been used to determine the fracturation profile of the roof.

A straddle packer was installed in the hole and a 25 cm length of the hole was sealed off with the packer and exposed to a pressure difference of about 630-650 Torr or 63-65 cm Hg. The pressure loss in the closed system was observed for a 10 min period. If the pressure loss was less than 8 Torr per 10 min, the section was considered tight.

By moving the packer in the hole and repeating the test, the fracturation profile of the roof was established. No effort was made to calculate the permeability of the separate sections. The result of the test is presented in Appendix A.

The fracturation condition of the other holes were established by using only observation packer. The results of the investigation are:

No. of Hole	Length of Investigated Interval	Differential Pressure in Torr	Vacuum Loss Torr per 10 min	Interpretation
1	20 ft	650	5	No fracture, tight rock
2	20 ft	630	4	No fracture, tight rock
3	20 ft	635	6	No fracture, tight rock
4	20 ft	643	4	No fracture, tight rock
5	20 ft	638	4	No fracture, tight rock

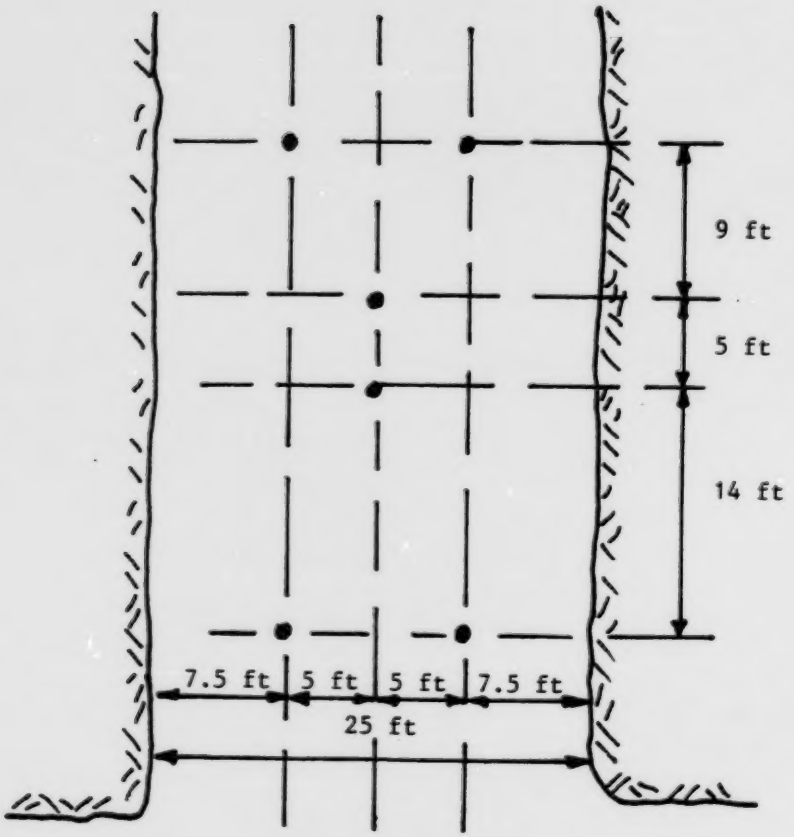

Type of hole: EX
Direction of hole: vertical
Length of holes: 25 ft (approx)
Hole size: ϕ 1.845 in = 37.72 mm

Fig. 10 - Drilling pattern for vacuum test holes in CAN-MET drift.

The investigation has indicated that the roof is very competent and no fractures are present in the roof despite the fact that the cores obtained from the holes exhibit fractures and separations. Furthermore, according to the test the thickness of the fractured zone due to blasting is about 40-60 cm.

PERMEABILITY OF UNFRACTURED ROCK

In order to evaluate the fracturation condition of the roof, it is necessary to know the permeability of the unfractured rock. The permeability of the unfractured rock is generally called the matrix permeability of the rock.

It was realized, based on the experience obtained during the fracturation profile determination, that the developed system is capable of conveniently measuring the in situ permeability of the unfractured rock with a high degree of accuracy.

No. 5 test hole in the CAN-MET drift has been used for the test. The general arrangement of the test and the pertinent information are shown in Appendices B and C.

According to the measurement the air permeability of the unfractured rock is: K_M = 0.002 millidarcies

In order to check the reliability of the measuring technique the measured matrix permeability was compared with the published permeability value of the quartzite and with the permeability of three quartzite core samples measured in the Elliot Lake Laboratory, using a helium permeameter.

The following tabulation is presenting the data for comparison.

Rock Type	Permeability of Unfractured Rock	Source
Quartzite	0.0020 md	In situ test at Denison
Quartzite	0.0019 md	Stuart, Brown and Rhodetiamel
Quartzite # 1	0.0035 md	Elliot Lake Lab, de Korompay
Quartzite # 2	0.0068 md	Elliot Lake Lab, de Korompay
Quartzite # 2	0.0095 md	Elliot Lake Lab, de Korompay

The general agreement between the magnitude of the permeability values is good. This fact indicates the feasibility of the method. It is important to realize that the test was conducted in the Elliot Lake Laboratory using helium and 'oven dry' samples, but during the in situ test in the CAN-MET drift the rock was in its original moist condition.

It is well known that the presence of a very small amount of water reduces the air permeability of the rock considerably. It is believed that in this case the water content influenced the measurements. The main conclusion of the investigation is that the permeability of the unfractured rock is very low, consequently a hole without fracture can hold a vacuum for a long period.

RESPONSE TEST

In order to establish the continuity of the fracture between holes it is necessary to observe the effect of the vacuum with a second packer installed in the adjacent hole.

A test was conducted by utilizing No. 4 hole as a vacuum hole and the effect of the vacuum was observed in the adjacent holes by using observation packers.

Despite the 700 Torr of vacuum created in No. 4 hole and the short distance between holes, no response was observe indicating the absence of horizontal fractures in the roof.

INVESTIGATION OF BLASTING EFFECTS

It is well known that a definite fractured zone will develop around an underground opening if blasting is used for excavation. Therefore it is very important to install the packers beyond this zone.

The thickness and the degree of fractures in the affected zone are directly related to the blasting technique used. It is possible, therefore, to

use the depth and permeability of this fractured zone as parameters to compare the effects of different blasting techniques.

An effort was made to establish the thickness of the fractured zone in the test holes. The investigation has indicated that the depth of the affected zone is about 40-60 cm.

LEAKAGE TEST

Small leakage in the system can falsify the vacuum measurement considerably. However, it is important to realize that any leakage always indicates a more dangerous situation than it actually is.

Checking the proper sealing of the equipment on the spot is very simple and only the packers installed in the hole require a different testing technique.

The airtight separation of the selected zone by packers during the test is of vital importance.

A simple method has been developed for checking the sealing performance of the packer installed in the hole.

It is necessary to measure only the flow rate under different packer pressures. When the flow rate remains constant at increasing packer pressure, this is the indication that no flow takes place at the contact of the rock and the packer elements. Therefore, the sealing performance of the packer in place can be conveniently established.

IMPROVEMENTS AND MODIFICATIONS

The vacuum measurement in the CAN-MET drift was the first full scale underground test conducted in a hard rock mine with the vacuum method.

The underground testing program has indicated that the air flow rate can be conveniently measured during testing.

The simultaneous flow rate and pressure measurements provide the necessary

information to calculate the permeability of the zone and estimate the size of the fracture, which were the final goals of the vacuum method.

However, to measure the air flow rate under negative pressure with a variable area flowmeter presents a very serious problem because of the large fluctuation of the float. The utilization of the conversion curves influences the accuracy of the measurement.

In order to solve the problem the vacuum pump was modified and the exhaust air at atmospheric condition was measured. A specially designed exhaust filter eliminates the oil mist from the air before entering the flowmeter. After the modification the flow rate was measured very accurately.

The testing programs conducted in the CAN-MET drift and in the selected stope require minimum mobility for the equipment, consequently mercury and water manometers were used as the simplest solution to measure the vacuum. However, it was realized that proper mobility is essential if the method is to be considered for roof monitoring. In order to eliminate the very cumbersome underground transportation of the mercury and water manometers, very accurate vacuum gauges should be used.

It was realized that with the introduction of high-vacuum thermistor gauges the vacuum method is capable of measuring permeability in situ as low as 1×10^{-11} darcies, which is necessary in connection with underground nuclear waste disposal.

VACUUM TEST IN THE SELECTED STOPE AT DENISON MINE

The 26060 - 26064 stope was selected to conduct the vacuum test simultaneously with other roof monitoring methods. The objectives of the vacuum test were to:

1. locate fractures, if present in the roof;
2. establish the continuity of the fracture between holes, using the method;
3. determine the fracture parameters, such as the location, width, dip, strike and the areal extension (roof mapping);
4. estimate the deterioration of the roof;
5. monitor the effect of blasting and air fracturing.

FRACTURATION PROFILE OF THE TEST STOPE

Number 231-74 and 231-76 test holes have been used to determine the fracturation profile of the roof in the test stope. A DEK - 1.5 in straddle packer with 25 cm testing interval was used for the test, see Fig. 6.

The measuring technique discussed in a previous chapter was used to determine the fracturation condition of the roof. The results of the investigation are presented in Appendices D and E.

The permeability and transmissibility of the rock and the 'equivalent fracture size' were calculated suing the formula given previously.

The location of the major fractures are shown on the geological cross-section of the test stope, see Fig. 11.

The main conclusions of the investigation are:

1. Four major fractural zones are present in the roof.
2. Air flow through the fractured zone was about 4000 times higher than through unfractured rock.
3. Estimated width of the fractures present in the roof is in the range of about 0.03 mm to 0.5 mm.

Scale: 1 in = 10 ft

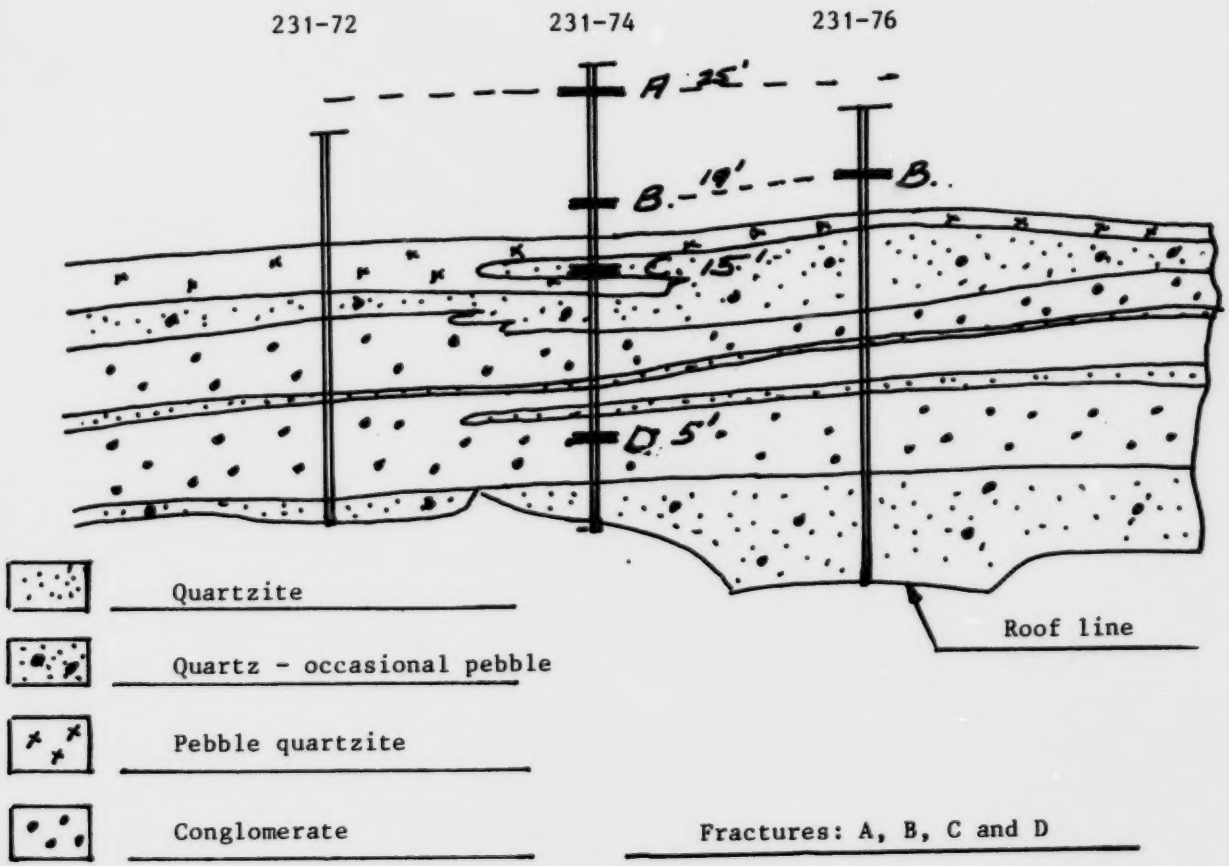

Fig. 11 - Location of fractures in the test stope's roof.

4. The positionsof Fracture A and B are practically horizontal, i.e., Dip = 0°.
5. The position of Fracture D corresponds to the end of the installed rockbolts.
6. Approximately 40 to 50 cm of the rock adjacent to the roof is affected by the blasting. However, according to the permeability measurement only hairline fractures developed in the zone.
7. One metre section of the roof section between Fracture D and the fractured rock E is very competent and may act as a self supporting beam.

CORRELATION OF THE FRACTURES BETWEEN HOLES

A short investigation has revealed that the roof stability depends entirely on the configuration of the fracture present in the roof. In other words, a large fracture developed parallel with the roof, but beyond the self-supporting beam's thickness may not affect its stability. However, a very small, but dipping separation may create an unstable roof condition.

It is obvious that no meaningful relationship exists between the width of a fracture, that is the permeability and the stability of the roof.

In order to evaluate the roof stability, intimate knowledge is necessary about the location, dip, strike and areal extension of the fracture. It can be seen that the proper correlation needed to establish the continuity of a fracture between adjacent holes is a basic requirement for proper roof control.

Realizing the practical importance of the problem a special effort was made to check the correlation ability of the vacuum system. The general arrangement of the correlation test is shown on Fig. 12.

Fracture 'B' in Hole No. 231-76 was sealed by a DEK-1.5 in straddle packer and the created vacuum was observed in the adjacent holes, using observation packers. The results are as follows:

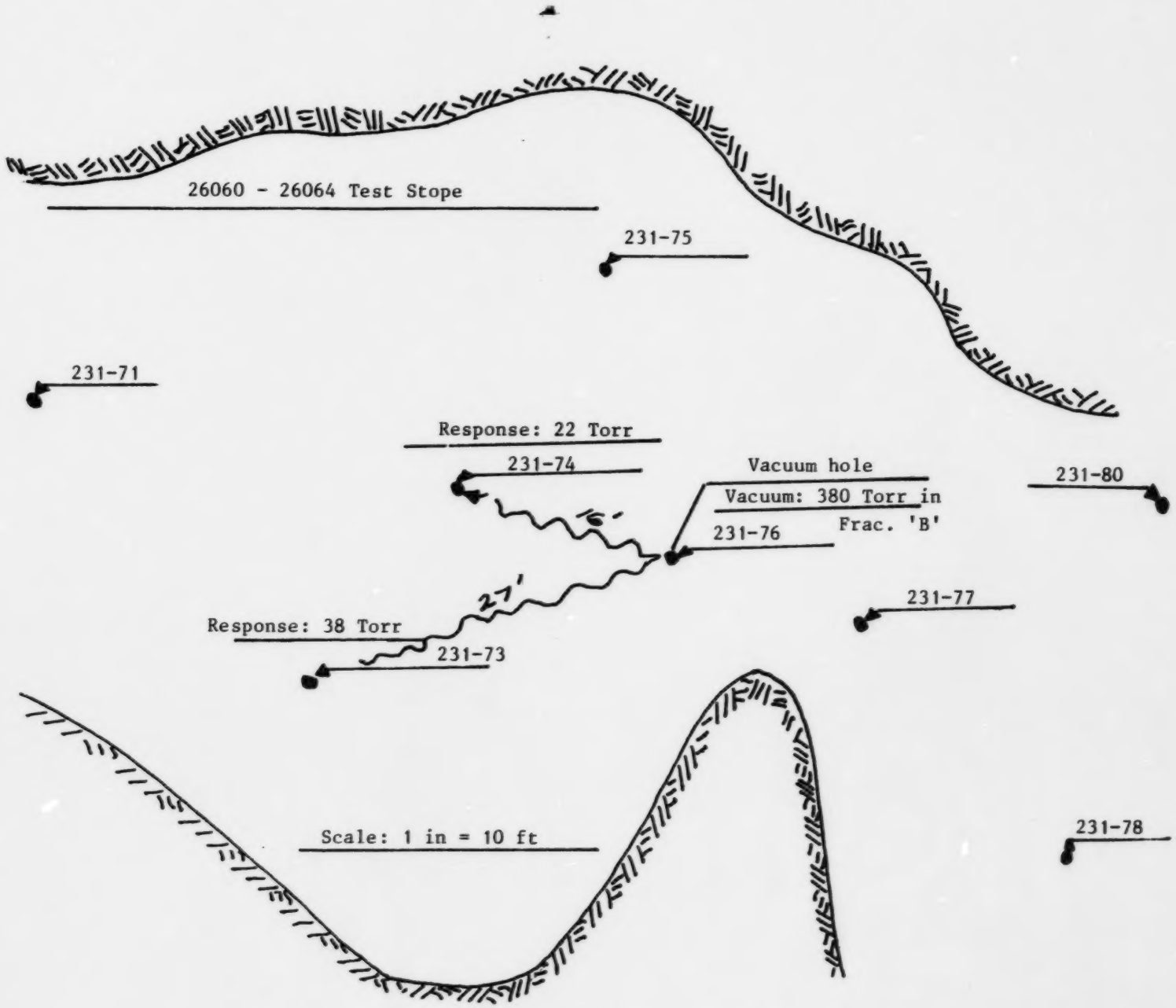

Fig. 12 - Arrangement of the fracture correlation test.

Vacuum Hole No. 231-76

Created vacuum in Fracture 'B' = 380 Torr.

Observation Hole No. 231-73

Observed response in the hole = 38 Torr.

Distance between Vacuum-Obs. hole = 27 ft.

Observation Hole No. 231-74

Observed response in the hole = 22 Torr.

Distance between Vacuum-Obs hole = 16 ft.

The test has indicated that the effect of moderate vacuum can be observed in wells situated 16 to 27 ft from the vacuum hole.

Furthermore, the measurement has revealed that the width of Fracture 'B' is not uniform.

ROOF MAPPING BY VACUUM METHOD

For routine roof control the mine operator generally uses the so-called 'Roof Mapping', which incorporates such activities as the visual inspection of the roof, sounding of the rock with scaling bar, mapping the visible faults and separations and examining and evaluating the pertinent core samples.

Where joints or faults do not intersect the roof line they are easily missed, whereas roof mapping by vacuum does provide the necessary fracture parameters, such as the location, width, dip, strike and areal extension.

Determining the size and shape of the unstable area is the key factor in effective roof control, as standard engineering methods can be used, either to support the unstable area or blast it down.

In order to demonstrate the feasibility of the vacuum method a roof mapping test has been conducted in the test stope as a very important part of testing program.

However, the conducted test must be considered only as a demonstration

of the measuring technique, because the roof mapping was not completed due to the lack of the second set of straddle packers, limited manpower and time.

Two vacuum holes and six observation holes were used for the test. According to the fracturation profile log, four major fractured zones, namely A, B, C and D, have been recognized. The deepest Fracture A was not intercepted by any of the observation holes, consequently the areal extension of it is unknown. However, lack of interception by the observation holes suggests that Fracture A is a horizontal fracture.

The areal extensions of Fractures B, C and D are presented in Fig. 13, 14 and 15, respectively. Furthermore, the limited information obtained from Hole No. 231-74 and No. 231-76 indicates that Fracture B is also a horizontal fracture. No direct information was available to determine the dip of Fracture C and D. However, the absence of any fracture strike in the roof suggests that fractures C and D are running parallel with the mine roof. The observed very similar fractures are developed around the centre of the stope, where the resistance against bending is minimum. This fact may indicate that the fractures were created by the sagging of the roof.

As a practical result the roof mapping indicated a very tight and competent immediate roof, which is self supporting. Based on this information it was predicted that the roof will not collapse after blasting off the rock bolts. The actual test has indicated the correctness of the prediction.

The main conclusions of the test are:

1. The width of the interconnected fractures in the roof is below 0.5 mm, consequently the visual detection and correlation of such fractures is very difficult.
2. The vacuum method can detect very small fractures and correlate them easily.

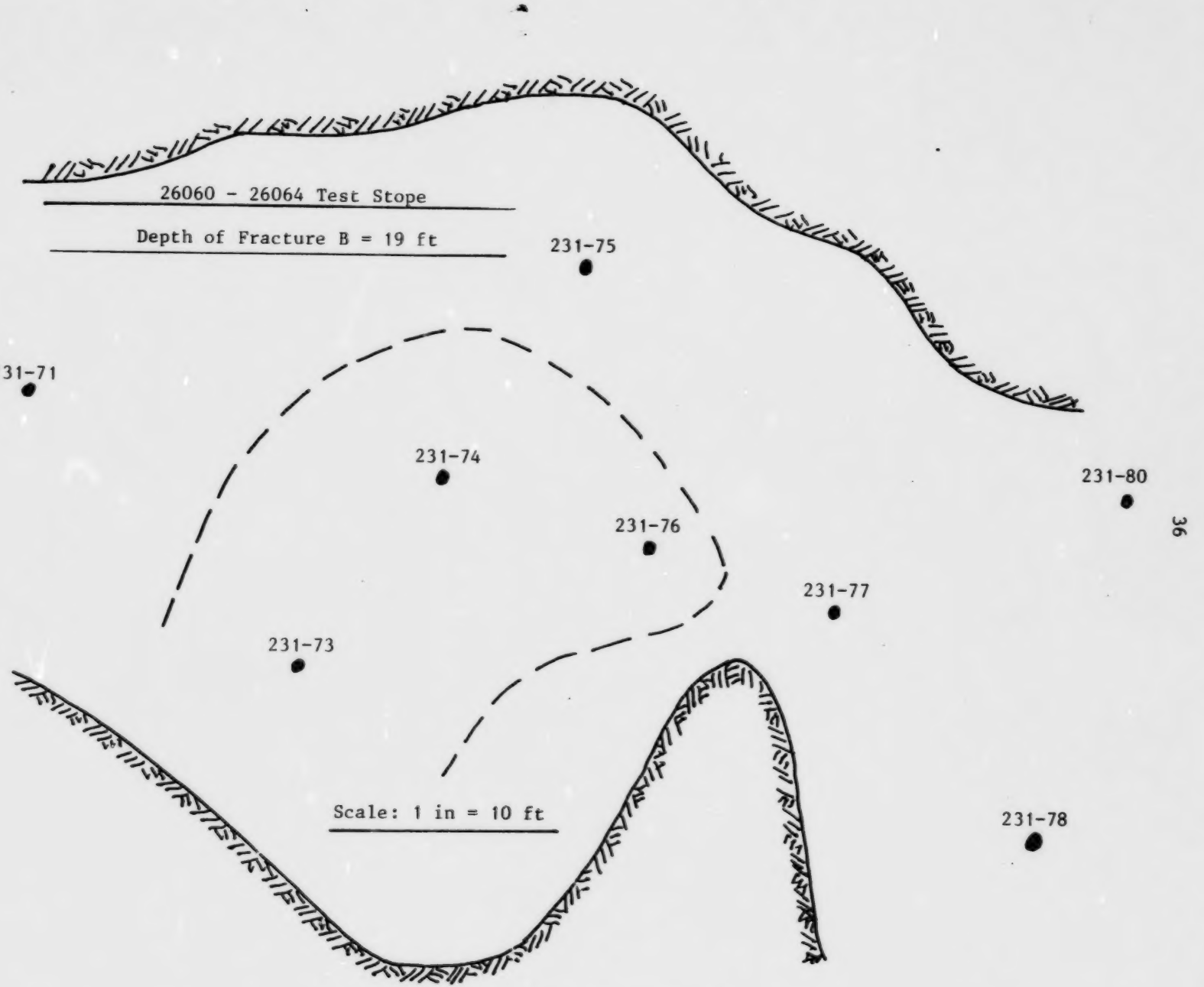

Fig. 13 - Areal extension of Fracture B.

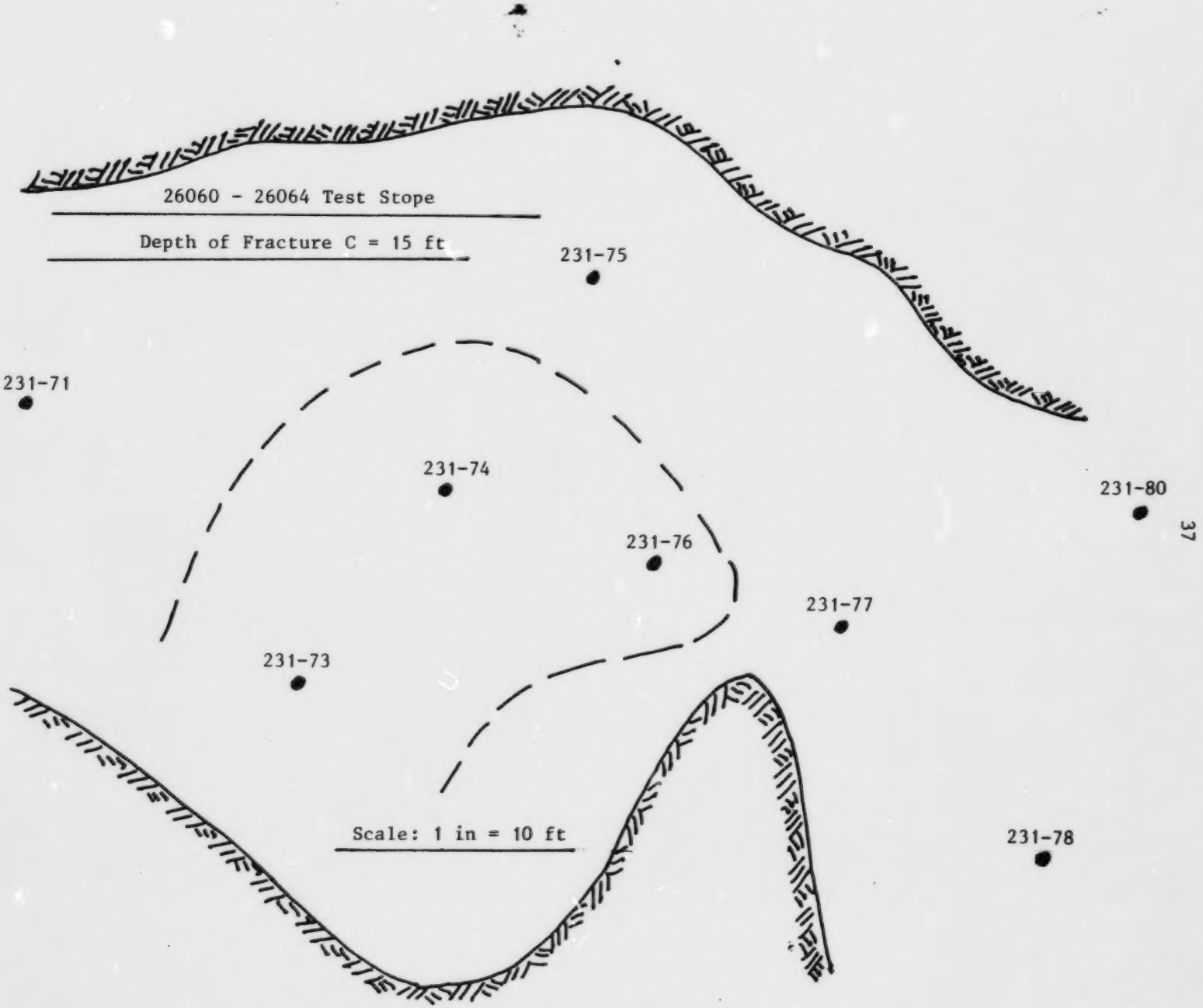

Fig. 14 - Areal extension of Fracture C.

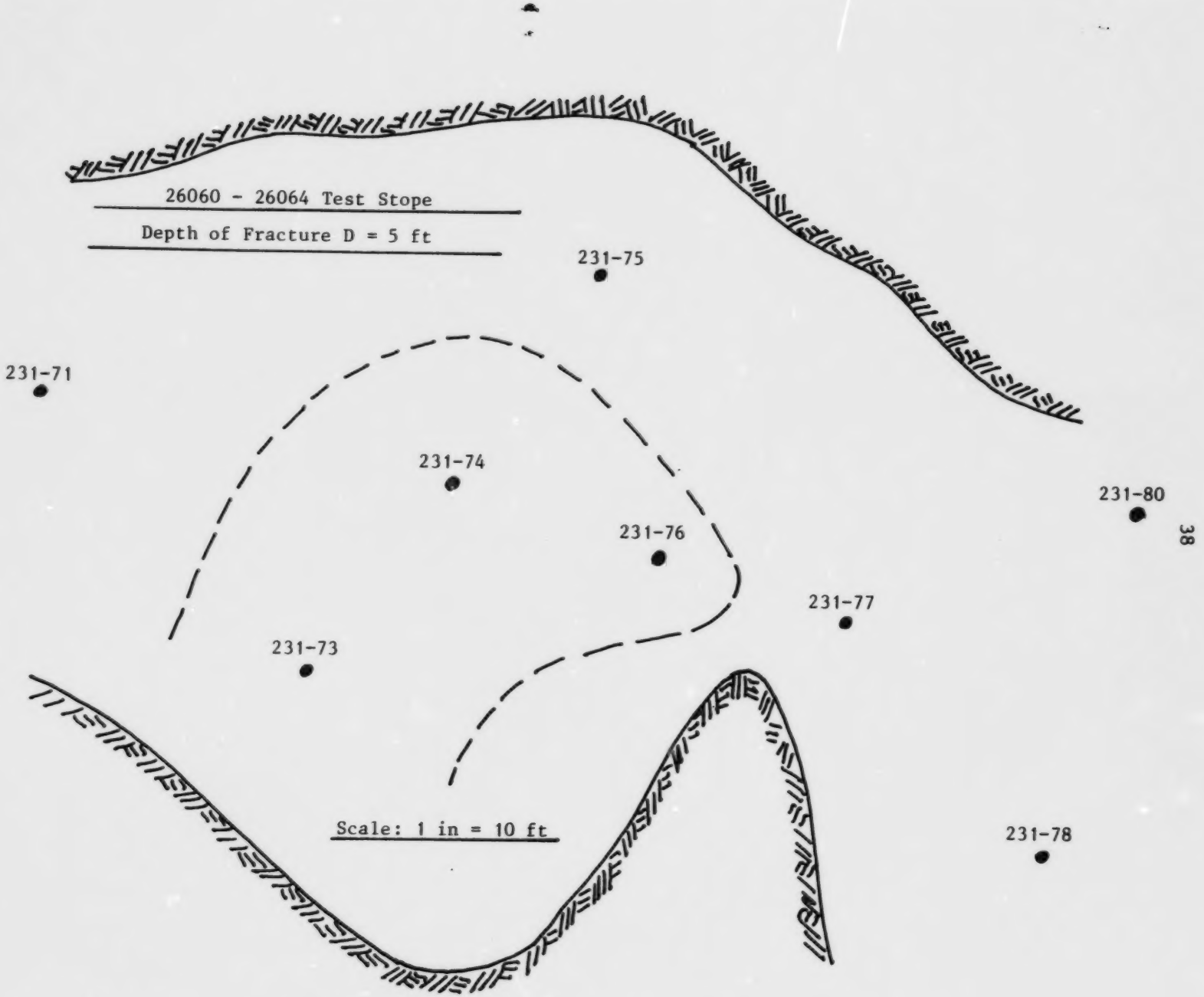

Fig. 15 - Areal extension of Fracture D.

3. The vacuum method can be a very helpful tool for the geologist and rock mechanics engineer for evaluating roof stability problems.

ROOF MONITORING

General

After the completion of the roof mapping program in the stope, heads were blasted off the rockbolts in the roof and compressed air was injected into the fractures.

The roof bolts were removed in three stages and the roof has been pressurized twice by compressed air. During this period an attempt was made to monitor the change of the physical conditions in the roof by using the selected methods. It was believed that such simultaneous tests may establish the practical merit of the different methods as potential warning devices.

Six holes equipped with DEK-1.5 in observation packers and special collar packers were used for the roof monitoring, see Fig. 16.

It was possible with the collar packer to monitor the immediate roof separately. Furthermore, the installation of the collar packer provided the possibility of checking the proper sealing of the DEK-1.5 in observation packer.

Hole No. 231-74 was converted and used as an air injection hole to pressurize the fractures. After the first blasting a remote observation station was used for measuring the pneumatic characteristics of the holes via tygon tubing, see Fig. 17.

Rock Face Pressure Measurement

The calculation of the permeability of the observation hole during the roof monitoring requires the determination of the so-called 'Rock face pressure'. Generally, the rock face pressure can be calculated by subtracting the friction pressure of the tubing line from the total observed pressure. However the

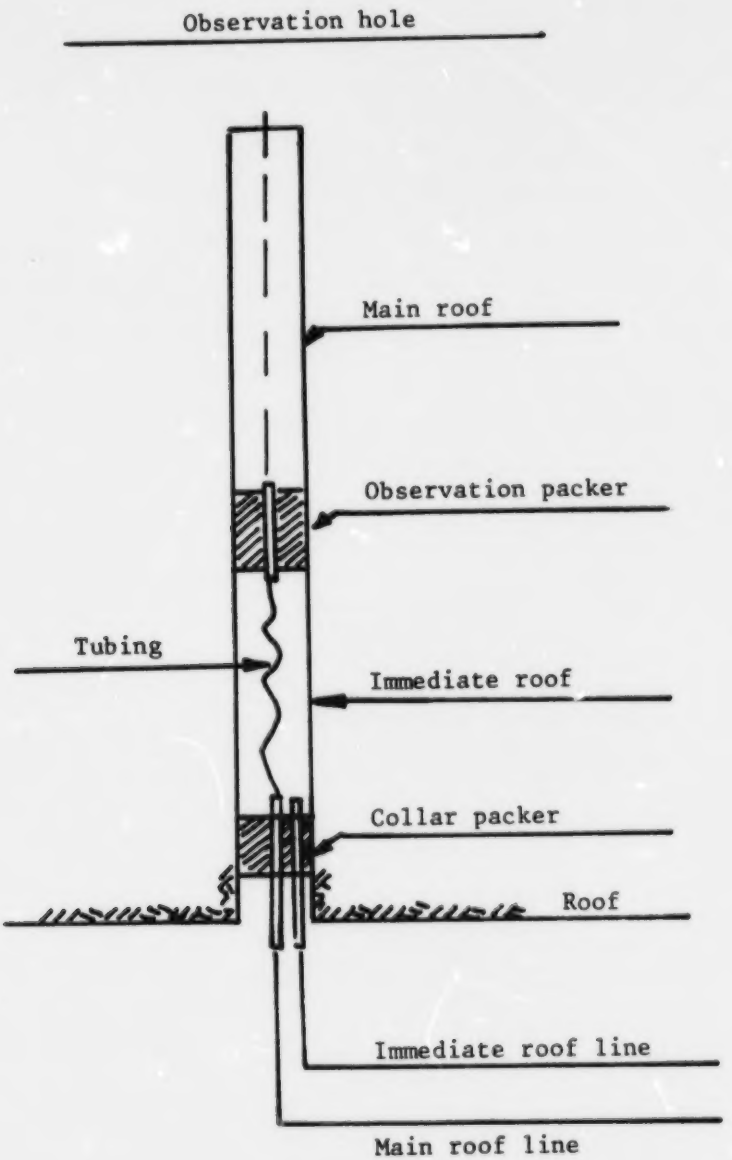

Fig. 16 - Hole construction for roof monitoring.

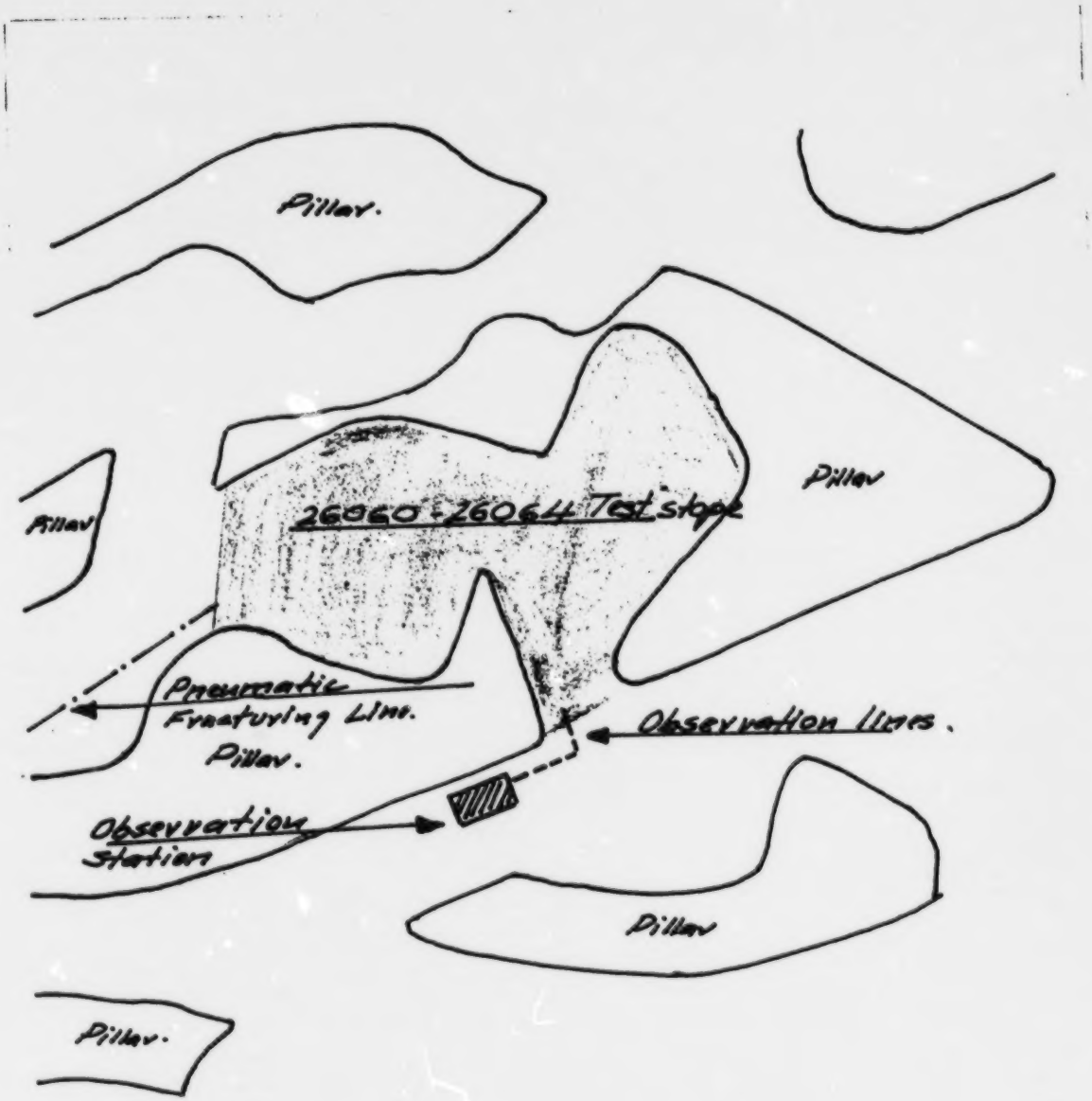

Fig. 17 - General arrangement of the roof monitoring.

investigation of the problem revealed the following very interesting facts:

1. The utilization of long vacuum line is not common, consequently friction loss tabulation could not be calculated.
2. The laboratory test indicated that the friction loss of a tygon tubing for air flow under vacuum is not proportional with its length.
3. The friction resistance of the identical size of tygon tubing of Fisher brand and clear vinyl tubing of Downs brand are different.

Therefore, it is necessary to remove the packers from the observation holes and establish the relationship between the flow rate and friction loss of the individual holes.

Pneumatic Fracturing

The fracturation profile of the test stope has indicated the presence of a very competent immediate roof, which may act as a self supporting beam.

Therefore, preparation was made to use compressed air to induce caving if necessary. It was planned to inject 70 psi compressed air into Fracture D, through Hole No. 231-74, using a simple mechanical packer. The predicted tensile stress was calculated by using the formula given on page 12 supposing 20 m span and 1.80 m immediate roof thickness.

The predicted tensile stress due to the weight of the beam and the pneumatic pressure is:

$$\sigma_{max} = \frac{0.003 \times 2000^2}{2 \times 180} + \frac{4.76 \times 2000^2}{2 \times 180^2}$$

$$\sigma_{max} = 33 + 294 = 327 \text{ Kg/cm}^2$$

The actual test revealed that the pneumatic pressure was insufficient to induce caving of the roof.

Effect of Blasting and Pneumatic Fracturing of the Roof

The rock bolts were removed in three stages by blasting on July 20,

investigation of the problem revealed the following very interesting facts:

1. The utilization of long vacuum line is not common, consequently friction loss tabulation could not be calculated.
2. The laboratory test indicated that the friction loss of a tygon tubing for air flow under vacuum is not proportional with its length.
3. The friction resistance of the identical size of tygon tubing of Fisher brand and clear vinyl tubing of Downs brand are different.

Therefore, it is necessary to remove the packers from the observation holes and establish the relationship between the flow rate and friction loss of the individual holes.

Pneumatic Fracturing

The fracturation profile of the test stope has indicated the presence of a very competent immediate roof, which may act as a self supporting beam.

Therefore, preparation was made to use compressed air to induce caving if necessary. It was planned to inject 70 psi compressed air into Fracture D, through Hole No. 231-74, using a simple mechanical packer. The predicted tensile stress was calculated by using the formula given on page 12 supposing 20 m span and 1.80 m immediate roof thickness.

The predicted tensile stress due to the weight of the beam and the pneumatic pressure is:

$$\sigma_{max} = \frac{0.003 \times 2000^2}{2 \times 180} + \frac{4.76 \times 2000^2}{2 \times 180^2}$$

$$\sigma_{max} = 33 + 294 = 327 \text{ Kg/cm}^2$$

The actual test revealed that the pneumatic pressure was insufficient to induce caving of the roof.

Effect of Blasting and Pneumatic Fracturing of the Roof

The rock bolts were removed in three stages by blasting on July 20,

July 28 and August 4th, 1981. The roof was fractured with compressed air on July 24th and August 7th, 1981 using Hole No. 231-74.

The pneumatic properties of the roof had been measured before and after the blasting and air fracturing operation, using observation holes.

Two separate fractured systems, namely Fractures West, consisting of Fractures A, B, C and D and Fractures East were recognized.

Observation sheets registering the response of the holes to the blasting and air fracturing are attached, see Appendices F to K. The registered values represent the combined effect of fractures present in the holes.

After every blasting and fracturing, an attempt was made to establish pneumatic contact between holes and the results are presented in Fig. 18 to 22.

Analysis of the blasting and fracturing operations are:

First Blasting (Fig. 18): The first blasting on July 20th, using 100 shaped charges had no effect on the Fracture West and Fracture East. The blasting damaged the flow line of Hole No. 231-71, creating erroneous flow measurement. The damage was repaired and protective tubing was installed on every flow line.

First Pneumatic Fracturing (Fig. 19): The first air fracturing was conducted on July 24th, 1981, using Hole No. 231-74 as an air injection hole. Maximum 20 psi injection pressure was used in order to protect the measuring lines against breakage at the connections.

No effort was made to measure the air flow rate and the developed air pressure in the observation holes during testing. A simple air bubble was used to observe the air flow from the hole. First, for a short period, water was produced from Hole No. 231-73.

The observed pneumatic connections are:

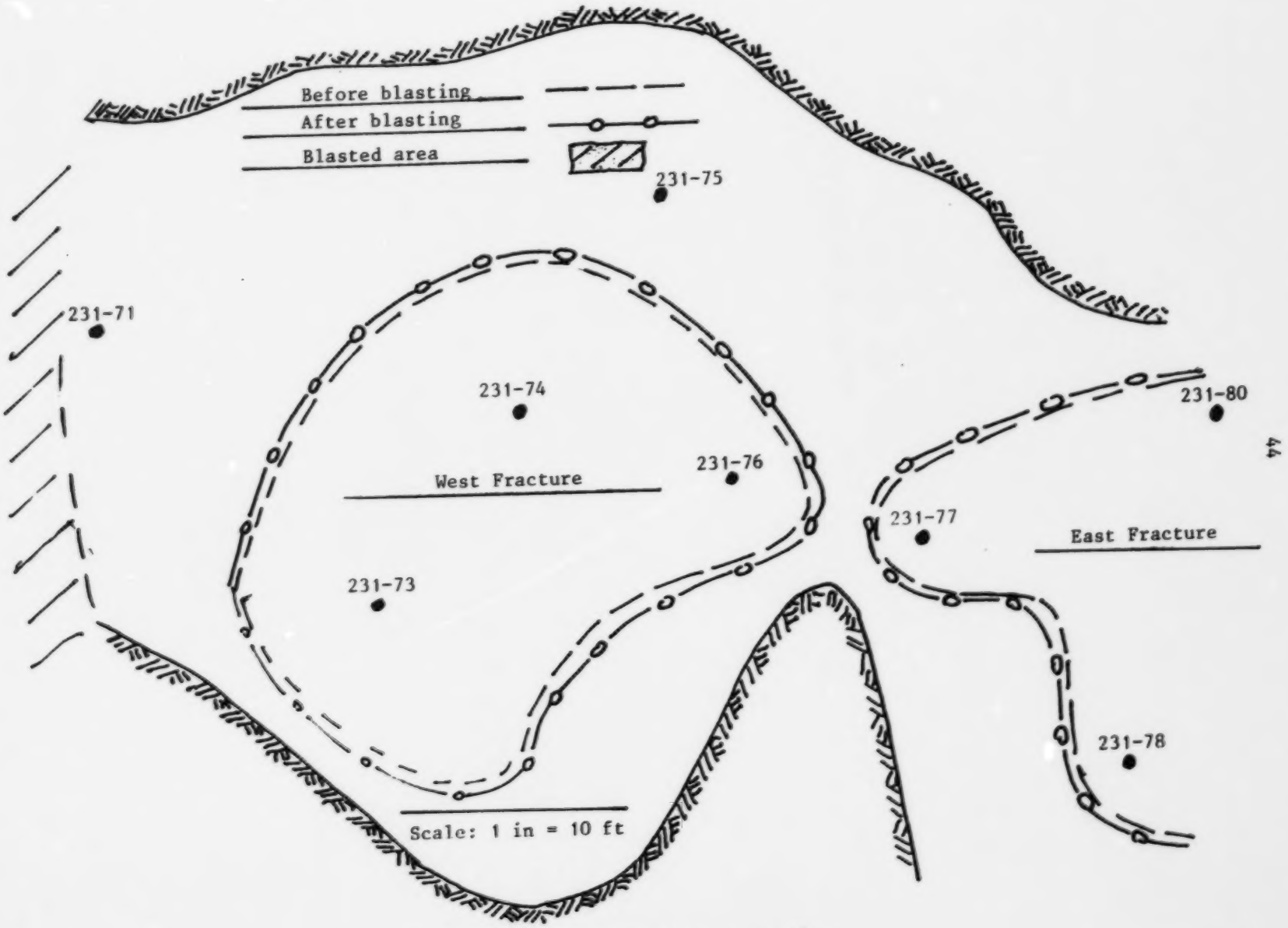

Fig. 18 - Effect of the first blasting.

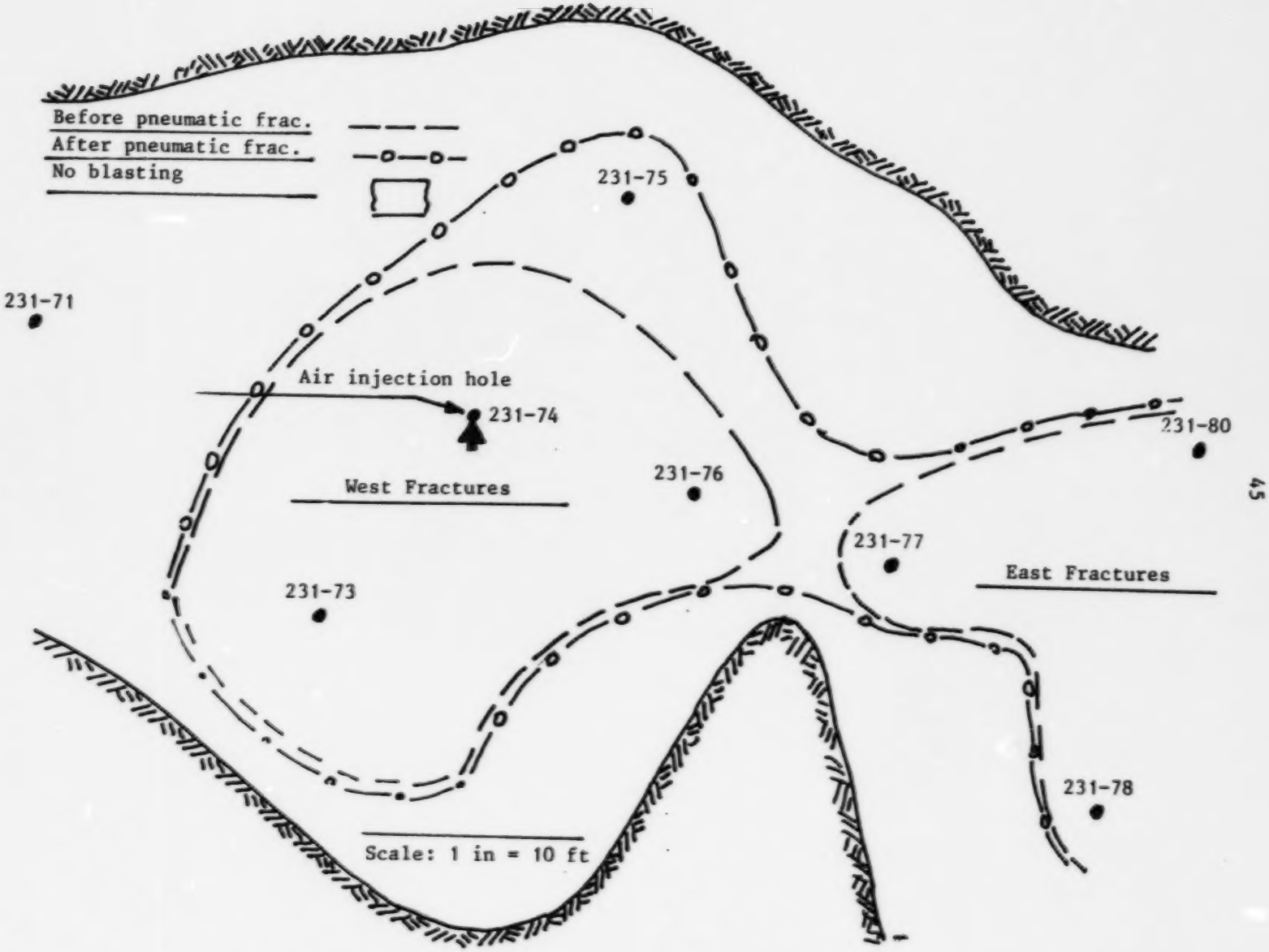

Fig. 19 - Effect of the first pneumatic fracturing.

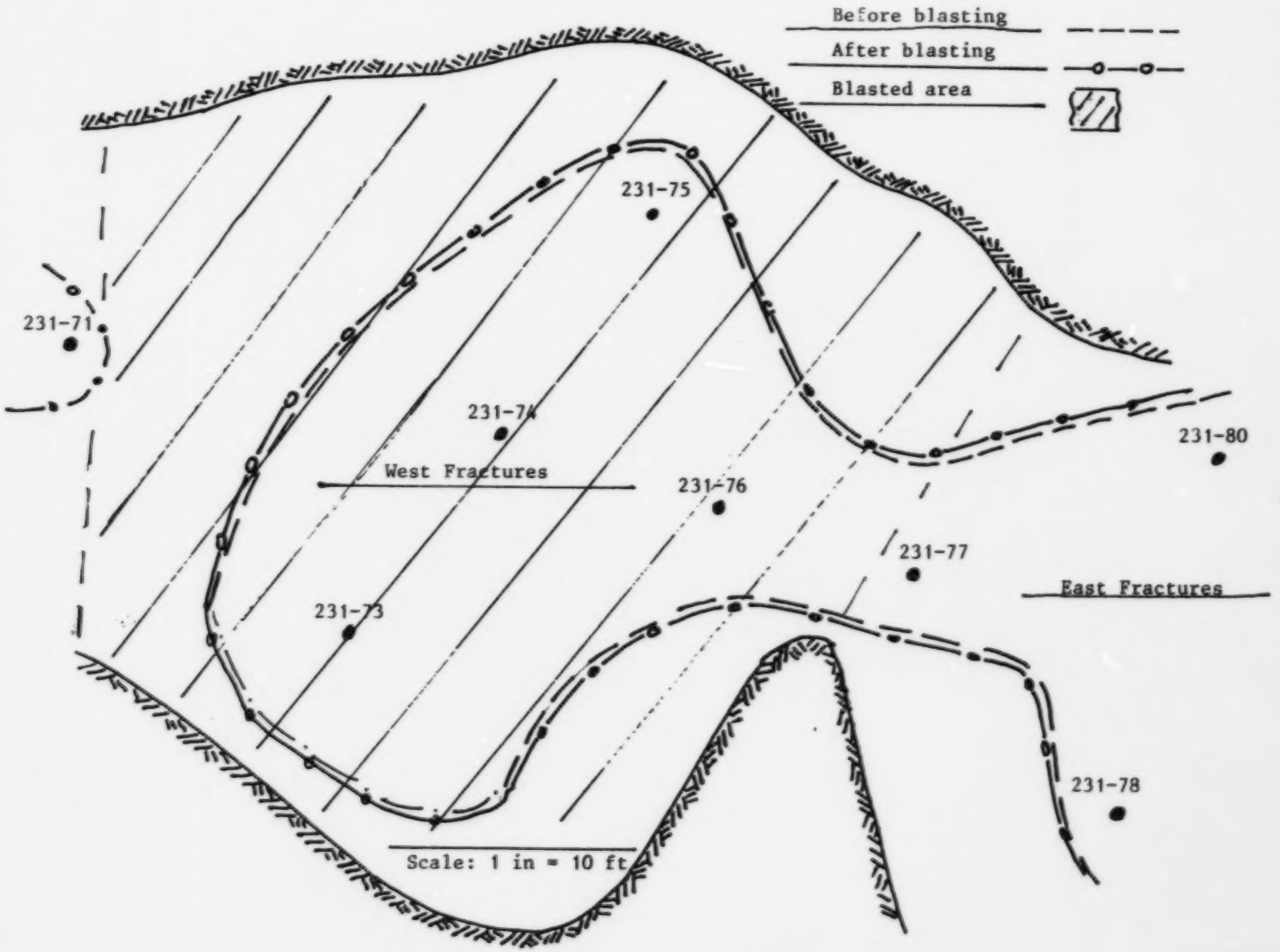

Fig. 20 - Effect of the second blasting.

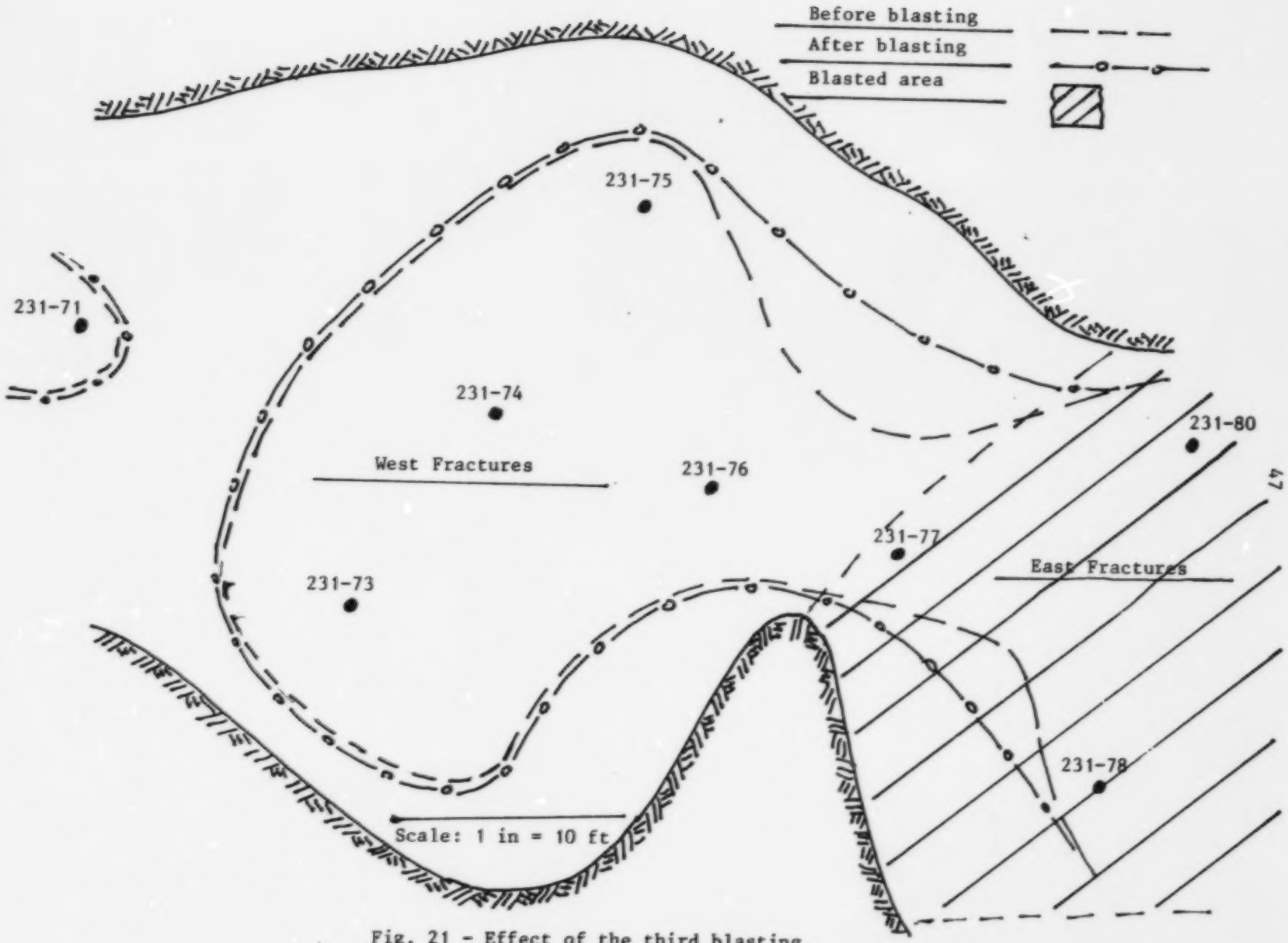

Fig. 21 - Effect of the third blasting.

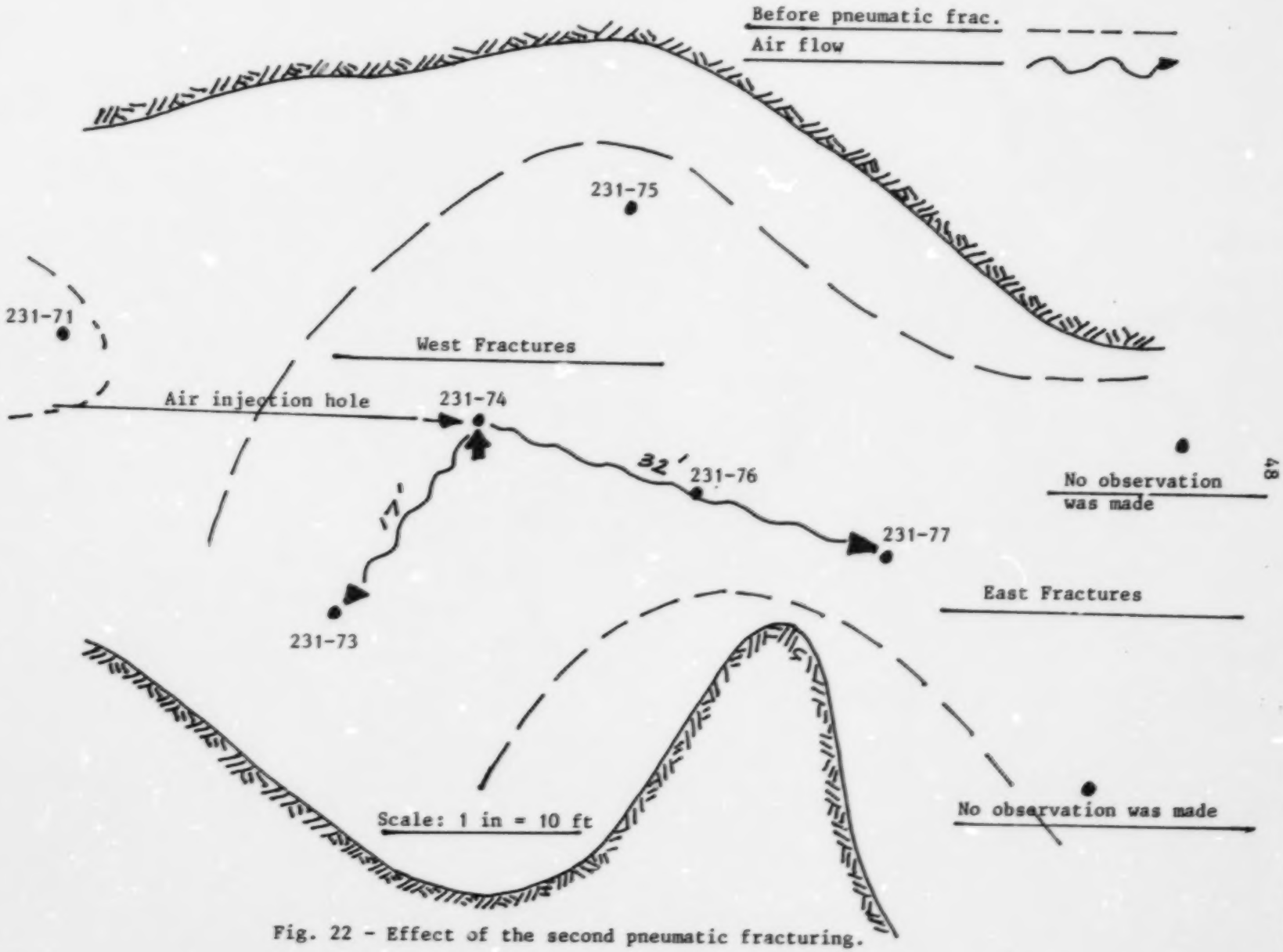

Fig. 22 - Effect of the second pneumatic fracturing.

Injection Pressure	Observed Air Flow from:
5 psi	Hole No. 231-77
10 psi	Hole No. 231-73, 231-77
20 psi	Hole No. 231-73, 231-75, 231-77

The pneumatic fracturing effectively extended the West Fractures in the north direction and connected the West and East fracture groups.

No pneumatic connection was observed between Hole No. 231-71 and 231-74, indicating unchanged fracturation conditions between holes.

Second Blasting (Fig. 20): The large flow rate increment at Holes No. 231-73, 231-75 and 231-77 has indicated that the second blasting on July 28th, 1981, using 250 shaped charges considerably enlarged the fractures on the West side of the stope, but the blasting had no effect on the fractures situated on the West side of the stope.

The flow rate increment at Hole No. 231-71 suggests that new fractures developed due to blasting, which had pneumatic connection in the West direction only.

Third Blasting (Fig. 21): The third blasting on August 4th, 1981, using 180 shaped charges had a strong effect on Holes No. 231-77 and 231-78, but the blasting had practically no effect on Hole No. 231-80 which is very close to the pillar. The areal extension of the fractures on the East side was considerably enlarged after blasting. The blasting had no effect on the fractures situated on the West side of the stope.

The roof in the vicinity of Hole No. 231-71 has sagged considerably between July 28th and August 4th, but no pneumatic connection has developed with the main fracture system.

Second Pneumatic Fracturing (Fig. 22): After completion of the blasting operation the roof in the stope remained practically intact. Therefore, the main objective of the second pneumatic fracturing was to induce roof collapse, which was necessary to evaluate the monitoring performance of the other methods. 70 psi air was injected in the fracture system through Hole No. 231-74 and Pneumatic connection was observed in Holes No. 231-73 and 231-74. Hole No. 231-75 was destroyed by local roof fall.

Due to the limited amount of measuring equipment no effort was made to monitor Hole No. 231-78 or 231-80 during testing.

The results of the test were:

Response Test

70 psi air was injected in Hole No. 231-74. The observed pressure and flow rate in Hole No. 231-77 were at:

9 psi - 8 l/m
14 psi - 9 l/m
17.5 psi - 10.5 l/m

Pressure Build-Up Test

70 psi air was injected in Hole No. 231-74. The observed pressure build-up on Hole No. 231-77 was:

3 min - 20 psi
4 min - 30 psi
5 min - 35 psi

At 35 psi pressure the tygon measuring line separated at the connection. The pressure build-up test has indicated that the air pressure in Fracture D, located at 1.8 m depth in the roof was about 50 psi.

The tensile stress due to the pneumatic pressure was calculated using the formula given on page 12. A beam span of 20 m was assumed for the calculation. The tensile stress is:

$$\sigma_{max} \frac{0.003 \times 2000^2}{2 \times 180} + \frac{3.4 \times 2000^2}{2 \times 180^2} = 243 \text{ kg/cm}^2$$

The fact that the roof did not collapse under this load has clearly indicated the important effect of the horizontal forces on the roof stability.

The main conclusions of the blasting test are:

1. The vacuum method has accurately monitored the roof deterioration during the testing period.
2. The agreement between the theoretical effect of the blasting and the actual vacuum measurement was very good.
3. The utilization of the vacuum method provides direct information about the fracturation condition of the roof.

ROOF STABILITY

The main objective of the recent research project is to develop a monitoring system, which can provide the necessary information for monitoring the stability of the mine roof.

It was realized that the determination of the configuration of the fractures is the key problem, because it determines the method in which the roof can collapse.

The vacuum method can provide these basic fracture parameters.

First, the development of the unstable roof condition is briefly reviewed and the stability calculation for the immediate and main roof are presented in simplified form. Considering the complexity of the problem the calculation methods must be considered as technical estimations only.

DEVELOPMENT OF UNSTABLE ROOFS

In order to develop an effective preventive system capable of indicating unstable roof conditions on time, it is necessary to briefly review the geological and rock mechanics aspects of the very complex roof control problem.

Two types of roofs are recognized in connection with an underground

opening, namely the immediate roof and the main roof, see Fig. 23. An unstable roof may develop in the immediate roof and in the main roof.

The mechanism of the development of an unstable roof in the immediate and in the main roof is different mainly because the stability of the immediate roof is controlled by rock bolts. It is necessary, therefore, to discuss the problems separately.

Rocks encountered in underground mines are considered heterogeneous. The rock mass due to its geological conditions contains fractures, fissures, joints, solution channels, cracks, faults and other mechanical discontinuities which create interfaces within the rock mass. Bond or tensile strengths across interfaces or partings can vary from zero to a value equal to the tensile strength of the rock.

During the excavation of an underground opening time-dependent deformations take place which tend to open fractures, joints and faults creating instability in the roof.

If the bond or tensile strength across the interface is zero or very small, the rock in the roof over the opening can become detached from the rock above to form a slab loaded by its own weight only. This slab is known as the immediate roof, and the rock mass above it is the main roof, see Fig. 23.

The main function of the rock bolts is to control the stability of the immediate roof. This stability can be achieved by:

1. consolidating several layers of rock into a thick laminated self supporting beam; or by
2. anchoring the loose and exposed rock to the more stable and competent main roof.

It is obvious that the rock bolts must be of sufficient length to create a self supporting beam spanning the opening. If the rock bolts are anchored to an incompetent rock mass, unstable roof conditions can develop.

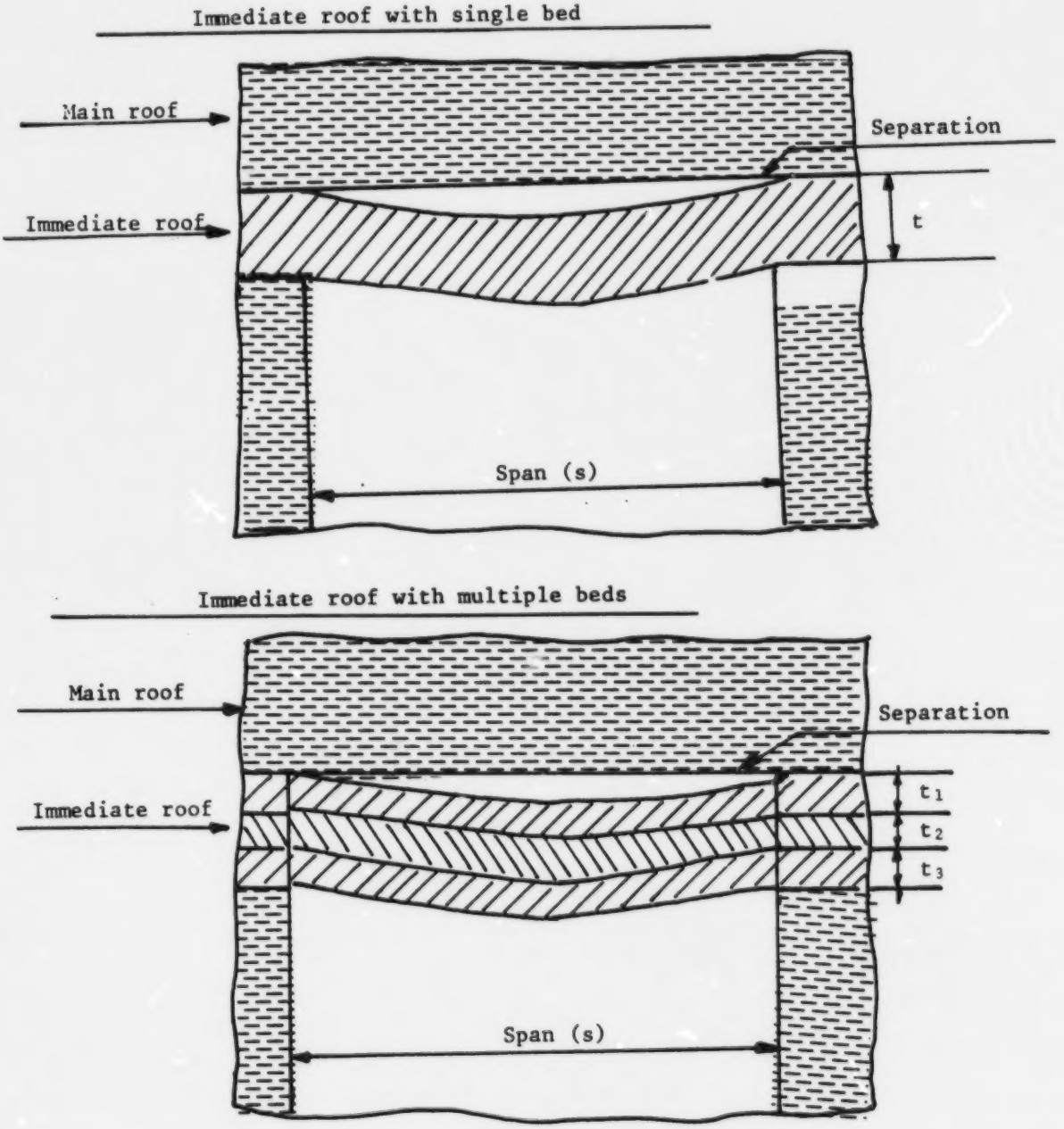

Fig. 23 - Typical mine roof.

Dipping interfaces, faults or separations that are present in the main roof can create a completely separated block of rock which is very weak or not bonded at all to the main rock mass. Such a loose block is called a wedge or a coffin type roof, see Fig. 24 and 25.

If the support under such a structure is gradually excavated then roof failure is imminent.

The real danger of this type of roof is that routine geological mapping sometimes does not reveal the presence of the loose rock mass because the planes of interfacesare invisible in the stope. Rock bolts around the edge intersect the weakness planes and will respond to any sagging of the rock mass. However, rock bolts in the central area may be anchored below the weakness planes and hence provide no direct support.

The coffin or wedge type roof is responsible for several roof collapses, where the weight of the caved-in rock mass was in some cases 1,000 to 1,600 tons.

It can be seen that this type of roof represents a dead weight problem, where the stability of the roof depends entirely on the configuration of the fractures. It is obvious that an effective roof monitoring system has to provide information about the configuration of the fractures present in the roof.

IMMEDIATE ROOF STABILITY EVALUATION

Three types of fractures may affect the stability of the immediate roof. These are:

1. Fractures parallel to the roof;
2. Dipping fractures where the strike of the fracture is visible from the opening;
3. Dipping fractures where the fracture plane is not intercepting the opening.

Vacuum tests or viewing systems conducted in rock bolt holes before the placement of the rock bolts provide the necessary information for the

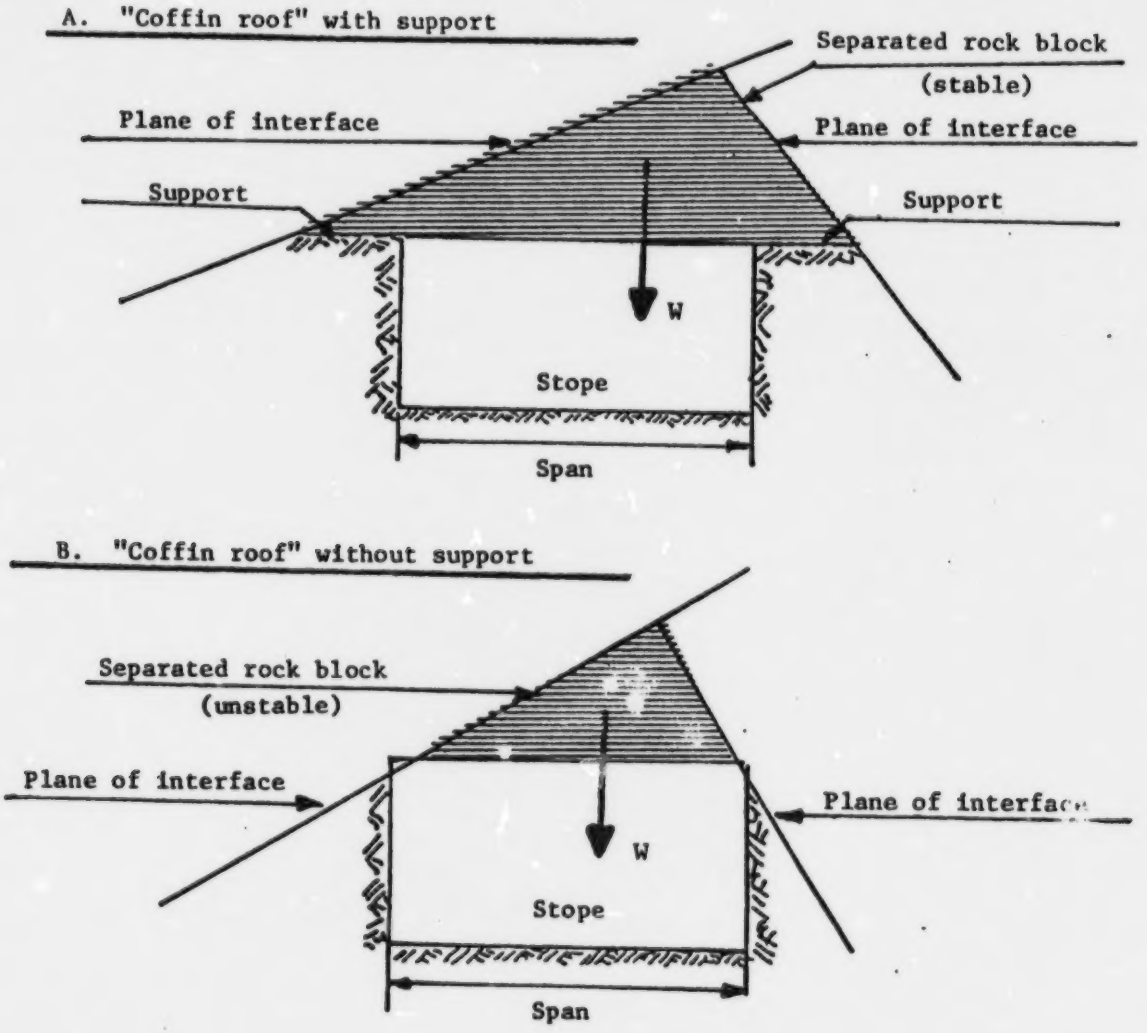

W = pulling force due to the weight of the rock block.

Remark: Strike of the plane of interfaces is parallel with the direction of the excavation.

Fig. 24 - Development of coffin roof, parallel to the stope.

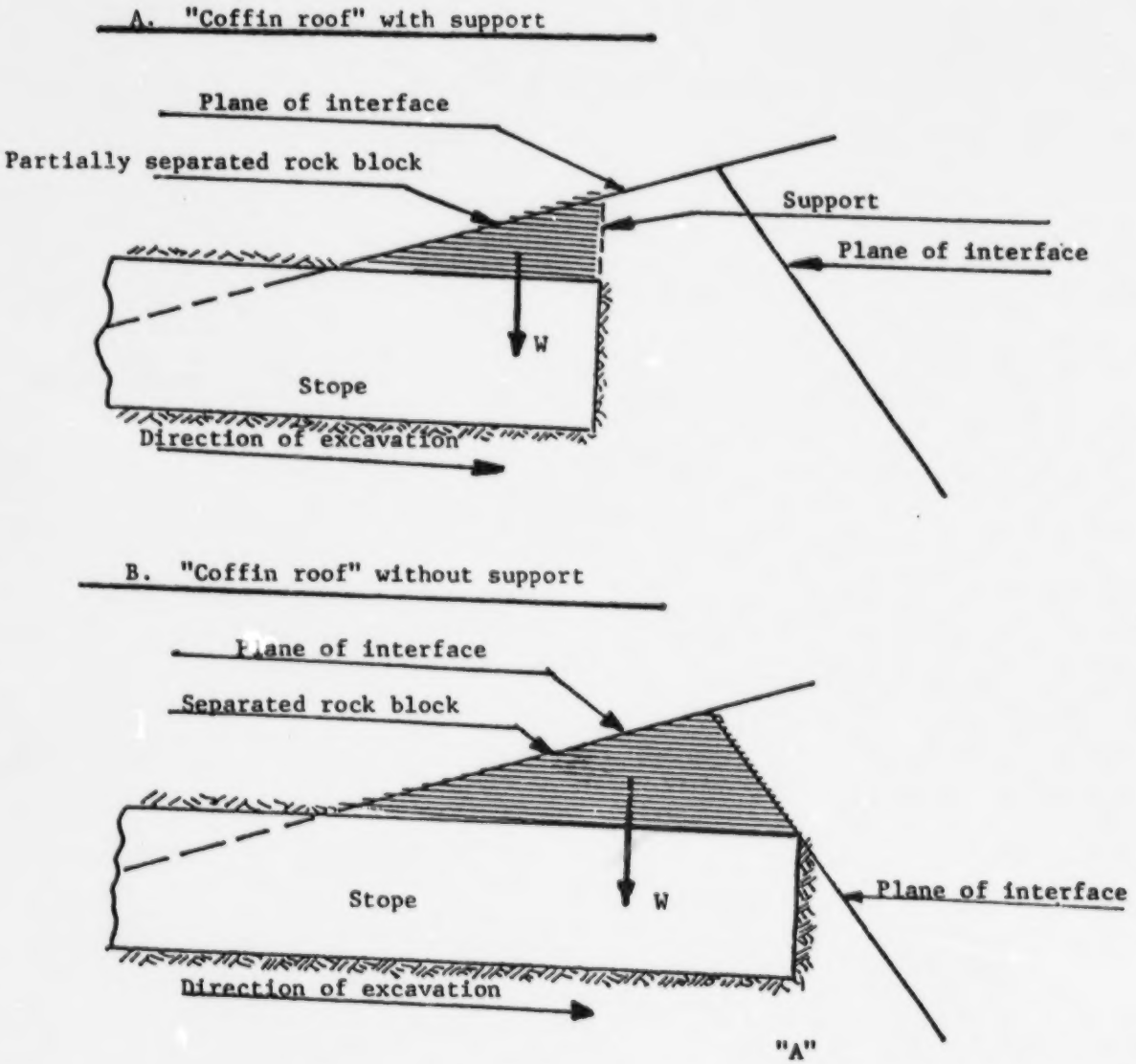

W = pulling force due to the weight of the rock block.

Remarks: When excavation has extended to "A" no support is under the separated rock block.
Strike of the plane of interfaces is perpendicular to the direction of the excavation.

Fig. 25 - Development of coffin roof, perpendicular to the stope.

type 1 and 2 fractures.

The information regarding the fracture system in the rock bolt holes is very important because:

1. The rock bolts must be anchored in competent rock;
2. Effective rock bolts must cross the dipping fractures.

One of the rock bolt's main functions is to bind a discontinuous rock mass together, such as a mass containing natural joints or fractures in order to create a self-supporting roof.

The evaluation of the stability of the immediate roof affected by a horizontal plane which is not controlled by rock bolts requires the definition of the plane.

The formula to calculate the tensile stress created by its own weight of the roof according to the beam theory is:

$$\sigma_{max} = \frac{\gamma S^2}{2h}$$

where: σ_{max} = maximum tensile stress

γ = unit weight of the rock

S = span of the opening

h = thickness of the separated roof

The safety factor against roof collapse is calculated by using the following relationship:

$$\text{Safety Factor} = \frac{\sigma_M}{\sigma_{max}}$$

where: σ_M = tensile strength of the material

σ_{max} = maximum tensile stress in the beam

It is recognized that the actual safety factor due to the horizontal stress can be considerably higher.

The procedure of calculation in connection with dipping fractures is presented in the next chapter.

MAIN ROOF STABILITY EVALUATION

A sketch showing the development of a coffin or wedge type roof in the main roof is presented in Fig. 26. The configuration of the fractures could be established by the vacuum measurement, conducted in test holes 1, 2, 3 and 4.

This evaluation would reveal that a separated rock block is present in the roof which is sitting on support A and B. The block exerts a pulling force of 'W' due to its own weight.

For the static calculation a, b, c d block is considered as a beam clamped at both ends and loaded by its own weight plus a triangular load sitting on the beam. No horizontal forces are acting on the block because of the presence of the open fractures. The formula to calculate the thickness of the beam is:

$$h = Z_1 - l \, tg\alpha$$

where: h = thickness of the beam

Z_1 = distance between roof and fracture in the test hole

l = distance between test hole and the stope's wall

α = dip of the fracture. It is calculated by using Z_1 and Z_2.

The maximum bending moment and stress due to the combined load is calculated according to the beam theory. The maximum bending moment is:

$$M_{max} = \frac{W_1 L^2}{12} + \frac{5W_2 L^2}{96}$$

where: M_{max} = maximum bending moment

L = span of the stope

W_1 = unit load due to the weight of the beam

W_2 = unit load due to the triangular load

The formula to calculate the maximum stress is:

$$\sigma_{max} = \frac{M_{max}}{Z}$$

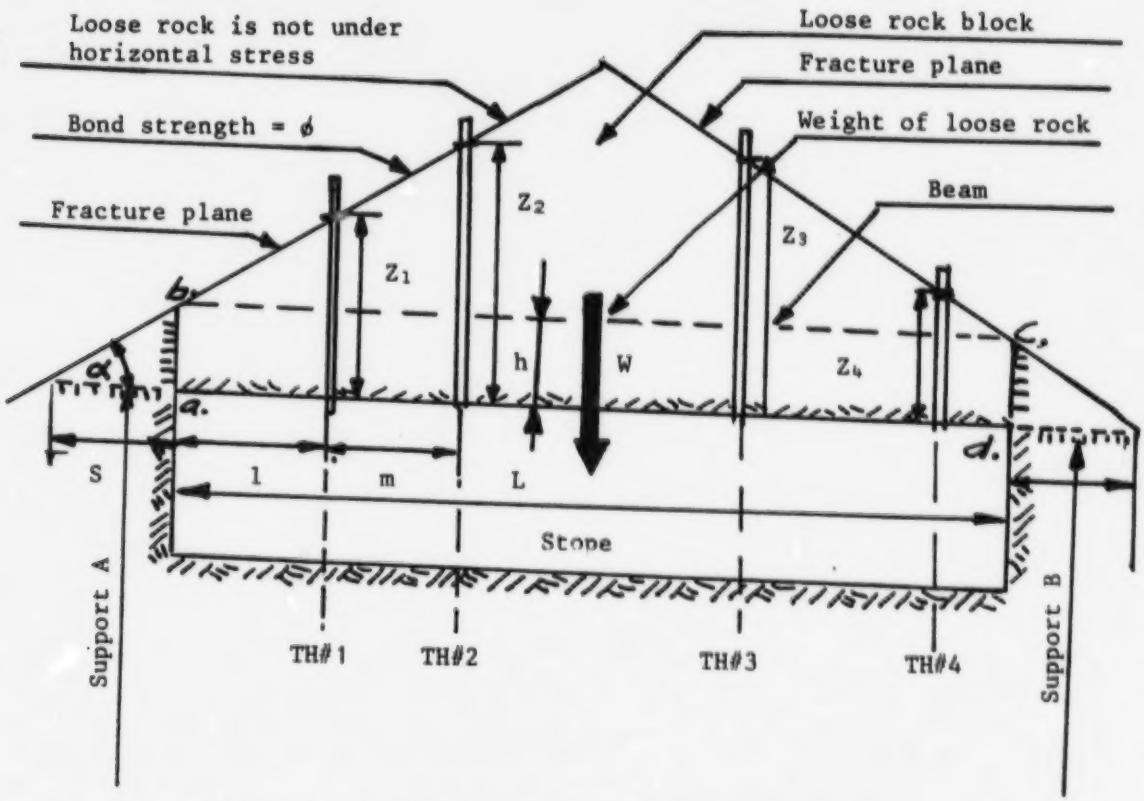

The loose rock block is not under horizontal stress due to the gap created by the fracture planes.

Thickness of the beam a-b-c-d: $h = Z_1 - l\,tg\alpha$

Dip of the fracture: $Tg\alpha = \frac{Z_2 - Z_1}{m}$

Maximum bending momentum:

$$max = \frac{W_1 L^2}{12} + \frac{5W_2 L^2}{96}$$

where: W_1 = unit load of beam
W_2 = unit load of triangle

Maximum Stress: $\sigma_{max} = \frac{M_{max}}{Z}$

Z = modulus of beam

Safety Factor: $B = \frac{\sigma_M}{\sigma_{max}}$

σ_M = tension strength of material

Supported length of beam: $S = \frac{h}{tg\alpha}$

Pressure in the Support: $p = \frac{W_B}{2S}$. W_B = unit load of rock block.

Fig. 26 - Sketch of the coffin type for stability calculation.

σ_{max} = maximum bending stress in the beam

Z = section modulus of the beam.

The safety factor against roof collapse is established by the following relationship:

$$SF = \frac{\sigma_M}{\sigma_{max}}$$

where: SF = safety factor

σ_M = tensile strength of the material

σ_{max} = maximum bending stress

The drawing clearly indicates that as the span of the opening increases, the thickness of the beam decreases, consequently the safety factor against roof collapse decreases.

The support at both ends of the loose block has an overwhelming effect on its stability. The formula to calculate the supported length of the loose block is:

$$S = \frac{h}{tg\alpha}$$

where: S = supported length of the block

h = thickness of the beam

α = dip of the fracture plane

The pressure generated on the support by the loose block is:

$$P = \frac{W_B}{2S}$$

where: P = unit pressure in the support

W_B = unit load due to the weight of the block

S = supported length of the block.

The present calculation has indicated that the roof stability can be readily established if the configuration of the fractures is known. It can be seen that the vacuum method can provide the necessary basic information for the static calculation.

STABILITY OF THE ROOF IN THE TEST STOPE

The fracturation profile has indicated the presence of Fracture D located 1.8 m depth in the roof. The fracture running parallel with the roof creates a 1.8 m thick immediate roof, which is separated from the main rock mass and acts as a self-supporting beam.

A beam span of 20 m is supposed for the tensile stress calculation. The calculated tensile stress, using the formula given on page 12 is:

$$\sigma_{max} = \frac{0.003 \times 2000^2}{2 \times 180} = 33 \text{ kg/cm}^2$$

Since the tensile strength of the rock mass is generally considered as zero this means that the horizontal compressive stresses must be at least 33 kg/cm^2 to preserve the beam.

FORMATION WATER INVESTIGATION

During the testing period a small amount of water, about 70-100 cm per day entered the test stope through Holes No. 231-71 and 231-73. The presence of the water in the formation created a simultaneous flow of water and air which considerably complicated the evaluation of the pneumatic parameters of the hole.

The drastic reduction of the air flow rate due to the presence of water is illustrated on the diagram presented in Fig. 27. This diagram illustrates the drastic reduction of the air flow rate when water is present in the formation.

The terms 'Effective Permeability' and 'Relative Permeability' are used by the oil reservoir engineers to describe this special flow condition. (See Glossary for definitions.)

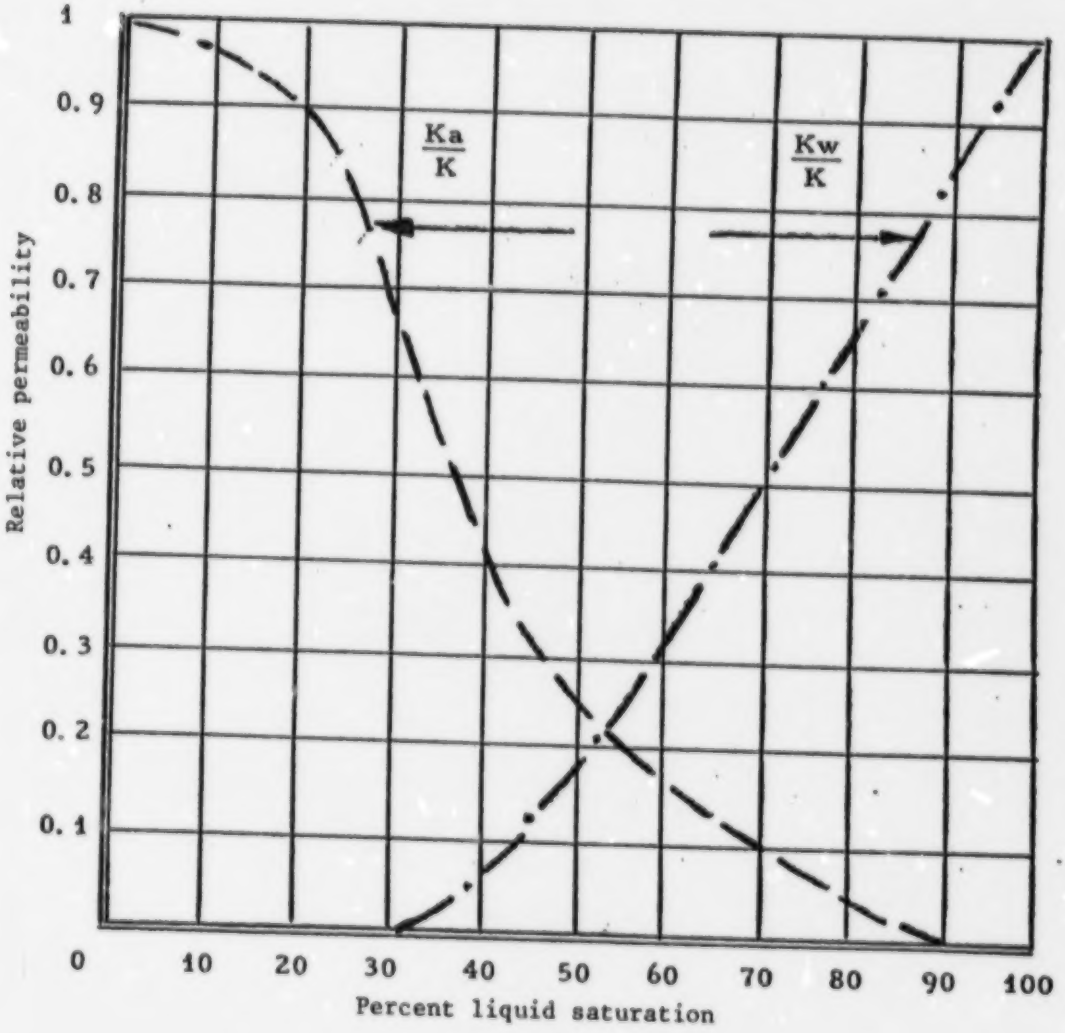

K = Absolute permeability
Ka = Effective permeability to air
Kw = Effective permeability to water

Fig. 27 - A typical relative permeability - saturation relationship.

VACUUM TEST AT RIO ALGOM MINE

The main objective of the underground test conducted at Rio Algom Mine was to check the performance of the method under different roof conditions. As an extra benefit the Rio Algom test provided the opportunity of testing the Convectron Series 275, digital and analog type vacuum gauges in order to increase the measuring accuracy and to improve the underground mobility of the system.

DESCRIPTION OF THE TEST STOPE

Stope No. 847 at New Quirke Mine was selected for conducting the in situ test program. The test stope is situated 1679 ft below the shaft collar, and the elevation of the stope is 305 ft below sea level.

Five EX diamond drill bore holes drilled in the roof were used to establish the fracturation condition of the roof. The layout of the selected test stope and the location of the test holes are shown on Fig. 28. No water seepage was observed during the vacuum test.

FRACTURATION PROFILE LOGS

The field test in the selected stope of No. 847 was conducted between March 1st to March 10th, 1982.

The Fracturation Profile Log of VH-1, VH-3, VH-4, VH-9 and VH-11 was measured by using a conventional straddle packer and measuring technique as discussed previously.

The flow rate in 1/m and the differential static pressure in Torr, i.e., mm Hg, were measured during the testing in order to calculate the pneumatic parameters of the section.

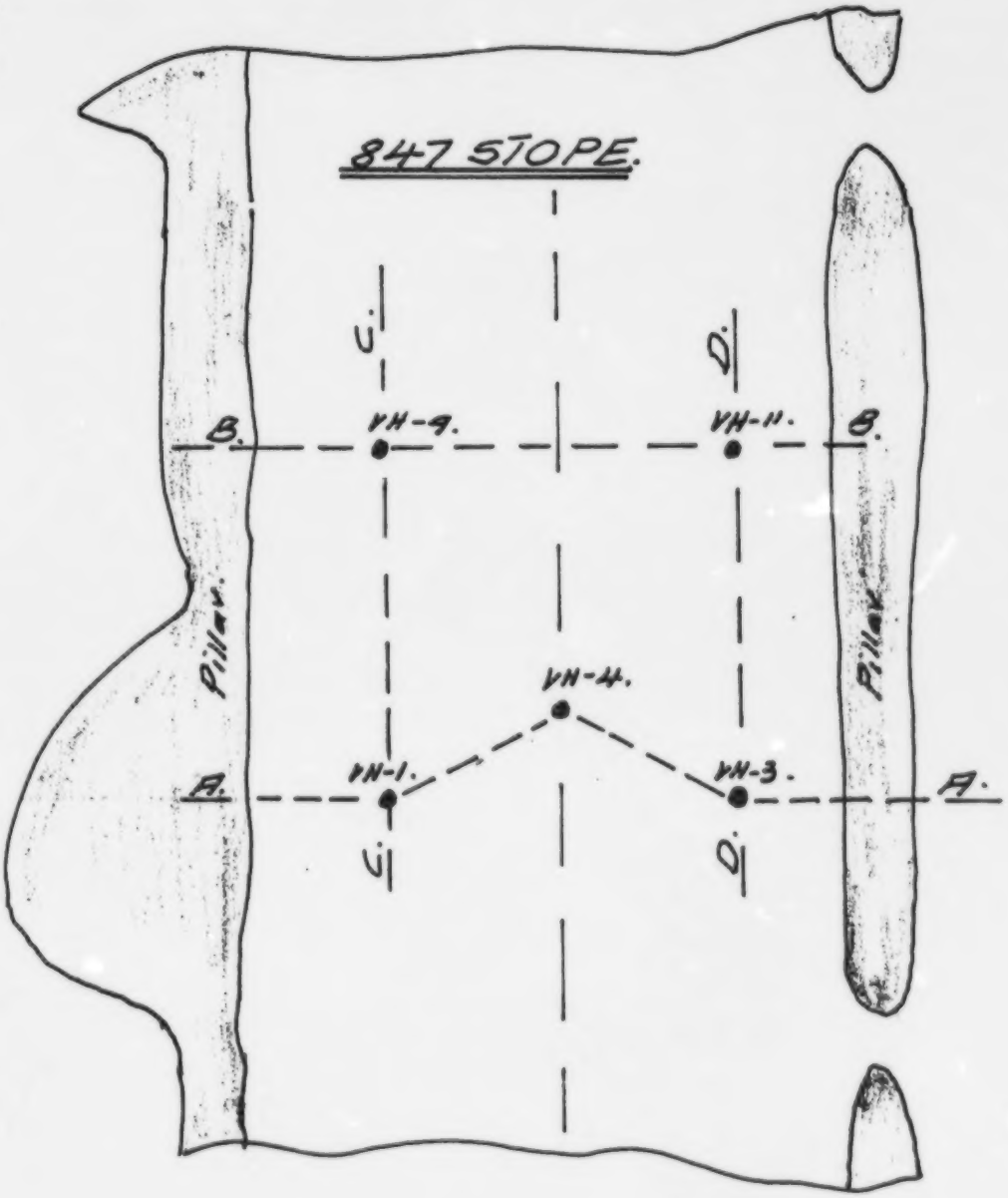

Fig. 28 - Layout of the Rio Algom test stope.

In the case of a tight formation when the very small flow rate cannot be measured, the differential static pressure in Torr and the pressure loss Torr per minute were used to calculate the pneumatic parameters of the section.

Formulae used for the log interpretation are:

Permeability - Tight Formation

$$K = 3.6 \frac{Pl}{P_e^2 - P_w^2}$$

where: K = permeability, md

Pl = pressure loss Torr, per min

P_e = formation pressure psi a

P_w = pressure at the rock face psi a.

Transmissibility - Tight Formation

$$T = \frac{0.82K}{1000}$$

where: K = permeability, md

T = transmissibility, d/ft.

Equivalent Fracture Size - Tight Formation

$$W_{mm} = \frac{\sqrt[3]{12T}}{14.88}$$

where: K = permeability, md

T = transmissibility, d/ft.

Transmissibility - Fractured Zone

$$T = 3.77 \frac{Q}{P_e^2 - P_w^2}$$

where: T = Transmissibility, d/ft

Q = flow rate, l/m

P_e = formation pressure, psi a

P_w = pressure at the rock face, psi a.

Equivalent Fracture Size - Fractured Zone

$$W_{mm} = \frac{\sqrt[3]{12T}}{14.88}$$

$$W_{in} = \frac{\sqrt[3]{12T}}{378}$$

where: W_{mm} = equivalent fracture size, mm

W_{in} = equivalent fracture size, in

T = transmissibility, d/ft.

Permeability of Fracture

$$K_f = 54.10^6 \, W_{in}^2$$

where: K_f = permeability of fracture, darcies

W_{in} = width of fracture, in.

For log interpretation it was supposed that permeability less than 0.1 md represents the matrix permeability of the unfractured rock.

In some cases during testing very large fractures were intercepted, however, it was not possible to calculate the pneumatic parameters of such fractures because the theoretical calculation has indicated that the limited flow rate creates a pressure drop of less than 1 Torr in the fracture.

The fracturation profile log of the holes is presented in Appendices M, N, O, P and Q.

The transmissibility of the individual sections was used as the best parameter to compare the air transmitting capacity of the different zones. The results are shown on Fig. 29, 30, 31, 32 and 33.

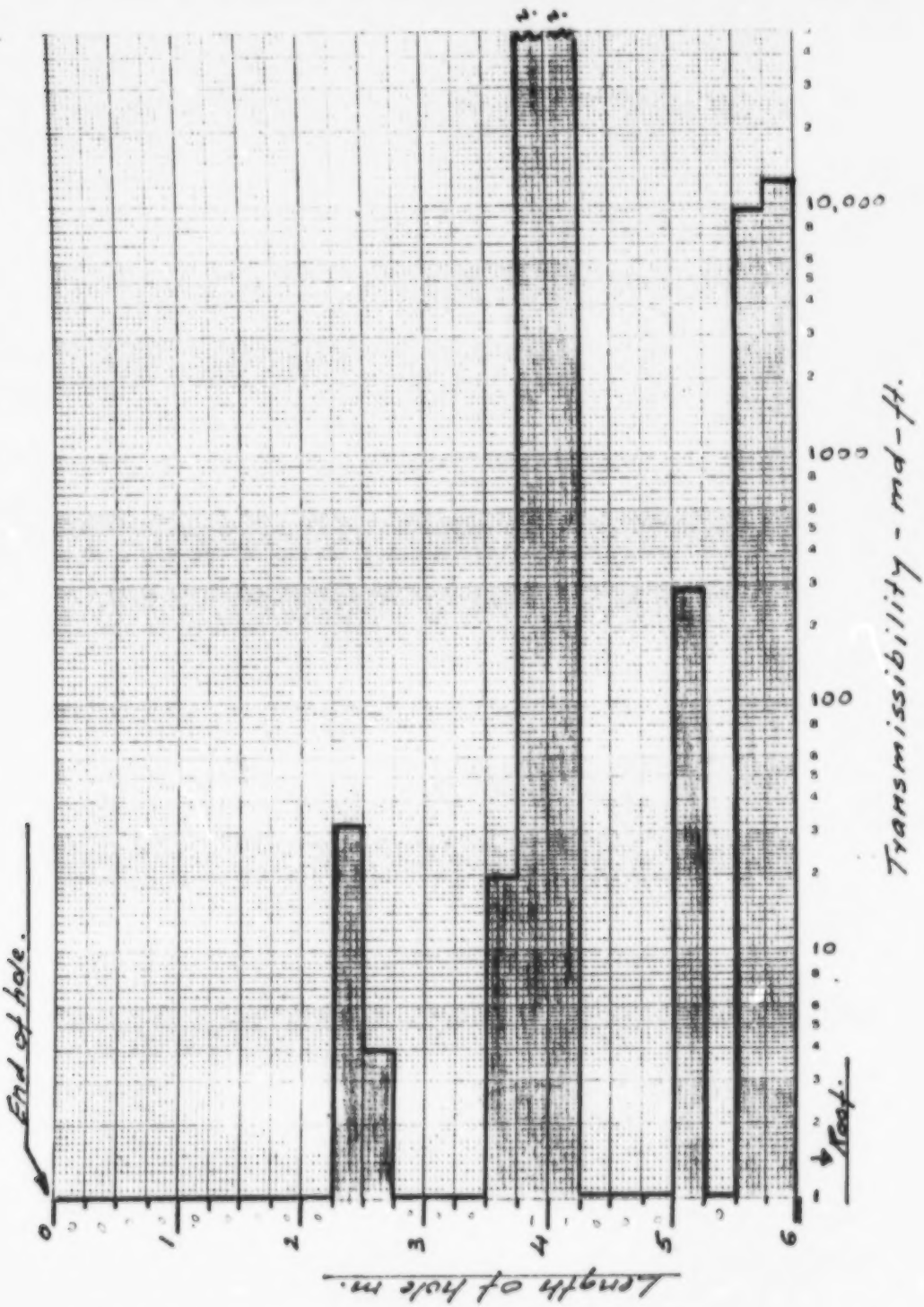

Fig. 29 - Vacuum hole transmissibility graph. Hole: VH-1.

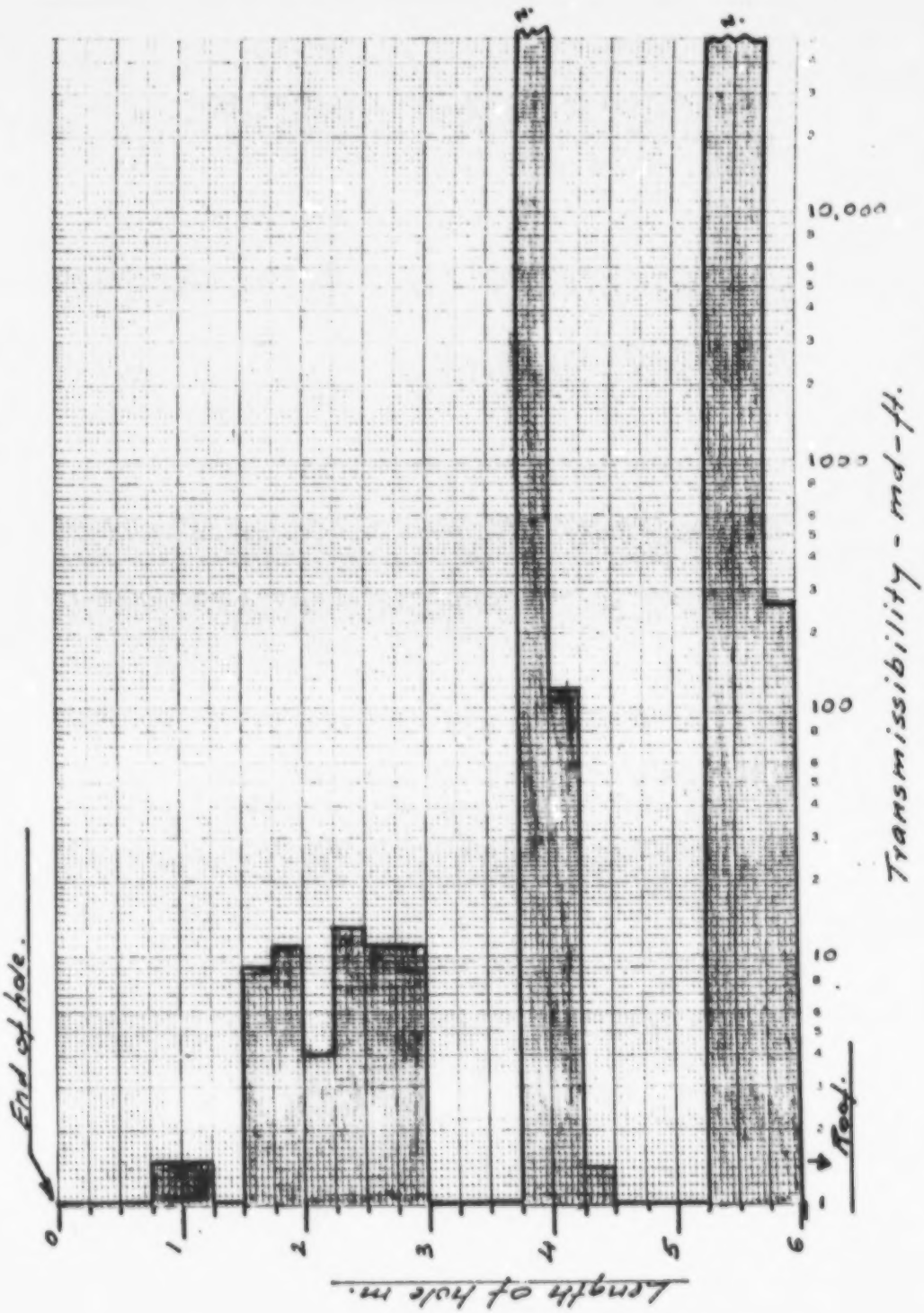

Fig. 30 - Vacuum hole transmissibility graph. Hole: VH-3.

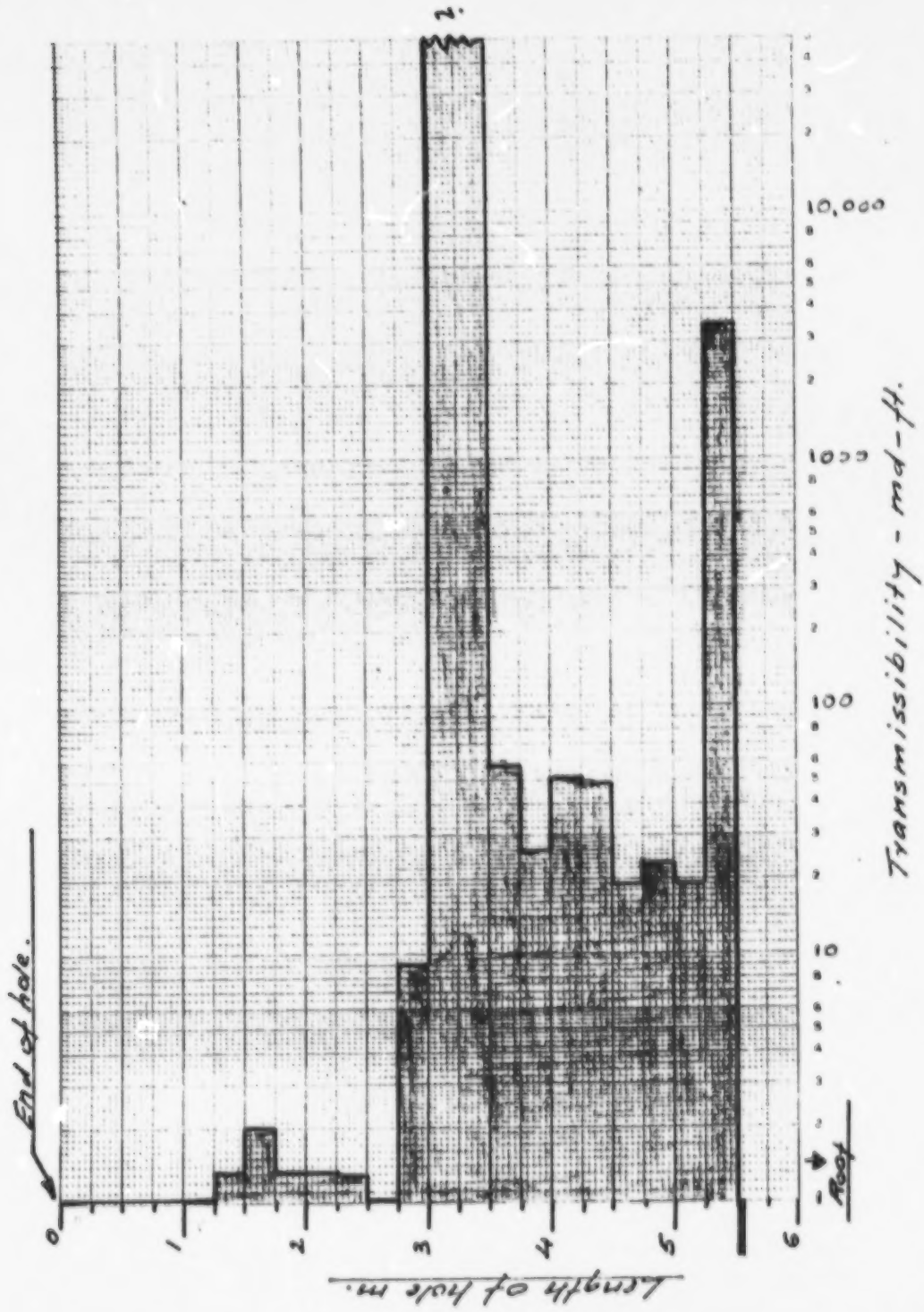

Fig. 31 - Vacuum hole transmissibility graph. Hole: VH-4.

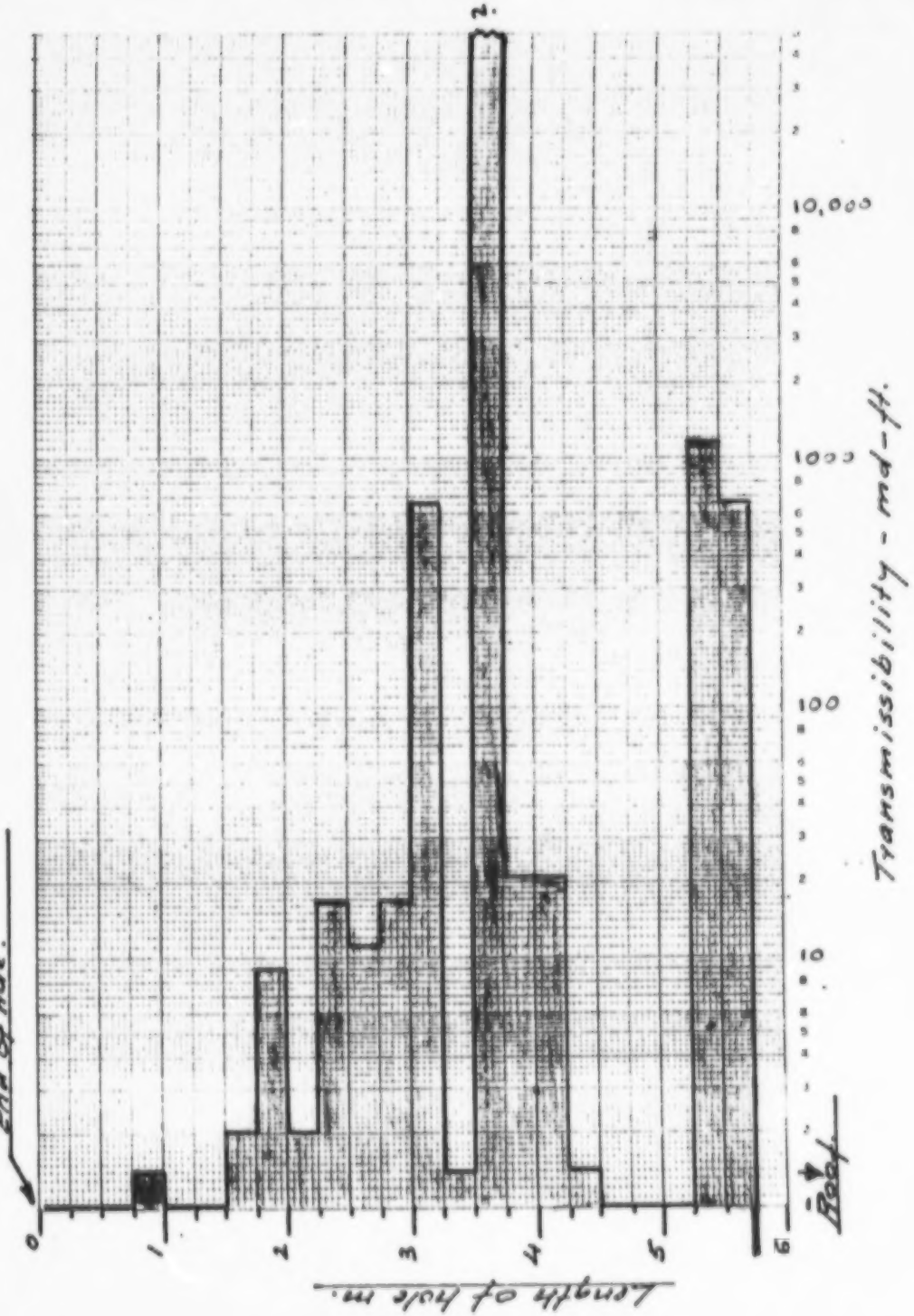

Fig. 32 - Vacuum hole transmissibility graph. Hole: VH-9.

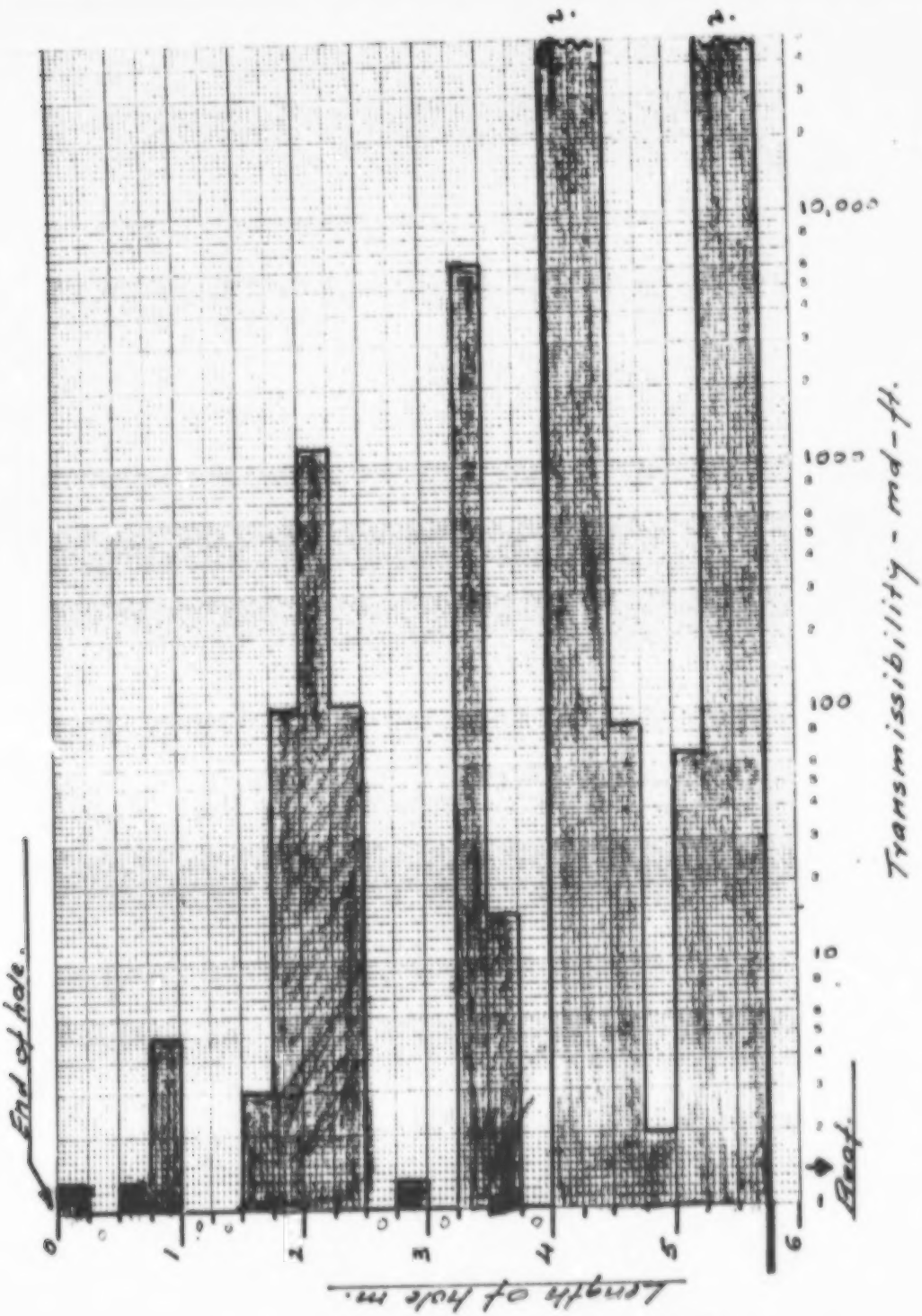

Fig. 33 - Vacuum hole transmissibility graph. Hole: VH-11.

CORRELATION OF FRACTURES

No attempt was made, due to the limited time, to establish the continuation of fractures between holes by observing the actual pneumatic connection between holes by using straddle packers. However, the main fracture zone, which exhibits extraordinarily large permeability can be easily correlated without pneumatic observation.

In order to establish the basic parameters of the main fractured zone, four cross sections, namely: A-A, B-B, C-C and D-D have been prepared and presented on Fig. 34, 35, 36 and 37, respectively. The locations of the cross sections are shown on Fig. 28.

The interpretation has revealed the presence of major separations located about 2 m deep in the roof. The depth of the separations corresponds closely with the length of the installed rock bolts. The separations run parallel with the roof line. The major separation is completely overlying the test stope.

The dip of the main fractured zone in the direction of the axis of the stope is about 3-4° and the dip in the perpendicular direction to the axis is about 2-4°.

To establish the continuation of fracture between holes without the actual response test is very problematic. For this reason no effort was made to correlate the large number of fractures present above and below the main fractured zone between holes.

The fractured zone created by the blasting operation can be distinguished clearly and correlated easily.

INTERPRETATION OF THE VACUUM TEST

Generally the agreement between the vacuum and TV camera measurements regarding the location of the major fractures is good. However, Holes VH-1,

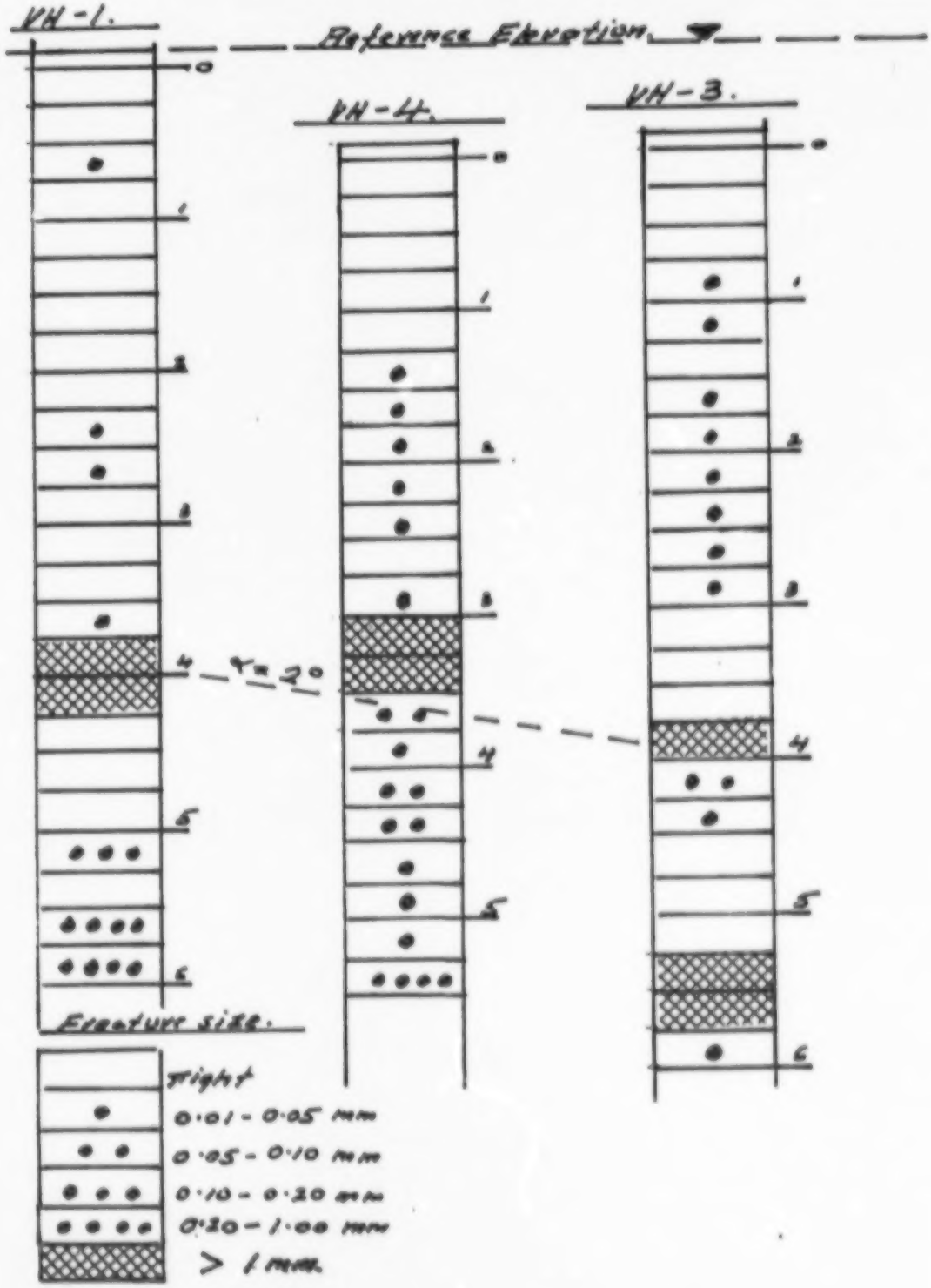

Fig. 34 - Cross-section A-A. R.A. 847 stope.

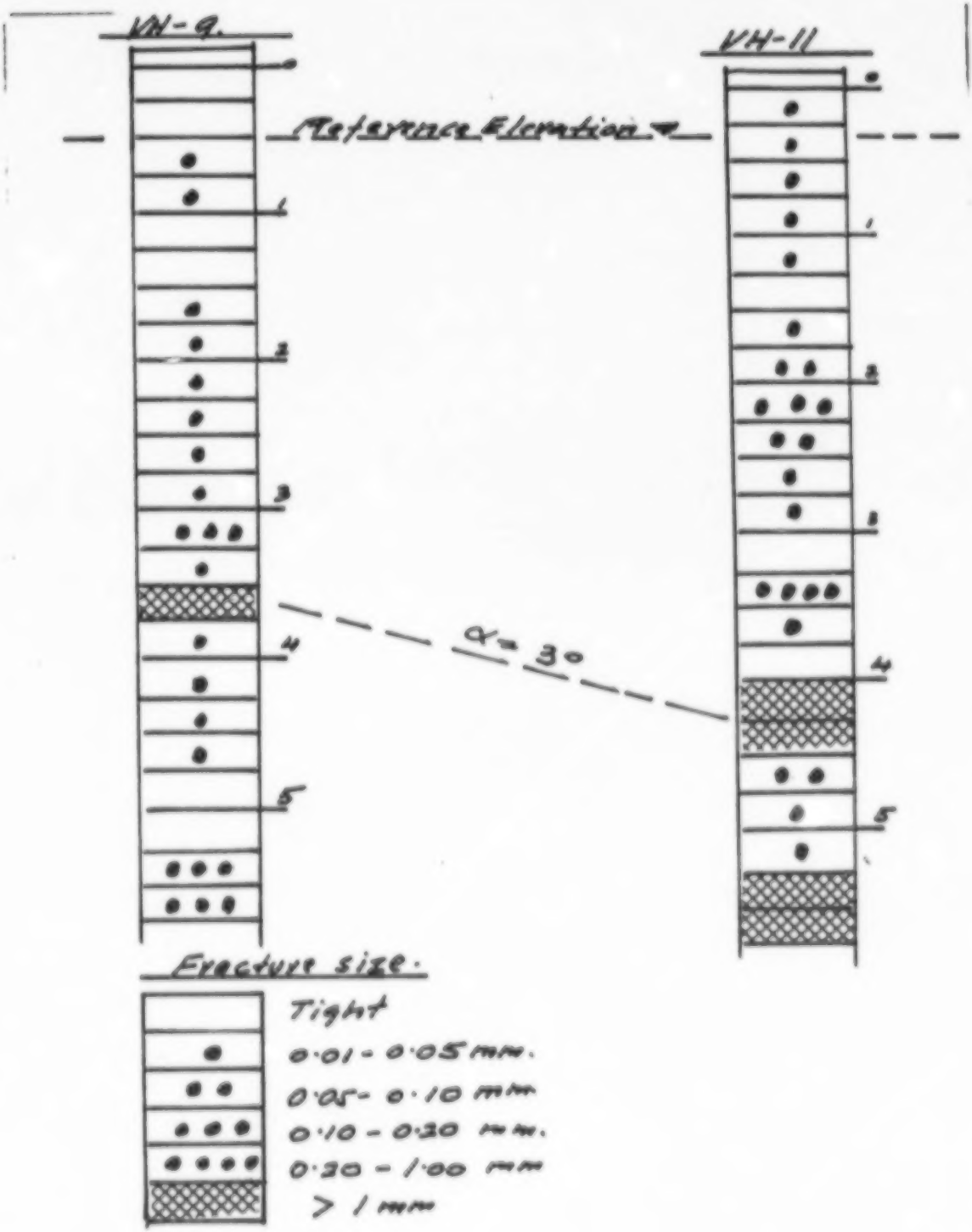

Fig. 35 - Cross-section B-B. R.A. 847 stope.

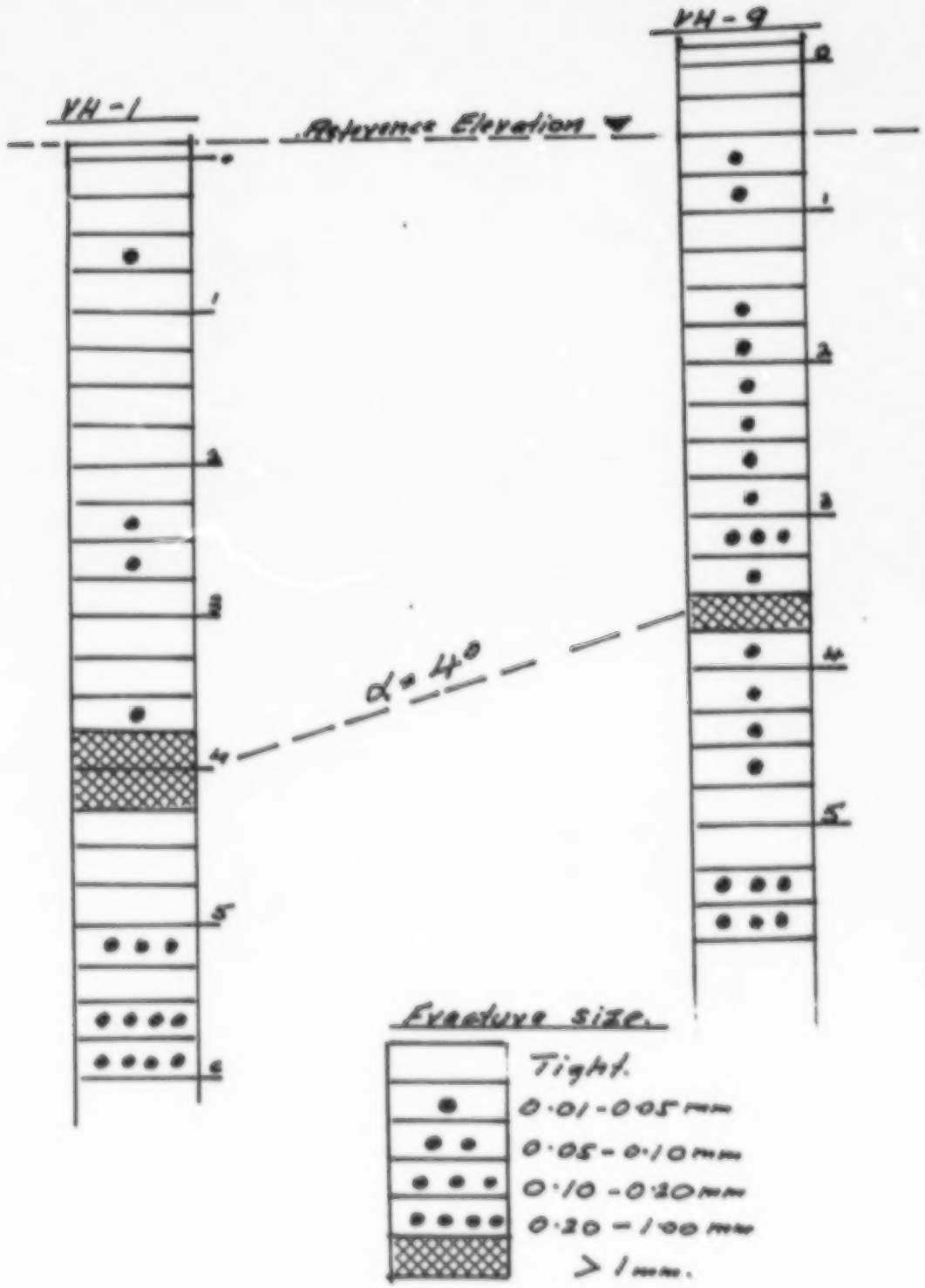

Fig. 36 - Cross-section C-C. R.A. 847 stope.

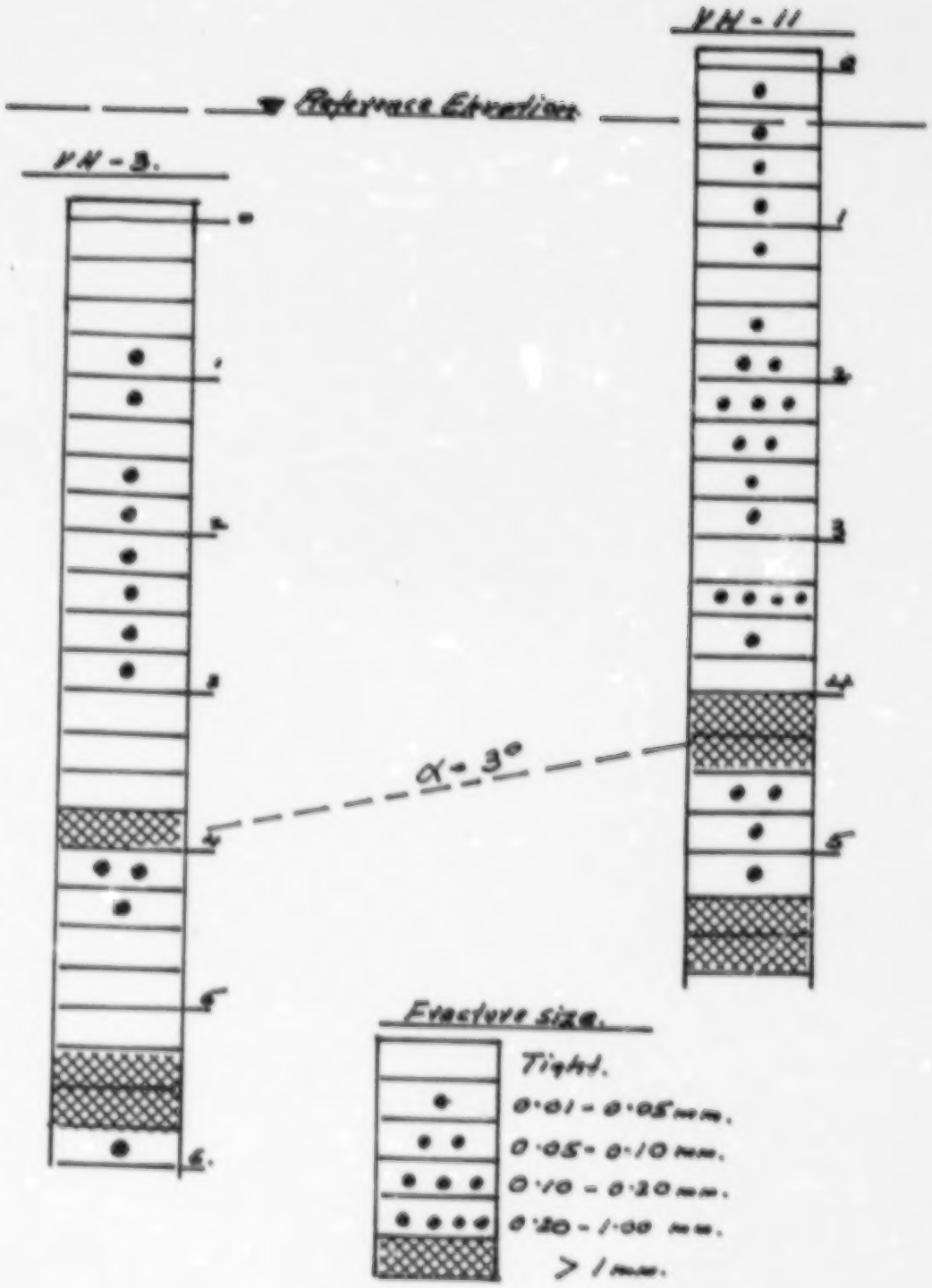

Fig. 37 - Cross-section D-D. R.A. 847 stope.

VH-4 and VH-11 have indicated the presence of more than one large fracture within an interval of 50 cm, instead of obe observed by the TV camera.

The vacuum test has revealed that the roof in the test stope is fractured and the fractures are secondary, created by the excavation of the stope. The estimated width of the fractures is in the range of 0.010 to 0.350 cm, except the major slip. The most severe sagging is developed at the centre of the stope as indicated by Hole VH-4.

However, considerable fracturation was also observed in Holes VH-9 and VH-11, which are located closer to the regular pillars.

Hole VH-3 indicates moderate roof deterioration, but better roof condition was observed in Hole VH-1 which is located close to a large pillar.

The vacuum test has indicated the following:

1. A continuous horizontal fracture plane at a depth of 2 m spanning the complete stope.
2. Regular pillars cannot prevent the development of fractures in the roof.
3. Practically no fractures have developed below and above the main fracture in the vicinity of a large pillar.

The vacuum measurement has provided accurate information on the thickness of the rock section affected by blasting.

The short analysis of the vacuum test holes are as follows:

Hole VH-1

The thickness of the zone affected by the blasting is about 66 cm. The main fractured zone is located at 2.16 m depth in the roof and the thickness of the zone is about 50 cm.

A very tight zone, 75 cm thick, is directly underlying the main fractured zone and the roof above the fractured zone is very competent. The hole is located close to a large safety pillar.

Hole VH-3

The thickness of the zone affected by blasting is about 88 cm. The main fractured zone is located at 2.26 m depth in the roof and the thickness of the zone is about 25 cm.

A very tight zone, 75 cm thick, is underlying the main fractured zone and the roof above the fractured zone is moderately competent. A 75 cm thick very competent rock is directly overlying the fractured zone. The hole is located close to a regular sized pillar.

Hole VH-4

The thickness of the zone affected by blasting is about 55 cm. The main fractured zone is located at 2.55 m depth in the roof and the thickness of the zone is about 50 cm.

The roof below the main fractured zone is severely fractured. A 150 cm thick fractured zone is directly overlying the main fractured zone. The hole is located at the centre of the stope where the maximum roof deformation has taken place.

Hole VH-9

The thickness of the zone affected by blasting is about 76 cm. The main fractured zone is located at 2.39 m depth in the roof and the thickness of the zone is about 25 cm.

The roof below and above the main fractured zone is moderately fractured. The hole is located close to a regular size pillar.

Hole VH-11

The thickness of the zone affected by blasting is about 73 cm. The main fractured zone is located at 1.73 m depth in the roof and the thickness of the zone is about 50 cm.

The roof below and above the main fractured zone is severely fractured. The hole is located close to a regular size pillar.

ROOF STABILITY OF THE RIO ALGOM TEST STOPE

The stability of the roof, as was discussed previously, depends mainly on the configuration of the fractures and the separations present in the roof.

The vacuum test conducted in Rio Algom's test stope has established the physical parameters of the main fractured zone, but due to limited time for the test no attempt was made to determine the configuration of the numerous separations encountered below and above the main fractured zone. Therefore, the stability analysis presented here can be considered only as a demonstration of the evaluation procedure.

No major roof fall was observed in the tesc stope. This fact suggests that all fractures and separations must be parallel with the roof and no wedge shaped separate rock blocks have developed in the rock mass.

The fracturation profile logs have indicated a very prominent separation located about 2 m depth in the roof. The separation running parallel with the roof line creates a 2 m thick self supporting laminated beam controlled by rock bolts.

The general arrangement of the test stope for stability evaluation is presented in Fig. 38.

The span of the beam is 20.4 m and the beam is supported at both ends by mine pillars 3 m thick. The approximate weight of the separated rock block resting on the two safety mine pillars is about 3000 tons. The tensile stress in the beam is calculated according to the formulae given on page 12.

$$\sigma_{max} = \frac{0.003 \times 2040^2}{2 \times 200} = 31.2 \text{ kg/cm}^2$$

This means that the tensile strength of the rock mass is greater than 31.2 kg/cm^2, or more likely the horizontal compressive stresses are greater than this value.

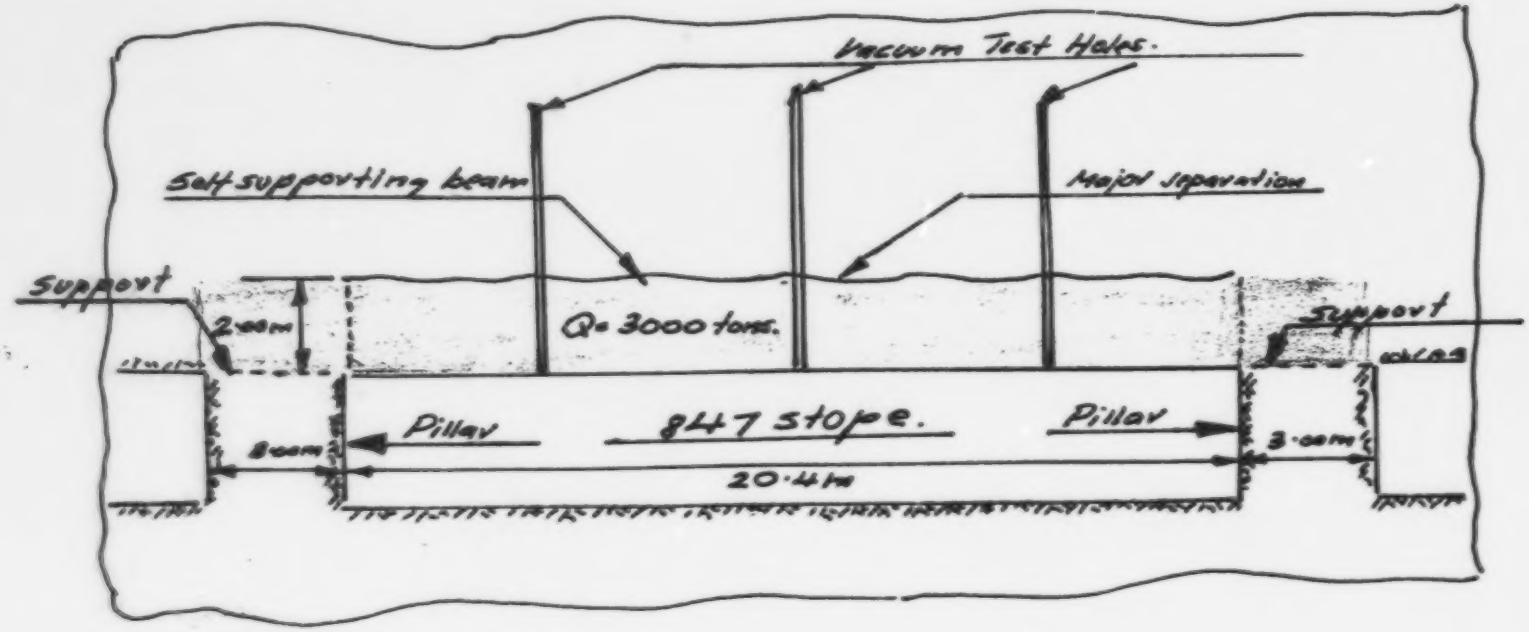

Fig. 38 - Cross section of the 847 stope for roof stability calculation.

The stability of the roof section affected by blasting represents a completely different problem.

It is well established that the blasting creates radial fractures in the rock mass, therefore, the blasting promotes the development of small wedge shaped rock blocks which may cause local rock falls. Such small separate rock blocks must be removed or controlled by rock bolts.

It is of interest to note that at Rio Algom the vacuum test was conducted under a completely separated loose rock block of 3000 tons with safety, but in the other case a wedge shaped rock block developed a rock fall of 1600 tons occurred.

UTILIZATION OF CONVECTRON TYPE VACUUM GAUGES

The underground tests conducted at Denison and Rio Algom mines required only permanent observation stations. Therefore, the mobility of the system was secondary and for this reason water and mercury manometers, as the simplest and most convenient instruments,were used for measuring vacuum during testing.

However, it is recognized that the basic function of the vacuum system is to monitor the roof condition in stopes where mining activities are carried out. The regular monitoring of the roof in stopes scattered on a relatively large area requires light and portable instruments and equipment.

The underground transportation and handling of water and mercury manometers is very cumbersome. For this reason Convectron Series 275 digital and analog type electrically operated vacuum gauges were introduced and sucessfully tested during the Rio Algom test.

The introduction of the vacuum gauges considerably simplified the measuring procedure and increased the mobility of the system. A mercury manometer is only used to calibrate the vacuum gauges from time to time.

CORRELATION OF LARGE FRACTURES BY USING CO_2

The correlation of large fractures between adjacent holes presents a special problem, because the pressure loss in large fractures created by a very moderate air flow is very small. In this case water from the drilling operations indicated a connection between all holes. Another solution is to use CO_2 as a tracer gas to detect the continuation of fractures between holes. The measuring technique using CO_2 as a tracer gas is presented on Fig. 39. The simple testing procedure is as follows:

a) A vacuum is created in the vacuum test hole in order to induce an air flow from the hole.

b) Straddle packer is used to isolate the hole section under investigation.

c) The air removed from the section flows through a Fyrite type CO_2 analyzer.

d) Simultaneously CO_2 is introduced in selected sections of the observation hole by using a CO_2 bottle with pressure reducer and a second straddle packer.

The feeding pressure of the CO_2 is less than 0.1 psi in order to eliminate the development of any extra load on the roof.

The presence of CO_2 at the Fyrite Analyzer is a direct indication of the pneumatic contact between the fractures.

Utilization of CO_2 as a tracer gas is safe and it requires a very simple gas detection instrument which is available on the market.

AIR PERMEABILITY - WATER PERMEABILITY

Sometimes, after conducting the permeability measurement with air, it is desirable to establish the permeability of the material to water. However, the measured air permeability of a porous material cannot be used to establish the water transmitting capacity of the material as the permeability of a porous

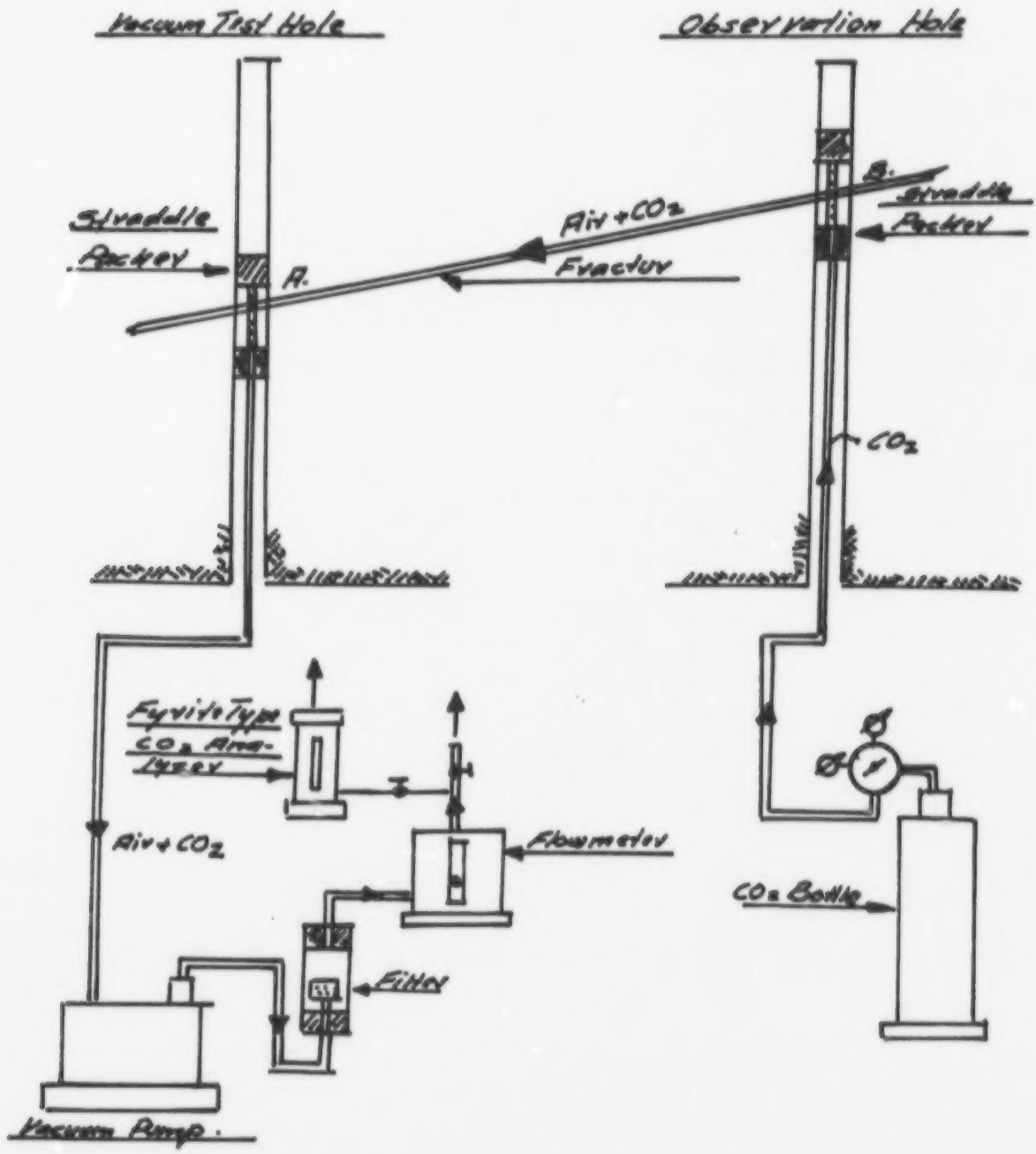

Fig. 39 - Correlation of large fracture by using CO_2.

material to air is always greater than to water.

The explanation given for this behaviour is that the water has a zero velocity at the solid water contact, but the gas has a finite velocity at the solid - gas contact, i.e., at the wall (5).

The proper correlation between gas and liquid permeability was developed by Klinkenberg, who has introduced the so called 'Klinkenberg permeability', i.e., the gas permeability at infinite pressure in order to establish the correlation between gas and liquid permeability (6).

The gas permeability at infinite pressure is called the equivalent liquid permeability of the porous material, because it is accepted that the gas permeability of the material at infinite pressure is equal to the water permeability. The measuring technique is presented on Fig. 40.

First, the air permeability Ka is measured at different mean pressure Pm. Ka and the reciprocal of the mean pressure 1/Pm are plotted and the result of the plot will be a straight line.

The interception of this line with the Ka axis will determine the value of the air permeability at infinite pressure K_∞ which is the equivalent water permeability of the material.

The air permeability at different mean pressures can be conveniently determined during the test, consequently the vacuum method can provide the equivalent liquid permeability of the rock if necessary.

POSSIBLE FURTHER APPLICATION OF THE METHOD

The vacuum method has potential in the following areas of application:

1. Establish and monitor fracturing of mine pillars.
2. Monitor the mine roof fractures in coal mines.
3. Monitor large underground openings, such as power stations, shaft stations, etc.

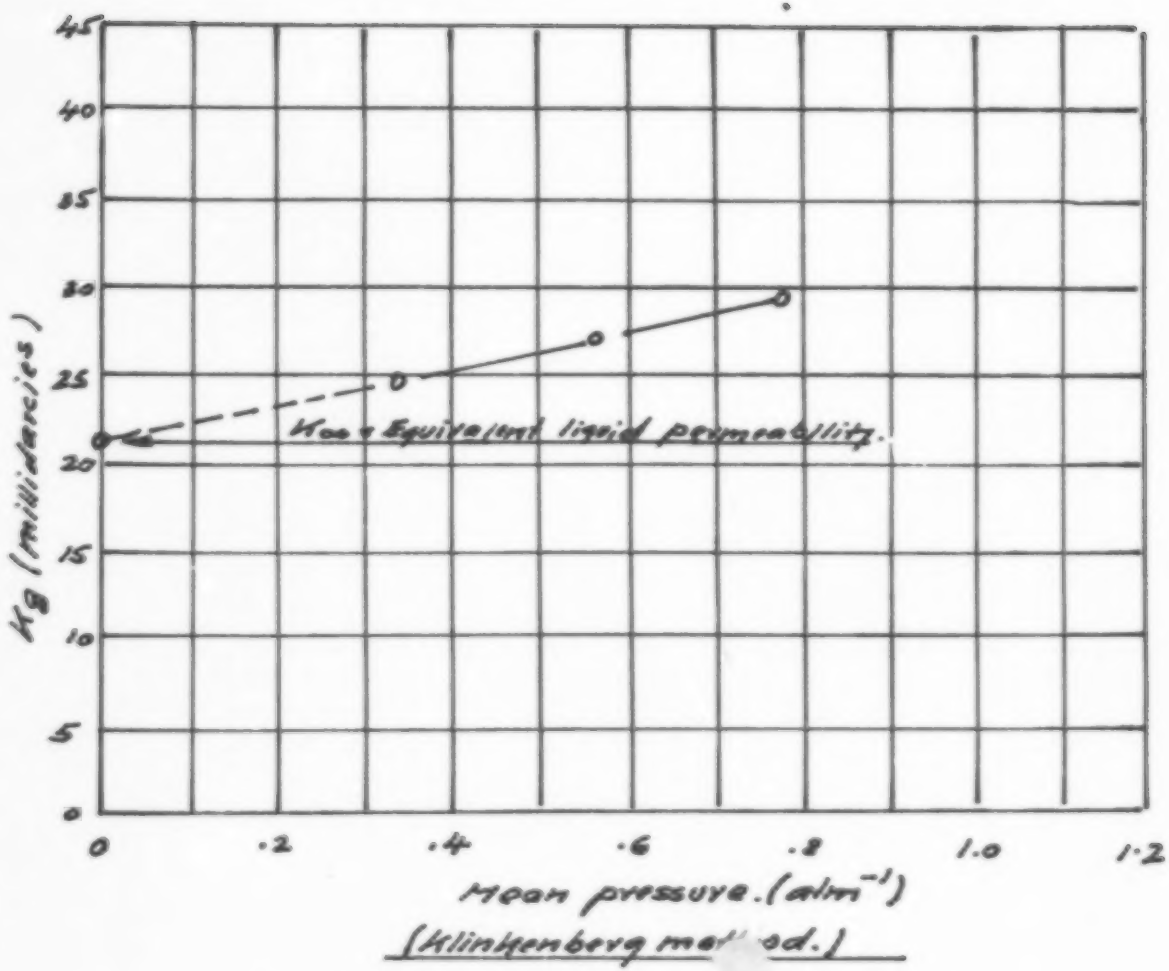

Fig. 40 - Equivalent liquid permeability determination.

4. Measuring the effect of heat and pressure on rock permeability in connection with nuclear waste disposal (7).
5. Measuring the fracture and pore volume of radon concentration in uranium mines.
6. Investigate the effect of blasting.
7. Detect and monitor fractures in structures, such as dams, foundations, etc., (8).
8. Monitor fractures in connection with pit slope stability problems.
9. High pressure gas bearing reefs detection in connection with potash mining in Saskatchewan (9).
10. Monitor the behaviour of sagging salt back in connection with the introduction of backfill in potash mines.
11. Utilization of the method in connection with routine geological roof mapping.
12. Using the measuring technique in connection with complex rock stability investigation, where the knowledge of the fracture parameter, such as the location, width, dip, strike and areal extension is essential.

CONCLUSIONS

The vacuum monitoring system is a new method of determining the fracture conditions inside a rock mass. It is capable of establishing the inter-connection of fractures between boreholes, and hence their areal extent. The location and dip of such fractures can thus be determined and using simple beam models a preliminary assessment of roof stability can be made.

One of the major benefits of the vacuum system is that a very small opening of a fracture results in a large change in the air flow characteristics. Consequently, small deformations are readily detected.

The components of the system (i.e., vacuum pump, manometers, air flow meters, etc.) are readily available and easy to use, only the borehole packers require careful manufacturing and installation inside a borehole.

ACKNOWLEDGEMENTS

The author feels very obligated to the Management of Denison Mine Ltd. and Rio Algom Ltd. for providing the test sites and facilities for conducting the underground testing program.

Acknowledgement is also due to N. Whitton and S.N. Muppalaneni of Rio Algom, and P. Townsend and R. Gunning of Denison Mines for supporting the testing program.

The author is very grateful to A.T. Jakubick and R. Klein of Ontario Hydro for their valuable help during the underground testing.

The author also wishes to thank W. Zawadski and B. Muir of CANMET, Elliot Lake Laboratory for conducting the measurements during the underground testing.

REFERENCES

1. "Towards safe production"; Report of the Joint Federal-Provincial Inquiry Commission into Safety in Mines and Mining Plants in Ontario. vol 2, April 1981.

2. Jones, P.J., "Production engineering and reservoir mechanics"; Oil and Gas J. Tulsa, p 76; 1945.

3. SME Mining Engineering Handbook; New York, 1973.

4. Hedley, D.G.F., "Roof Classification at the New Quirke Mine, Rio Algom Mines Ltd."; Dept. of Energy, Mines and Resources Mines Branch, Mining Research Centre; Internal Report 72/151; 1972.

5. Calhoun, J., J.C., "Fundamentals of Reservoir Engineering"; University of Oklahoma Press: Normal; p 417; 1953.

6. Klinkenberg, L.J., "The permeability of Porous Media to Liquids and Gases"; API Drill and Prod Pract; p 200 ff; 1941.

7. Jakubick, A.T. and de Korompay, V., "Monitoring the Permeability of the Near Field and Far Field Interface of the Nuclear Repository"; Oral presentation at 5th Int. Symp. on the Scientific Basis for Radioactive Waste Management, Berlin (West), Germany, June 7-10, 1982.

8. de Korompay, V., "An Advanced Method to Detect and Monitor Fractures in Structures"; L.C. Lang & Assoc., Inc., consulting engineering report, October 1981.

9. de Korompay, V., "Winnipegosis Reefs and the Safety of the Sylvite Potash Mining at Rovanville, Sask"; Unpublished working note; November 1977.

GLOSSARY OF TERMS USED IN CONNECTION WITH THE VACUUM METHOD

Absolute permeability: expresses the fluid transmitting capacity of the medium when the pore space is 100% saturated with the fluid flowing in the medium.

Absolute pressure: In vacuum technology pressure always corresponds to absolute pressure and not to gauge pressure.

darcy: Unit of permeability. One darcy is defined as the permeability which allows the flow of 1 cc. per second of fluid or 1 cp viscosity through an area of 1 sq cm under a pressure gradient of 1 atm per cm, when the flow condition is viscuous.

Effective permeability: The ability of porous material to conduct fluid when the saturation of that fluid is less than 100% of the pore space is called effective permeability of the material to that fluid. Subscript Ka, Kg and Kw mean, respectively, the effective permeability to air, to gas and to water.

Equivalent fracture size of a section is the fracture size, which has the same fluid transmitting capacity as the section itself.

Matrix permeability: If the fluid movement takes place only in the pores, the permeability is called 'matrix permeability'.

Millidarcy: md is one thousandth of a darcy.

Millimeter of mercury: A unit of pressure corresponding to a column of mercury 1 mm high at 0 C and 980.665 cm/sec acceleration. Abbreviated as mm Hg.

Relative permeability is defined as the ratio of the effective permeability to a given fluid at a definite saturation to the permeability at 100% saturation. The terminology used is simply Ka/K, Kg/K, Kw/K.

Rock face pressure is the pressure at the wall in the bore hole between the two rubber elements of the straddle packer.

Torr: International standard term to replace the term of mm of mercury, i.e., mm of Hg.

Transmissibility is the product os section thickness and section permeability. It expresses the 'permeability capacity' of a section. K x h is commonly referred to in terms of millidarcy, feet or darcy, feet.

Vacuum: In vacuum technology the term 'vacuum' refers to a given space filled with gas at pressure below atmospheric pressure.

Vacuum gauge: A manometer for pressures below 760 torr.

Appendix A - Fracturation profile log of Can-Met drift

Date: March 18-19, 1981 Hole No: Test hole no. 6

Logged by: V. de Korompay Tool: Straddle packer no. 1

Length of Hole m	Section	Vacuum Used Torr	Vacuum Loss for 10 m Torr	Interpretation
	0.25	650	2	Tight
	0.25	625	1	Tight
	0.25	630	0	Tight
1.00	0.25	630	3	Tight
	0.25	640	2.5	Tight
	0.25	644	0	Tight
	0.25	632	0	Tight
2.00	0.25	627	1.5	Tight
	0.25	652	2	Tight
	0.25	647	2.5	Tight
	0.25	632	2	Tight
3.00	0.25	629	2	Tight
	0.25	632	3	Tight
	0.25	641	0	Tight
	0.25	648	2	Tight
4.00	0.25	638	3	Tight
	0.25	651	0	Tight
	0.25	630	2	Tight
	0.25	644	3	Tight
5.00	0.25	641	3	Tight
	0.25	655	3.5	Tight
	0.25	618	3	Tight
	0.25	642	2	Tight
6.00	0.25	622	2	Tight
	0.25	633	3	Tight
	0.25	644	3.5	Tight
	0.25	420	N/A	Fractures present
7.00	0.25	315	N/A	Fractured zone
	0.25	320	N/A	Fractured zone
	Roof			

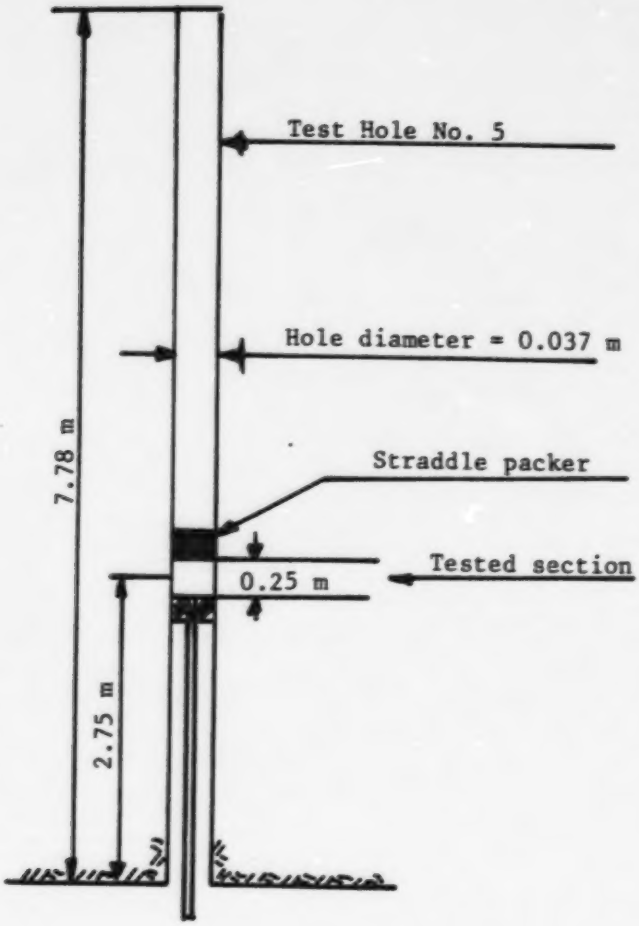

Basic information

Diameter of the hole:	D = 3.77 cm
Length of tested section:	L = 25 cm = 0.82 ft
Volume of the closed system:	V = 438 cm^3
Closed system temperature:	T_C = 60°F
Rock temperature:	T_R = 522°R
Vacuum loss during test:	H_1-H_2 = 14 Torr
Length of test:	t = 95 min
Differential pressure:	$P_e^2-P_w^2$ = 173
Hole geometry:	In re/rw = 5
Viscosity of air:	μ = 0.018 cp

Appendix B - Matrix permeability determination - basic information.

Appendix C - Matrix permeability determination - calculation

Flow Rate Calculation

$$Q = \frac{(H_1 - H_2)\ 520\ V}{760\ t\ (460 + T_c)}$$

$$Q = \frac{14.520 \times 438}{760 \times 95 \times (460 + 60)} = 0.085\ cm^3/min$$

$$Q\ cu\ ft/day = \frac{0.085 \times 1440}{28317} = 0.0043\ cu\ ft/day$$

Matrix Permeability Calculation

Darcy's Equation - Radial Flow.

$$K = \frac{Q\ \mu\ In\ \frac{r_e}{r_w}\ T_R\ 14.65}{10320\ h\ (P_e^2 - P_w^2)}$$

$$K = \frac{0.0043 \times 0.018 \times 5\ 522 \times 14.65}{10329 \times 0.82 \times 173} = 0.000002\ darcies$$

or

$$K = 2 \times 10^{-6}\ darcies$$

or

$$K = 0.002\ millidarcies$$

Appendix D - Fracturation profile log of Hole No. 231-74

Length of Hole	Station	Section	Diff. Static Pressure	Pressure Loss	Differential Pressure		Flow Rate	Transmissibility	Permeability	Equiv. Fracture size
					Dynamic	Static				
m	No.		Torr	Torr/m	Torr	Torr	L/m	Draft	md.	mm
	1	Frac. A	758	0.1					0.0007	
	2	F			585	300	1.5	0.04	0.2×10^6	0.05
	3	?	695	53					0.44	
1.00	4		662	0.1					0.001	
	5		705	0.1					0.001	
	6		645	0.1					0.001	
	7		715	0.1					0.001	
2.00	8		722	0.2					0.002	
	9	Frac. B	692	0.1					0.001	
	10	FF			355	75	4	0.38	1×10^6	0.11
	11	FF			366	86	3.8	0.31	0.8×10^6	0.10
3.00	12		691	0.1					0.001	
	13	Frac. C	631	0.1					0.001	
	14	F			698	580	0.7	0.013	0.1×10^6	0.04
	15	F			728	652	0.4	0.007	0.08×10^6	0.03
4.00	16		735	0.2				0.002		
	17		705	0.2					0.002	
	18		743	0.3					0.004	
	19		744	0.1					0.0007	
5.00	20		715	0.2					0.002	
	21		705	0.1					0.001	
	22		655	0.2					0.002	
	23		700	0.3					0.004	
6.00	24		662	0.1					0.001	
	25		699	0.1					0.001	
	26	Frac. D	701	0.2					0.002	
	27	F			655	365	1.2	0.03	0.2×10^6	0.05
7.00	28		707	0.1						
	29		704	0.1						
	30		728	0.4						
	31		724	0.1						
8.00	32	FFF			330	0.3	4.5	12.76	10.6×10^6	0.36
	33	FFF			330	-0.1	4.5	36.77	21.6×10^6	0.51

Fracture due to blasting
Roof Line

Date: May 11th to June 12
Logged by: V. de Korompay
Hole No. 231-74
Tool: Straddle packer No. 1

Appendix E - Fracturation profile log of Hole No. 231-76

Length of Hole	Station	Section	Diff. Static Pressure	Pressure Loss	Differential Pressure		Flow Rate	Transmissibility	Permeability	Equiv. Fracture size
					Dynamic	Static				
m	No.		Torr	Torr/m	Torr	Torr	L/m	Draft	md.	mm
	1		725	5					0.072	
	2		510	7.2					0.102	
	3		610	5					0.080	
1.00	4	Frac. B	600	1					0.013	
	5	F			380					?
		?								

Total length of hole: 26.5 ft

No flowmeter, no static line were used during testing.

The hole was temporarily used as a vacuum hole.

Date: May 6th

Logged by: V. de Korompay

Hole No. 231-76

Tool: Straddle Packer No. 1

Appendix F - Observation sheet of Hole No. 231-71

Datum	Operation	Flow Rate L/m	Diff. Press. cm Hg	Remarks
June 16		0.2	74	
June 17		0.6	72	
July 20	Before blasting	0.1	74	
July 24	After blasting	0.2	75	Blasting damaged flow line
July 24	Before pneu frac	0.2	75	
July 24	Pneumatic frac		No communication was observed	
July 28	After pneu frac	0.5	73	
July 28	Before blasting	0.5	73	
July 28	After blasting	0.5	25	
Aug. 4	Before blasting	3.0	30.2	Measured by Denison
Aug. 4	After blasting	3.0	29	Measured by Denison
Aug. 7	Before pneu frac	3.0	27.6	
Aug. 7	Pneumatic frac		No communication was observed	

Remarks: The flow line was damaged by the blasting on July 24th. Water seepage was observed during testing.

PAGE NO.

Appendix G - Observation sheet of Hole No. 231-73

Datum	Operation	Flow Rate L/m	Diff. Press. cm Hg	Remarks
July 20	Before blasting	0.6	68	
July 20	After blasting	1.0	70	
July 24	Before pneu frac	1.0	70	
July 24	Pneumatic frac		At 10 psi good air blow was observed	
July 28	After pneu frac	1.8	69	
July 28	Before blasting	1.8	69	
July 28	After blasting	4	58	
July 29		5.0	53.6	Measured by Denison
July 30		5.0	52.8	Measured by Denison
Aug. 4	Before blasting	3.0	31.0	Measured by Denison
Aug. 4	After blasting	3.0	29.4	Measured by Denison
Aug. 7	Before pneu frac	3.0	33.4	
Aug. 7	Pneumatic frac		Flow rate at 10 psi → 5.5 L/m	

Remarks: Water seepage was observed during testing.

Appendix H - Observation sheet of Hole No. 231-75

Datum	Operation	Flow Rate L/m	Diff. Press. cm Hg	Remarks
July 17			72	Press. loss = 0.1 mm Hg/m
July 20	Before blasting	Tight	71	Press. loss = 0.2 mm Hg/m
July 20	After blasting	Tight	71	Press. loss = 0.2 mm Hg/m
July 24	Before pneu frac	Tight	71	Press. loss = 0.2 mm Hg/m
July 24	Pneumatic frac		Good air blow at 20 psi	
July 28	After pneu frac	0.5	70	
July 28	Before blasting	0.5	70	
July 28	After blasting	3.0	18.6	
July 29		5.0	53.6	Measured by Denison
July 30			Rock fall destroyed the hole.	

Remarks: Local rock fall destroyed the hole between July 30th and August 4th.

PAGE NO.

Appendix I - Observation sheet of Hole No. 231-77

Datum	Operation	Flow Rate L/m	Diff. Press. cm Hg	Remarks
July 17		2	44	Re-set packer
July 20	Before blasting	2.4	64	
July 24	After blasting	2.4	64	
July 24	Before pneu frac	2.4	64	
July 24	Pneumatic frac		Good air blow at 5 psi	
July 28	After pneu frac	2.6	47.6	
July 28	Before blasting	2.6	47.6	
July 28	After blasting	1.3	17.4	
July 29		2.6	62	Measured by Denison
July 30		2.8	62.4	Measured by Denison
Aug. 4	Before blasting	3.0	63	Measured by Denison
Aug. 4	After blasting	3.0	37.0	Measured by Denison
Aug. 7	Before pneu frac	3.0	40	
Aug. 7	Pneumatic frac		See remarks below	

Remarks: Flow rate during pneumatic fracture on August 7th:

9 psi 8 L/m

14 psi 9 L/m

17.5 psi 10.5 L/m

Maximum observed pressure before the air line separated at connector was 35 psi.

PAGE NO.

Appendix J - Observation sheet of Hole No. 231-78

Datum	Operation	Flow Rate L/min	Diff. Press. cm Hg	Remarks
July 17		3	19.2	
July 20	Before blasting	3	19.0	
July 24	After blasting	3	19.0	
July 24	Before pneu frac	3	19.0	
July 24	Pneumatic frac		No communication was observed	
July 28	After pneu frac	3.5	23	
July 28	Before blasting	3.5	23	
July 28	After blasting	3.5	22	
July 29		5.5	52	Measured by Denison
July 30		5.5	52	Measured by Denison
Aug. 4	Before blasting	3	18.6	Measured by Denison
Aug. 4	After blasting	3	12.4	Measured by Denison
Aug. 7	Before pneu frac	3	13.6	
Aug. 7	Pneumatic frac		No observation was made	

PAGE NO.

Appendix K - Observation sheet of Hole No. 231-80

Datum	Operation	Flow Rate L/m	Diff. Press. cm Hg	Remarks
July 14		3	30.6	
July 16		4	39.2	
July 17		3	28.6	
July 20	Before blasting	3	28.4	
July 24	After blasting	3	27.0	
July 24	Before pneu frac	3	27.0	
July 24	Pneumatic frac		No communication was observed	
July 28	After pneu frac	3.8	34.8	
July 28	Before blasting	3.8	34.8	
July 28	After blasting	3.8	35.0	
July 29		4.5	57	Measured by Denison
July 30		4.25	57.5	Measured by Denison
Aug. 4	Before blasting	3.0	28.2	Measured by Denison
Aug. 4	After blasting	3.0	26.2	Measured by Denison
Aug. 7	Before pneu frac	3.0	29.6	
Aug. 7	Pneumatic frac		No observation was made	

Appendix L - Fracturation profile log - hole no. VH-1

Length of Hole	Station	Section	Diff. Static Pressure	Pressure Loss	Differential Pressure		Flow Rate	Transmis-sibility	Permea-bility	Equiv. Fracture size
					Dynamic	Static				
m	No.		Torr	Torr/m	Torr	Torr	L/m	Draft	md.	mm
	1	T	685	2.0				-	0.034	-
	2	T	690	2.0				-	0.034	-
	3	●	637	22.7				-	0.397	0.010
1.00	4	T	706	0.7				-	0.012	-
	5	T	690	1.3				-	0.022	-
	6	T	698	0.7				-	0.012	-
	7	T	683	2.0				-	0.034	-
2.00	8	T	684	0.7				-	0.012	-
	9	T	678	0.7				-	0.012	-
	10	●	468	304.0				0.032	6.25	0.029
	11	●			760	693	0.2	0.004	51×10^3	0.025
3.00	12	T	708	0.7				-	0.012	-
	13	T	701	2.0				-	0.034	-
	14	T	698	1.0				-	0.017	-
	15	●			730	600	1.1	0.020	145.10^3	0.042
4.00	16	XXXXXX			470	<1	7.7	?	?	>1
	17	XXXXXX			463	<1	7.5	?	?	>1
	18	T	693	5.0				-	0.085	-
	19	T	690	1.3				-	0.022	-
5.00	20	T	692	0.7				-	0.012	-
	21	●●●			527	155	6.0	0.186	860.10^3	0.101
	22	T	698	1.3				-	0.022	-
	23	●●●●			466	5	7.75	9.740	869.10^4	0.323
6.00	24	●●●●			460	4	7.5	12.850	105.10^5	0.354

Fracture size (mm): T = Tight
● = 0.01 to 0.05
●● = 0.05 to 0.10
●●● = 0.10 to 0.20
●●●● = 0.20 to 1.00
XXXXXX = >1 mm

Appendix M - Fracturation profile log - hole no. VH-3

Length of Hole	Station	Section	Diff. Static Pressure	Pressure Loss	Differential Pressure		Flow Rate	Transmissibility	Permeability	Equiv. Fracture size
					Dynamic	Static				
m	No.		Torr	Torr/m	Torr	Torr	L/m	Draft	md.	mm
	1	T	706	1.9				-	0.034	-
	2	T	707	2.0				-	0.034	-
	3	T	694	4.0				-	0.067	-
1.00	4	●	573	44.7				0.001	0.793	0.014
	5	●	572	55.0				0.001	0.621	0.012
	6	T	637	15.3				-	0.261	0.009
	7	●			755	668	0.5	0.009	87.10^3	0.032
2.00	8	●			760	680	0.6	0.011	97.10^3	0.034
	9	●			763	690	0.2	0.004	51.10^3	0.020
	10	●			750	640	0.7	0.013	107.10^3	0.036
	11	●			770	710	0.15	0.011	100.10^3	0.034
3.00	12	●			750	633	0.6	0.011	98.10^3	0.034
	13	T	736	3.0				-	0.050	-
	14	T	715	3.0				-	0.050	-
	15	T	699	0.7				-	0.012	-
4.00	16	XXXXX			453	<1	8.0	?		>1.000
	17	●●			570	283	4.25	0.122	846.10^3	0.076
	18	●	610	100.0				0.001	1.731	0.017
	19	T	750	0.1				-	0.002	-
5.00	20	T	708	0.7				-	0.012	-
	21	T	727	0.7				-	0.012	-
	22	XXXXX			463	<1	7.5	?	?	>1.000
	23	XXXXX			465	<1	7.5	?	?	>1.000
6.00	24	●			530	150	5.5	0.269	817.10^3	0.099

Fracture size (mm): T = Tight
● = 0.01 to 0.05
●● = 0.05 to 0.10
●●● = 0.10 to 0.20
●●●● = 0.20 to 1.00
XXXXX = >1 mm

Appendix N – Fracturation profile log – hole no. VH-4

Length of Hole	Station	Section	Diff. Static Pressure	Pressure Loss	Differential Pressure		Flow Rate	Transmissibility	Permeability	Equiv. Fracture size
					Dynamic	Static				
m	No.		Torr	Torr/m	Torr	Torr	L/m	Draft	md.	mm
	1	T	690	0.3	–	–	–	–	0.005	–
	2	T	688	1.3	–	–	–	–	0.022	–
	3	T	707	2.0	–	–	–	–	0.033	–
1.00	4	T	748	4.8				–	0.080	–
	5	T	756	1.3				–	0.022	–
	6	●	708	62				0.001	1.038	0.015
	7	●	662	116				0.002	1.961	0.018
2.00	8	●	685	70				0.001	1.178	0.016
	9	●	682	56				0.001	0.742	0.014
	10	●	603	58				0.001	1.009	0.015
	11	T	748	8				–	0.133	–
3.00	12	●	405	490				0.009	11.381	0.032
	13	XXXXX			490	<1	7.0	?	?	>1
	14	XXXXX			580	<1	5.0	?	?	>1
	15	●●			649	380	2.4	0.056	290.10^3	0.059
4.00	16	●			705	505	1.3	0.026	175.10^3	0.046
	17	●●			650	380	2.2	0.051	273.10^3	0.057
	18	●●			670	408	2.2	0.049	266.10^3	0.056
	19	●			736	546	1.0	0.019	141.10^3	0.041
5.00	20	●			720	550	1.2	0.023	160.10^3	0.044
	21	●			720	562	1.0	0.019	141.10^3	0.041
	22	●●●●			520	12	6.5	3.501	445.10^4	0.230

Fracture size (mm):

T = Tight
● = 0.01 to 0.05
●● = 0.05 to 0.10
●●● = 0.10 to 0.20
●●●● = 0.20 to 1.00
XXXXX = >1 mm

Appendix O - Fracturation profile log - hole no. VH-9

Length of Hole	Station	Section	Diff. Static Pressure	Pressure Loss	Differential Pressure		Flow Rate	Transmissibility	Permeability	Equiv. Fracture size
					Dynamic	Static				
m	No.		Torr	Torr/m	Torr	Torr	L/m	Draft	md.	mm
	1	T	720	0.6				-	0.012	-
	2	T	734	0.7				-	0.012	-
	3	●	690	20.0				-	0.336	0.011
1.00	4	●	548	91.0				0.001	1.638	0.017
	5	T	716	2.7				-	0.045	-
	6	T	615	3.3				-	0.057	-
	7	●	578	164.0				0.002	2.894	0.021
2.00	8	●			750	630	0.5	0.009	87.10^3	0.032
	9	●	613	134.0				0.002	2.319	0.019
	10	●			740	570	0.9	0.017	131.10^3	0.040
	11	●			740	600	0.6	0.011	98.10^3	0.034
3.00	12	●			720	555	0.9	0.017	131.10^3	0.040
	13	●●●			605	42	4.0	0.656	147.10^4	0.133
	14	●	655	36.7				0.001	0.623	0.013
	15	XXXXX			568	<1	5.0	?	?	>1.000
4.00	16	●			730	540	1.1	0.021	152.10^3	0.043
	17	●			720	500	1.1	0.021	152.10^3	0.043
	18	●	660	80.0				0.001	0.352	0.016
	19	●	726	6.7				-	0.112	0.037
5.00	20		735	0.7				-	0.012	-
	21		678	1.3				-	0.022	-
	22	●●●			570	28	5.0	1.178	217.10^4	0.161
	23	●●●			600	41	3.9	0.656	147.10^4	0.133
6.00										

Fracture size (mm):

T = Tight
● = 0.01 to 0.05
●● = 0.05 to 0.10
●●● = 0.10 to 0.20
●●●● = 0.20 to 1.00
XXXXX = >1 mm

Appendix P - Fracturation profile log - hole no. VH-11

Length of Hole	Station	Section	Diff. Static Pressure	Pressure Loss	Differential Pressure		Flow Rate	Transmissibility	Permeability	Equiv. Fracture size
					Dynamic	Static				
m	No.		Torr	Torr/m	Torr	Torr	L/m	Draft	md.	mm
	1	●	660	80.0				0.001	1.352	0.016
	2	●	658	16.0				-	0.272	0.010
	3	●	588	44.0				0.001	0.773	0.013
1.00	4	●	470	300.0				0.005	5.838	0.026
	5	●	650	20.0				-	0.341	0.010
	6	T	695	3.3				-	0.055	-
	7	●	545	230				0.003	4.161	0.023
2.00	8	●●			743	45.0	0.7	0.105	442.10^3	0.072
	9	●●●			620	22	3.75	1.178	214.10^4	0.161
	10	●●			605	305	4.0	0.108	448.10^3	0.073
	11	●	688	21.3				-	0.358	0.010
3.00	12	●	635	50.0				0.001	0.857	0.014
	13	T	733	4.7				-	0.078	-
	14	●●●●			570	6	5.0	6.283	653.10^4	0.280
	15	●			750	565	0.9	0.015	122.10^3	0.038
4.00	16	T	734	4.0				-	0.067	-
	17	XXXXX			693	<1	4.5	?	?	>1
	18	XXXXX			575	<1	5.0	?	?	>1
	19	●●			660	280	3.0	0.087	388.10^3	0.068
5.00	20	●	554	172				0.002	2.935	0.021
	21	●			670	305	2.6	0.067	327.10	0.063
	22	XXXXX			560	<1	5.0	?	?	>1
	23	XXXXX			540	<1	4.9	?	?	>1
6.00										

Fracture size (mm):

T = Tight
● = 0.01 to 0.05
●● = 0.05 to 0.10
●●● = 0.10 to 0.20
●●●● = 0.20 to 1.00
XXXXX = >1 mm